National Library of Canada

Acquisitions and Bibliographic Services Branch

395 Wellington Street
Ottawa, Ontario
K1A 0N4

Bibliothèque nationale du Canada

Direction des acquisitions et des services bibliographiques

395, rue Wellington
Ottawa (Ontario)
K1A 0N4

Your file Votre référence

Our file Notre référence

NOTICE

The quality of this microform is heavily dependent upon the quality of the original thesis submitted for microfilming. Every effort has been made to ensure the highest quality of reproduction possible.

If pages are missing, contact the university which granted the degree.

Some pages may have indistinct print especially if the original pages were typed with a poor typewriter ribbon or if the university sent us an inferior photocopy.

Reproduction in full or in part of this microform is governed by the Canadian Copyright Act, R.S.C. 1970, c. C-30, and subsequent amendments.

AVIS

La qualité de cette microforme dépend grandement de la qualité de la thèse soumise au microfilmage. Nous avons tout fait pour assurer une qualité supérieure de reproduction.

S'il manque des pages, veuillez communiquer avec l'université qui a conféré le grade.

La qualité d'impression de certaines pages peut laisser à désirer, surtout si les pages originales ont été dactylographiées à l'aide d'un ruban usé ou si l'université nous a fait parvenir une photocopie de qualité inférieure.

La reproduction, même partielle, de cette microforme est soumise à la Loi canadienne sur le droit d'auteur, SRC 1970, c. C-30, et ses amendements subséquents.

Canada

UNIVERSITY OF ALBERTA

TWO-DIMENSIONAL FINITE ELEMENT MODELING OF FLOW IN AQUATIC HABITATS

by

ASHRAF H. M. GHANEM ©

A Thesis
submitted to the Faculty of Graduate Studies and Research
in partial fulfillment of the requirements for the degree of
Doctor of Philosophy

in

WATER RESOURCES ENGINEERING

DEPARTMENT OF CIVIL ENGINEERING

Edmonton, Alberta
Spring, 1995

National Library of Canada
Acquisitions and Bibliographic Services Branch
395 Wellington Street
Ottawa, Ontario
K1A 0N4

Bibliothèque nationale du Canada
Direction des acquisitions et des services bibliographiques
395, rue Wellington
Ottawa (Ontario)
K1A 0N4

Your file *Votre référence*

Our file *Notre référence*

THE AUTHOR HAS GRANTED AN IRREVOCABLE NON-EXCLUSIVE LICENCE ALLOWING THE NATIONAL LIBRARY OF CANADA TO REPRODUCE, LOAN, DISTRIBUTE OR SELL COPIES OF HIS/HER THESIS BY ANY MEANS AND IN ANY FORM OR FORMAT, MAKING THIS THESIS AVAILABLE TO INTERESTED PERSONS.

L'AUTEUR A ACCORDE UNE LICENCE IRREVOCABLE ET NON EXCLUSIVE PERMETTANT A LA BIBLIOTHEQUE NATIONALE DU CANADA DE REPRODUIRE, PRETER, DISTRIBUER OU VENDRE DES COPIES DE SA THESE DE QUELQUE MANIERE ET SOUS QUELQUE FORME QUE CE SOIT POUR METTRE DES EXEMPLAIRES DE CETTE THESE A LA DISPOSITION DES PERSONNE INTERESSEES.

THE AUTHOR RETAINS OWNERSHIP OF THE COPYRIGHT IN HIS/HER THESIS. NEITHER THE THESIS NOR SUBSTANTIAL EXTRACTS FROM IT MAY BE PRINTED OR OTHERWISE REPRODUCED WITHOUT HIS/HER PERMISSION.

L'AUTEUR CONSERVE LA PROPRIETE DU DROIT D'AUTEUR QUI PROTEGE SA THESE. NI LA THESE NI DES EXTRAITS SUBSTANTIELS DE CELLE-CI NE DOIVENT ETRE IMPRIMES OU AUTREMENT REPRODUITS SANS SON AUTORISATION.

ISBN 0-612-01694-3

Canada

UNIVERSITY OF ALBERTA

Library Release Form

Name of Author: Ashraf H. M. Ghanem

Title of Thesis: Two-Dimensional Finite Element Modeling of Flow in Aquatic Habitats

Degree: Doctor of Philosophy

Year this Degree Granted: 1995

Permission is hereby granted to the University of Alberta Library to reproduce single copies of this thesis and to lend or sell such copies for private, scholarly, or scientific research purposes only.

The author reserves all other publication and other rights in association with the copyright in the thesis, and except as hereinbefore provided, neither the thesis nor any substantial portion thereof may be printed or otherwise reproduced in any material form whatever without the author's prior written permission.

Ashraf H. M. Ghanem
25 a Ismail Mohammed Street
Zamalek, Cairo, Egypt

Dated: March 28, 95

بِسْمِ اللهِ الرَّحْمَنِ الرَّحِيمِ

أَوَلَمْ يَرَ الَّذِينَ كَفَرُوا أَنَّ السَّماوَاتِ
وَالأَرْضَ كَانَتَا رَتْقًا فَفَتَقْنَاهُمَا وَجَعَلْنَا مِنَ الْمَاءِ
كُلَّ شَيْءٍ حَيٍّ أَفَلا يُؤْمِنُونَ .

(سورة الأنبياء — آية ٣٠)

In the Name of Allah the Most Gracious, the Most Merciful

"Do not those who disbelieve see that the
heavens and the earth were joined together,
then We (God Almighty) tore them asunder?
And We made of water every living thing.
Will they not then believe?"

The Quran, 21:30

UNIVERSITY OF ALBERTA

Faculty of Graduate Studies and Research

The undersigned certify that they have read, and recommend to the Faculty of Graduate Studies and Research for acceptance, a thesis entitled TWO-DIMENSIONAL FINITE ELEMENT MODELING OF FLOW IN AQUATIC HABITATS by Ashraf H. M. Ghanem in partial fulfillment of the requirements for the degree of Doctor of Philosophy in Water Resources Engineering.

P. M. Steffler (Supervisor)

F. E. Hicks (Co-Supervisor)

T. Y. Gan

A. Elwi

B. Lipsett

M. Leclerc (External Examiner)

Date: March 28, 1995

Abstract

The simulation of the flow of water in natural streams and rivers is of importance to many disciplines. Hydraulic models are required for flood forecasting and designing of flood protection measures, for the design of dams and power stations, and for the analysis and design of stream diversions and water intakes. A correct understanding of the flow characteristics is also important for analyzing processes related to the flow of water such as sediment transport, water quality and aquatic habitat protection.

In many flow situations, a one-dimensional approach does not provide the required details of complex flow phenomena. Examples of these are flow in braided rivers, flow around islands, flow in estuaries and river deltas, or flow of a meandering river with a wide floodplain. In these situations, a two-dimensional model may be more appropriate.

A review of the literature on available two-dimensional flow models indicated several areas of difficulties which prevent the models from providing accurate solutions. Examples of these difficulties are the inability to represent complex topography and boundaries, poor conservation properties, the need for excessive artificial diffusion, cross-wind diffusion, and instabilities occurring when attempting to simulate domains containing wet and dry areas.

This thesis proposes a two-dimensional finite element method that overcomes many of the numerical difficulties encountered when solving the two-dimensional shallow water flow equations. The finite element method facilitates the use of an unstructured grid and thus is able to accommodate complex domain geometry. A routine has been developed which builds a two-dimensional finite element mesh from a standard one-dimensional input file. The solution of the flow equations is based on the Characteristic-Dissipative-Galerkin Finite Element technique, in which application of the Petrov Galerkin Finite Element Method results in a higher order artificial diffusion applied in the characteristic directions of disturbances. The upwinding matrices have the property of reducing correctly to the optimal one-dimensional system case, thus overcoming the problem of cross-wind diffusion. Numerical experiments showed that the method is able to accurately simulate complex flow features such as standing waves, dambreak problems, and changes

between super- and subcritical flows. As the scheme is based on the conservation form of the equations, it has excellent conservation properties (sections 3.2 and 3.4). Integration by parts of the governing equations facilitates a natural implementation of the boundary conditions.

A new method has been proposed to simulate flow on dry/wet domains. The method is simple to apply, yet it is accurate and stable in simulating steady and unsteady fully dynamic flow without limitations on domain complexity. The technique has been used to simulate an experiment of dambreak on a dry bed. The results were in excellent agreement with laboratory measurements. Simulation of flow in natural fish habitats with dry bed areas confirmed the robustness of the method. The simulated velocities agreed well with field measurements.

As the two-dimensional model provides a good representation of the flow field, it can serve as a tool to analyze the complex flows encountered in typical fish habitat reaches. The good conservation properties of the model make it suitable for further development to simulate transport phenomena and flow under ice cover. The finite element mesh could be utilized directly to integrate habitat quality parameters over the simulation domain.

Acknowledgements

First and Foremost I am thankful to Allah the Almighty (God) for His Grace and Mercy.

I wish to express my sincere thanks to my supervisor Dr. Peter Steffler for his valuable advice and support throughout the course of this study. His active interest in the subject was very inspiring and led to many fruitful discussions.

Thanks are due to my co-supervisor Dr. Faye Hicks for her support and guidance. Especially her advice in the phase of evaluating instream flow needs assessment methods and her valuable suggestions in structuring the thesis are greatly appreciated.

I would like to extend my thanks to Mr. Chris Katopodis, Department of Fisheries and Oceans, Government of Canada, for his valuable support and suggestions. His keen interest in the subject of fish habitat led to tying the developed computational modeling techniques to practical implementation in fish habitat simulation.

Many thanks are due to Mr. Allan Locke and Mr. Tom Olson, Alberta Fish and Wildlife, who kindly provided references and fish habitat data files, and helped in the practical aspects of fish habitat simulation.

Financial support for this study was provided by the Department of Fisheries and Oceans and the National Sciences and Engineering Research Council, Government of Canada.

A warm thank you to all my relatives in Canada, especially my brother Ayman, my cousin Refaat, my cousin Nelly and her husband Tarek, for their continued support and encouragement. Thanks are also extended to all my friends, in Edmonton in particular and elsewhere on the globe, just too many to mention here, who continually provided support and relief.

Finally, special thanks are extended to my mother Hayat Salem and my father Dr. Hassan Ghanem for always being there.

Table of Contents

Chapter 1 Introduction 1

Chapter 2 Finite Element Solution of the Two-Dimensional Shallow Water Flow Equations 9

2.1 Introduction 9

2.2 Equations of Two-Dimensional Depth Averaged Free Surface Flow 10

2.3 Boundary and Initial Conditions 16

2.3.1 No-Flow Boundary: 18

2.3.2 Inflow Boundary: 18

2.3.3 Outflow Boundary: 19

2.4 Finite Element Formulation 20

2.5 Dry Elements 30

2.5.1 General 30

2.5.2 Treatment of Domains with Partially Dry Beds 32

2.6 Mesh generation 37

2.6.1 Introduction 37

2.6.2 Unstructured Mesh Generation 38

2.6.3 Description of the mesh generation routine 38

2.6.3.1 Preparation of input file 39

2.6.3.2 Placement of boundary and interior nodes 39

2.6.3.3 Triangulation 40

2.6.3.4 Smoothing 40

2.6.3.5 Renumbering 41

2.6.3.6 Interpolation 41

2.7 Summary 43

Chapter 3 Model Evaluation 44

3.1 Introduction 44

3.2 Supercritical Flow Through a Channel Contraction 45

3.3 Circular Dam Break Problem 47

3.4 Partial Dam Failure 54
3.5 Directional Dependency of Upwinding 58
3.5.1 Hydraulic Jump 58
3.5.2 Dambreak Problem 58
3.6 Stability Range 62
3.7 Dambreak on Dry Bed 64
3.8 Flow in a Trapezoidal Channel With Partly Dry Side Slopes 66
3.9 Summary 68

Chapter 4 Simulation of Flow in Physical Fish Habitat 69

4.1 Introduction 69
4.2 Hypothetical Test Case: Flow over a Side Bar 70
4.3 Real Test Case: Simulation of Flow in a Fish Habitat 73
4.3.1 Simulation of High Flow 74
4.3.2 Simulation of Low Flow 79

Chapter 5 Summary and Conclusions 83

References 86

Appendix A Field Data Collection for Two-dimensional Flow Simulation of Fish Habitat 94

Appendix B Hydraulic Modeling in Instream Flow Needs Assessment Methods 98

B.1 Introduction 98
B.2 Single Variable Methods 99
B.2.1 Introduction 99
B.2.2 Discharge Methods 99
B.2.2.1 General 99
B.2.2.2 Tennant's Method (Montana Method) 100
B.2.2.3 Other Discharge Methods 101
B.2.2.4 Discussion 101
B.2.3 Methods based on Channel Hydraulic Characteristics 102
B.2.3.1 General 102

B.2.3.2 Wetted Perimeter Inflection Point Method 102
B.2.3.3 Other Methods Based on Channel Characteristics 105
B.2.3.4 Discussion 106
B.3 Multi-variable Methods 107
B.3.1 General 107
B.3.2 Empirical Methods 107
B.3.2.1 The Habitat Quality Index (HQI) Method 107
B.3.2.2 Other Empirical Methods 109
B.3.2.3 Discussion 109
B.3.3 Instream Flow Incremental Methodology 110
B.3.3.1 General 110
B.3.3.2 Method Description 111
B.3.3.3 Discussion 116
B.3.4 Other Multi-variable Methods 119
B.4 Discussion of IFN Methods 119
Appendix C Evaluation of the Square Root of the Convection Matrix 121

List of Figures

Figure 2.1	Two-Dimensional Depth Averaged Free Surface Flow: Definition Sketch	10
Figure 2.2	Boundary Condition Specification	17
Figure 2.3	Shape Functions for Linear Elements	21
Figure 2.4	Elements in Local and Global Coordinate Systems	21
Figure 2.5	Partially Dry Elements (Hervonet and Janin, 1994)	32
Figure 2.6	Wet and Dry Subdomains (right and left of point A respectively)	33
Figure 2.7	Dividing the Domain into Dry and Wet Regions	35
Figure 2.8	Element Generation Using the Advancing Front Method	40
Figure 2.9	Interpolation Procedure Using Areal Interpolation	42
Figure 3.1	Finite Element Mesh	45
Figure 3.2	Measured Depth Contours (Reproduced from Ippen and Dawson, 1951)	46
Figure 3.3	Simulated Depth Contours	46
Figure 3.4	Circular Dam Break: Initial Water Surface	47
Figure 3.5	Finite Element Mesh (Quadrilaterals)	48
Figure 3.6	Finite Element Mesh (Triangles)	48
Figure 3.7	Finite Element Mesh (Equilateral Triangles)	49
Figure 3.8	Depth Contours (Quadrilateral Elements) at t = 0.69 sec	49
Figure 3.9	Velocity Vectors (Quadrilateral Elements) at t = 0.69 sec	50
Figure 3.10	Depth Contours (Triangular Elements) at t = 0.69 sec	50
Figure 3.11	Velocity Vectors (Triangular Elements) at t = 0.69 sec	51
Figure 3.12	Depth Contours (Equilateral Triangular Elements) at t = 0.69 sec	51
Figure 3.13	Velocity Vectors (Equilateral Triangular Elements) at t = 0.69 sec	52
Figure 3.14	Computed Water Surface (quadrilateral mesh) at time t = 0.69 sec	53
Figure 3.15	Partial Dam Failure: Definition Sketch	54
Figure 3.16	Initial Water Surface	54
Figure 3.17	Finite Element Mesh	55
Figure 3.18	Computed Depth Contours	56
Figure 3.19	Velocity Vectors at time t = 7.1 seconds	56
Figure 3.20	Water Surface at time t = 7.1 seconds	57

Figure 3.21 Comparison Between Computed Water Surface Profiles at t = 7.1 seconds, y = 140 m 57

Figure 3.22 Hydraulic Jump Initially and after 100 Time Steps in the x-Direction and at 45 Using the CDG method 59

Figure 3.23 Water Surface After 60 seconds from Dam Break, Flow in the x-direction (one-dimensional CDG-method). 60

Figure 3.24 Water Surface After 60 seconds from Dam Break, Flow in the x-direction and at (CDG-solution) 60

Figure 3.25 Initial and Final Water Surface (at 10,000 steps) for = 0.65 62

Figure 3.26 Water Surface after 2000 time steps for = 0.6 63

Figure 3.27 Measured and Simulated Water Surfaces for Dambreak on Dry Bed (Measured Data from Schoklitsch, 1917) 65

Figure 3.28 Computed Longitudinal Water Surface Profiles at y = 15 m 66

Figure 3.29 Cross Section at x = 200 m after 500 seconds, Showing Wet and Dry Areas 67

Figure 3.30 Depth Contours at Steady State (t = 500 seconds) 67

Figure 3.31 Steady State Velocity Vectors 67

Figure 4.1 Flow Over a Side Bar 70

Figure 4.2 Transverse Distribution of Longitudinal Velocity at Sec. X1-X1 Q = 180 m^3/sec 71

Figure 4.3 Transverse Distribution of Longitudinal Velocity at Section X2-X2 Q = 1800 m^3/sec 72

Figure 4.4 Layout of Cross-Section Data Points and Cross-Section Numbers Waterton River 73

Figure 4.5 Interpolation Mesh (Waterton River) 74

Figure 4.6 Finite Element Calculation Mesh (Waterton River) 74

Figure 4.7 Interpolated Bed Contours, Waterton River 74

Figure 4.8 Longitudinal Section I-I 75

Figure 4.9 Longitudinal Section II-II 76

Figure 4.10 Computed Steady State Velocity Vectors 76

Figure 4.11 Comparison Between Measured and Simulated Velocities Cross Section 11 (Refer to Figure 4.4 for Cross Section Number) 77

Figure 4.12 Comparison Between Measured and Simulated Velocities Cross Section 10 (Refer to Figure 4.4 for Cross Section Numbers) 78

Figure 4.13 Depth Contours at Low Flow (Q = 1.52 m^3/sec) 79

Figure 4.14 Longitudinal Section X-X 79

Figure 4.15 Cross-Section Y-Y Through the Island 80

Figure 4.16 Velocity Vectors at Low Flow (Q = 1.52 m^3/sec) 80
Figure 4.17 Comparison Between Measured and Simulated Velocities at Low Flow (Cross-Section 11) 81
Figure 4.18 Comparison Between Measured and Simulated Velocities at Low Flow (Cross-Section 10) 82
Figure B.1 Wetted Perimeter Inflection Point Method 104
Figure B.2 Cross section in a Natural Stream 118

List of Symbols

x	horizontal space dimension (a subscript x with any variable refers to the x-component of that variable)
y	horizontal space dimension (a subscript y with any variable refers to the y-component of that variable)
$\mathbf{A}$	convection matrix
A	element area
$\mathbf{B}$	matrix of shape functions
$\hat{\mathbf{B}}_i$	weight function
$\overline{\mathbf{BK}}$	boundary stiffness matrix
$\overline{\mathbf{BC}}$	boundary condition codes matrix
b	shape function
$\mathbf{C}$	diffusion vector
c	wave celerity
$\overline{\mathbf{CBC}}$	complimentary boundary condition codes matrix
C_r	Courant number
C_s	dimensionless Chezy coefficient
$\mathbf{D}$	diffusion matrix
d	number of space dimensions
$\mathbf{F}$	force vector
$\overline{\mathbf{F}}$	source vector
F_r	Froude number

$\mathbf{G}$	source vector
g	gravitational acceleration
H	water depth
H_{min}	minimum depth specified for dry bed calculation
h	stage
$\mathbf{I}$	identity matrix
$\mathbf{J}$	jacobian matrix
$\mathbf{K}$	stiffness matrix
k_s	roughness height
$\mathbf{M}$	force matrix
$\mathbf{N}$	source matrix
NS	number of shape functions
$\mathbf{n}$	unit inward normal to the domain Γ
q	discharge per unit width in the x-direction
R	hydraulic radius
S_f	friction slope
S_o	bed slope
$\mathbf{S}$	capacity matrix
S	aquifer storativity
T	aquifer transmissivity
t	time
U	depth averaged velocity in the x-direction
u_s	shear velocity
V	depth averaged velocity in the y-direction

$\mathbf{W}$	total velocity vector
$\mathbf{W}$	upwinding matrix
z	bed elevation
Δx	discretization in the x-direction
Δy	discretization in the y-direction
Δ	discretization size
ε	convergence norm
Γ	domain boundary
ϕ	vector of unknowns H, qx and qy
Φ	nodal values of unknowns
$\hat{\Phi}$	vector of known boundary values
ν	turbulent exchange coefficient
Ω	domain
ω	upwinding coefficient
ρ	water density
τ	shear stress due to turbulence
Θ	angle the bed makes with the horizontal plane
θ	implicitness factor

Chapter 1

Introduction

The simulation of the flow of water in natural streams and rivers is of importance to many disciplines. Hydraulic models are required for flood forecasting and designing of flood protection measures, for the design of dams and power stations, and for the analysis and design of stream diversions and water intakes. A correct understanding of the flow characteristics is also important for analyzing processes related to the flow of water such as sediment transport, water quality and aquatic habitat protection.

The flow simulation approach can be classified with regards to the number of spatial dimensions as one-, two- or three-dimensional approaches. One-dimensional models treat the stream as a number of cross sections and provide the results in the form of cross-section average values. This approach is usually used to analyze long reaches of rivers extending over many kilometers, where the variation of flow across the channel is not of much interest. The reader is referred to Hicks and Steffler, (1990), for an overview of different approaches and approximations to solve the one-dimensional open channel flow equations.

For some practical applications, the variation of the flow across the stream might be important. Examples of these are flow in braided channels, estuaries and river deltas, or flow in a meandering river with a wide floodplain. Also, environmental impact assessment

models often require the distribution of the velocity across the stream as input to other chemical or biological models. In these situations, the solution of the two-dimensional shallow water flow equations can provide good estimates of complex flow features in the horizontal plane, such as recirculation, flow around islands and obstructions, and flow in braided channels.

However, because of the depth averaging in the two-dimensional equations, they are not able to resolve flow features of a three-dimensional nature. For example, when simulating a river bend, the two-dimensional model would be able to predict the redistribution of longitudinal velocity reasonably well, but it would not represent the helical vortex usually observed in bends. As this vortex has a large effect on the mixing characteristics and local bathymetry of the river, the direct application of the two-dimensional model to simulate water quality or sediment transport would provide only limited success.

The solution of the three-dimensional Reynolds equations would be able to account for secondary flows and other flow features, such as horseshoe vortices in the vicinity of bridge piers, and flow details around obstructions and bed forms. However, the solution of the three-dimensional equations is not an easy task. The equations are comprised of one equation of conservation of mass and three equations of conservation of momentum applied in the directions of the three space dimensions. The turbulent fluctuations of the flow are time averaged to yield additional turbulent stress terms in the momentum equations. The resulting system of four equations has a total of ten unknowns, and therefore closure models are required to relate the turbulent stresses to mean flow parameters. Further, the resolution required to obtain numerically stable solutions in a typical reach of a natural stream or river would involve an enormous number of computational nodes, having four unknowns each. The free water surface would further complicate the problem, as the three-dimensional mesh would have to change continually with time.

In view of the enormous data and computer requirements involved in solving the three-dimensional equations for flow in natural rivers, the solution of the two-dimensional depth averaged equations is attempted here. When the underlying assumptions and limitations are understood and considered, a two-dimensional model provides significantly more detailed information than the one-dimensional approach. As shown in Chapter 4, the use

of a two-dimensional model could actually result in a reduction in data requirements as compared to the one-dimensional approach for certain applications.

When solving the two-dimensional equations for natural streams, several difficulties arise. First, there are the challenges which are also encountered in the one-dimensional approach such as the simulation of shocks, and the production of wiggle-free solutions. In addition, new difficulties, related to the two-dimensional nature of the problem, have to be overcome. For example, in the two-dimensional case, the problem of cross-wind diffusion appears, which requires special treatment (Brooks and Hughes, 1982). Other difficulties are introduced by the complex boundaries often encountered in two-dimensional domains. The computational grid should be able to conform well to complex geometrical shapes. Another difficulty in two-dimensional modeling is the treatment of boundary conditions. Also, in the one-dimensional approach, if the water lever drops and the cross section is only partially full, the area at that cross section remains positive. On the other hand, any drop of water level in the two-dimensional domain usually results in exposing nodes and elements. These "dry areas" result in mathematical complications and require special treatment.

Several numerical techniques have been proposed to solve the two-dimensional shallow water flow equations. Benque et al. (1982) used a split operator Finite Difference (FD) technique together with the Alternating Direction Implicit (ADI) method to simulate tidal currents. However, it is not suitable for rapidly varying or highly nonlinear velocities (Benque et al., 1982). Jenkins and Keller (1990) applied a two-dimensional FD model using a boundary fitted coordinate system with subregion grid generation to simulate flow in a hypothetical river with flood plain. They used first order upwinding for the convective terms together with the ADI method.

The Finite Volume (FV) method, which is based on the integral form of the conservation equations, has the advantage of having good conservation properties (Hirsch, 1988). Soulis (1992) proposed a two-dimensional FV model to solve dambreak problems using body fitted non-orthogonal local coordinates. The method assumed the main flow to be in the positive x-direction and employed a first order upwind scheme. Other FV techniques classified under the approximate Riemann solvers, such as Flux Vector Splitting and Flux Difference Splitting have been proposed by Steger and Warming, (1981), Van

Leer, (1982) and Roe, (1981), (Hirsch, 1988). Glaister, (1988), proposed a Flux Difference Splitting Scheme to solve the shallow water equations. Zhou et al. (1994) overcame the problem of domain irregularity by allowing the use of an unstructured mesh of triangles and quadrilaterals together with the explicit FV method. The model used the Osher scheme as an approximate Riemann solver to give some allowance for discontinuities. Since the model was based on an explicit scheme, it suffered from the requirement of small computational time steps. The model was only first order accurate, which would result in excessive numerical damping. Further, the model could not adequately simulate domains having discontinuities and shocks (Zhou et al., 1994).

Generally, some limitations face the FD and FV methods. One is that boundary conditions are imposed artificially. Derivative boundary conditions require the use of fictitious nodes and/or a reduced accuracy at the boundary. Although the FD method is usually easier to program than the Finite Element (FE) method, it generally requires more nodes and computational time to achieve accuracy comparable to the FE method (Lee and Froehlich, 1986). Further, the FD method's inability to operate on an unstructured grid greatly limits its applicability to simulate flow in natural water bodies. As stated above, the FV method has been used on unstructured grids (Zhou et al., 1994). It should however be noted, that the advantage of ease of implementation attributed to the FV method as compared to the FE method starts becoming debatable in this class of FV methods.

The FE method is attractive for simulating flow of water in natural streams and water bodies having irregular boundaries and complex topography. The flexibility of the method allows the choice from a wide array of linear and higher order elements which can be combined to give the best representation of complex domains using an unstructured mesh. It is possible to concentrate nodes in regions of complex geometry and/or interesting flow features and have a more sparse layout in areas which are more uniform. Further, the FE method, through integration by parts of the governing equations, facilitates a natural implementation of boundary conditions. This, together with the overall consistency and accuracy of the method results in requiring usually less nodes than FD and FV methods to achieve similar accuracy. Therefore, the FE method has been chosen for this thesis.

As no variational formulation exists for most fluid flow equations (Lee and Froehlich, 1986), the Galerkin technique is usually chosen to solve flow problems using the FE

method. The technique is applied to a system of differential equations by requiring that the residual resulting from the integration of the weighted equations over the simulation domain be a minimum. In the Bubnov Galerkin method, using a weight function equal to the basis function results in minimizing the overall solution error. However, this technique was found to be unstable for many practical open channel flow problems, especially when shocks occur in the solution domain (Katopodes, 1984).

The majority of research and commercial FE codes developed to simulate the shallow water flow equations employ the concept of mixed interpolation, in which a higher order interpolation is used for the velocity than for the water surface. This technique is similar in concept to the staggered FD technique. Among the models based on this approach are the Finite Element Surface Water Modeling System (FESWMS) (Froehlich, 1989), RMA-2 (King and Norton, 1987), Leclerc et al., (1990), and FASTTABS (Boss Corporation and Brigham Young University, 1992). The success of this technique to suppress spurious oscillations has been attributed to error consistency (Lee and Froehlich, 1986). Walters (1983) explained that the use of mixed interpolation cuts off the short wave lengths for the depth at 4Δ (where Δ is the nodal grid spacing), and thereby eliminates the spurious oscillation mode.

However, the mixed interpolation technique is not free from problems. Walters (1983) applied the method to simulate flow in a rectangular basin with quadratically varying bathymetry and a periodic forcing function on one boundary. Although the oscillations in water surface were suppressed, significant spurious oscillations in the predicted velocity were observed. Walters (1983) explained that these velocity oscillations were due to poor phase speed behavior and that the solution was generally inferior to the velocity solution obtained using equal order interpolation. He also noted that the severity of these oscillations increased with increasing network complexity. An "eddy viscosity" three to four orders of magnitude higher than the expected natural values had to be used to damp these oscillations. No convergence could be achieved with zero eddy viscosity (Walters 1983). Excessive, element size dependent, values of "turbulent diffusion" were also recommended by King and Norton (1976) for use in the RMA-2 model. These large values of diffusion could have a distorting effect on the simulated flow, as they would smear out any interesting flow features. Norton and King (1976 and 1978), Walters and Cheng, (1980), and Froehlich (1989) reported conservation problems, especially at no flow boundaries

with sharp corners. Problems in satisfying continuity were also reported by Gee and McArthur (1978) and Bates et al. (1992). Walters and Cheng, (1980) noticed difficulties to apply head type boundary conditions. Some remedies were suggested but often led to problems in convergence. Bates et al. (1992) used a mixed interpolation FE method to simulate an 11 km river channel/floodplain reach. They identified stability problems in simulating steep lateral and longitudinal slopes, complex topography and sharp changes in flow direction. Unacceptable conservation properties were also observed. To achieve a converged solution they had to resort to "some relaxation" of the model representation of the physical environment and concluded that this may constrain certain applications of the scheme. In their paper they presented limiting values for the above features in order to avoid numerical instability. It should be noted that these limiting values were much more restrictive than the assumptions underlying the original governing flow equations. Another drawback of mixed interpolation is that although a large number of nodes is required for the higher order interpolation, the accuracy of the results is governed by the lower degree element.

Although the idea of a wiggle-free element might be attractive, in that it would eliminate the need for the much criticized artificial diffusion, the above shows that several problems face this element, including the need for excessive artificial diffusion. In view of the difficulties related to mixed interpolation, researchers investigated other possibilities for use with the FE method. Advances had been made in the field of Computational Fluid Dynamics to solve the Euler and the Navier Stokes Equations. Christie et. al., (1976), introduced the concept of modifying the weighting functions to achieve upwinding effects (known as the Petrov Galerkin Finite Element Method). Heinrich et al., (1977), extended the method to two-dimensional flow. Wang and Adeff (1987) applied a Petrov Galerkin technique to solve the depth integrated two-dimensional Navier Stokes equations and Katopodes (1987) applied a similar technique to simulate the surge resulting from a breached dam. The upwinding matrices chosen by Wang and Adeff and by Katopodes are discussed in section 3.4. The Streamline Upwind Petrov Galerkin (SUPG) Finite Element technique was introduced by Brooks and Hughes (1982). In this technique, modified weight functions and consideration of the characteristics in quantifying the upwinding led to a robust third order accurate scheme. Hicks and Steffler (1992) implemented the SUPG scheme for the one-dimensional open channel flow equations under the name of Charac-

teristic-Dissipative-Galerkin (CDG) Finite Element Method. In their study they examined and compared different FE and FD techniques for applicability in unsteady one-dimensional open channel flow modeling using a wide range of challenging test problems. They concluded that the CDG was the best suited method, as it performed well over a wide range of steady and unsteady flow problems.

In this thesis, the CDG method is extended to solve the two-dimensional free surface flow equations. In Chapter 2, the development of the two-dimensional model is provided. In section 2.2, the governing equations are presented along with the underlying assumptions and limitations. The initial and boundary conditions are discussed in section 2.3, and the finite element formulation including the new Petrov-Galerkin upwinding scheme is introduced in section 2.4. Section 2.5 presents a new technique that has been developed to simulate domains with partially dry areas, and section 2.6 discusses different aspects of the automatic generation of an unstructured computational mesh.

Numerical tests to evaluate the model performance are carried out in Chapter 3. The first test simulates the standing waves resulting from supercritical flow through a channel constriction. The computed results compare well to measurements taken by Ippen and Dawson, 1951. The second test (section 3.3) simulates the break of a hypothetical circular dam. The effect of element shape on the obtained solution is examined by computing the results on different meshes. The test in section 3.4 simulates the partial failure of a hypothetical dam. This test, proposed by Fennema and Chaudhry in 1990, has been used by several authors to examine two-dimensional schemes. In section 3.5, the directional dependency is examined through a one-dimensional hydraulic jump and a one-dimensional dambreak problem. The tests are run first in the direction of the x-coordinate and then at 45° to the coordinates. It is found that the solutions are independent of mesh orientation. The stability range with regard to the implicitness factor θ is examined in section 3.6. Finally, the performance of the dry bed simulation routine is tested in sections 3.7 and 3.8. Section 3.7 simulates a dambreak on a dry bed. Computed water surface profiles are compared to laboratory measurements taken by Schoklitsch (1917), and show excellent agreement. In section 3.8, a hypothetical test case of flow in a trapezoidal channel with partly dry side slopes is carried out.

One of the interesting and challenging applications for a two-dimensional model is the simulation of flow in natural fish habitats. The highly varying topography usually encountered in such domains, which results in rapid flow variations, and the complex boundary conditions, require a robust and accurate scheme. In Chapter 4, the model is applied to flow in physical fish habitat. Two study cases are examined. In section 4.2, a hypothetical test case of flow over a side bar is carried out. The test shows that significant difference between the results of a one-dimensional and a two-dimensional model can exist for certain flow situations. In section 4.3, flow in a real fish habitat site is simulated. Computed results compare well with field measurements.

Chapter 5 summarizes the major conclusions. In Appendix A, guidelines for field data collection, which could further improve the results of the two-dimensional model, are presented. As one important application of the two-dimensional model is in the field of simulation of flow in aquatic habitats, Appendix B reviews and discusses the different Instream Flow Needs (IFN) assessment methods, with emphasis on the hydraulic modeling aspects in these methods.

Chapter 2

Finite Element Solution of the Two-Dimensional Shallow Water Flow Equations

2.1 Introduction

The two-dimensional shallow water flow equations describe free surface flow in the horizontal plane. Section 2.2 provides a description of the equations together with the underlying assumptions and limitations. The appropriate boundary and initial conditions are discussed in section 2.3. The Characteristic-Dissipative-Galerkin finite element formulation is presented in section 2.4. Section 2.5 proposes a new technique to simulate fully dynamic flow on a partly dry domain. In section 2.6, the generation of an unstructured computational mesh for natural streams is discussed.

2.2 Equations of Two-Dimensional Depth Averaged Free Surface Flow

The equations describing shallow two-dimensional free surface flow can be obtained through integrating the three-dimensional Reynolds equations over the depth of flow (e.g. Weiyan, 1992), or by applying the basic principles of conservation of mass and momentum to a prismatic vertical water column (Figure 2.1) bounded by the bed from the bottom and the free water surface from the top (e.g. Daubert and Graffe, 1967, Van Rijn, 1990).

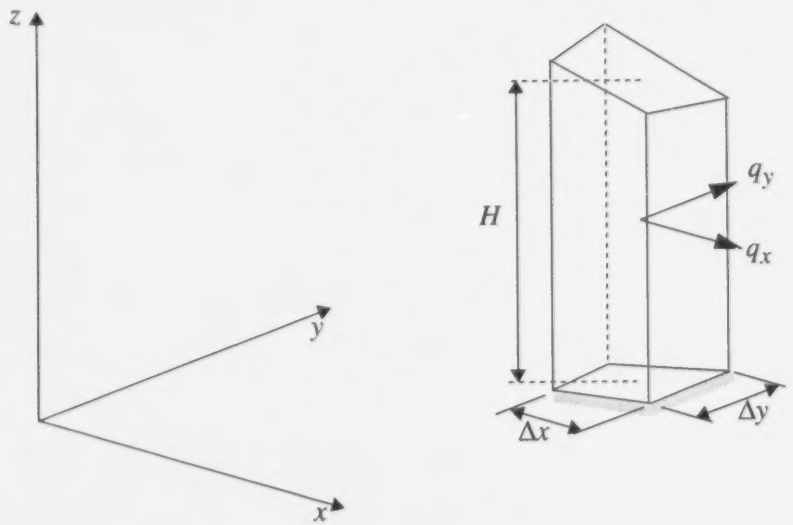

Figure 2.1 Two-Dimensional Depth Averaged Free Surface Flow: Definition Sketch

The equations are comprised of one equation of conservation of mass (continuity equation) and two equations of conservation of momentum.

Conservation of mass:

$$\frac{\partial H}{\partial t} + \frac{\partial q_x}{\partial x} + \frac{\partial q_y}{\partial y} = 0 \qquad [2.1]$$

Conservation of x-direction momentum:

$$\frac{\partial q_x}{\partial t} + \frac{\partial}{\partial x}(Uq_x) + \frac{\partial}{\partial y}(Vq_x) + \frac{g}{2}\left(\frac{\partial}{\partial x}(H^2)\right)$$

$$= gH(S_{ox} - S_{fx}) + \frac{1}{\rho}\left(\frac{\partial}{\partial x}(H\tau_{xx})\right) + \frac{1}{\rho}\left(\frac{\partial}{\partial y}(H\tau_{xy})\right) + fHV + \frac{1}{\rho}\tau_{a_x} \qquad [2.2]$$

Conservation of y-direction momentum:

$$\frac{\partial q_y}{\partial t} + \frac{\partial}{\partial x}(Uq_y) + \frac{\partial}{\partial y}(Vq_y) + \frac{g}{2}\left(\frac{\partial}{\partial y}(H^2)\right)$$

$$= gH(S_{oy} - S_{fy}) + \frac{1}{\rho}\left(\frac{\partial}{\partial x}(H\tau_{yx})\right) + \frac{1}{\rho}\left(\frac{\partial}{\partial y}(H\tau_{yy})\right) - fHU + \frac{1}{\rho}\tau_{a_y} \qquad [2.3]$$

where x and y are the cartesian coordinates in the horizontal plane and t refers to time. The dependent variables H, q_x and q_y are functions of the independent variables x, y and t, and represent point values, where H is the depth of flow (m) and q_x and q_y are the x- and y-components of discharge per unit width (m^2/sec); U and V are the depth averaged velocity components (m/sec) which are related to q_x, q_y through $U = q_x/H$ and $V = q_y/H$.

In the above equations S_{ox} and S_{oy} are bed slope components; S_{f_x} and S_{f_y} are friction slope components, given by:

$$S_{f_x} = \frac{U\sqrt{U^2 + V^2}}{C_s^2 gH} \qquad [2.4]$$

and

$$S_{f_y} = \frac{V\sqrt{U^2 + V^2}}{C_s^2 gH} \qquad [2.5]$$

C_s being the dimensionless Chezy coefficient, calculated using the formula

$$C_s = K + 5.75\log\left(\frac{H}{k_s}\right) \qquad [2.6]$$

(Van Rijn, 1990), where k_s is the height of the bed roughness (m) and K is a constant. Van Rijn (1990) suggested a value of $K = 6.2$ for hydraulically rough flow. The same value has been used by Hicks and Steffler (1990) for the one-dimensional St. Venant Equations, and is also used here for the two-dimensional model. Numerical experiments show satisfactory agreement with measurements for this value of K (e.g. section 3.7.6).

In the above equations g is the gravitational acceleration (m/sec^2), ρ is the density of water (kg/m^3), and t denotes time (sec). The depth averaged fluid shear stresses caused by turbulence are represented by τ_{xx}, τ_{xy}, τ_{yx}, and τ_{yy}. Numerous relations have been proposed to relate these stresses to different parameters of the mean flow. The reader is referred to the ASCE Task Committee on Turbulence Models (1988), or Rodi, (1984) for details on this topic. In this thesis, a simple turbulence model is used. More sophisticated models could be readily incorporated later. It should be mentioned that the turbulence stress terms generally have a stabilizing effect on the numerical solution process, and are thus sometimes exploited by modelers to stabilize unstable schemes through addition of excessive and unrealistic values. The turbulence model used relates the turbulence stresses to the mean flow velocity gradients. For example,

$$\tau_{xy} = \rho \nu_{xy} \left(\frac{\partial U}{\partial y} + \frac{\partial V}{\partial x} \right) \qquad [2.7]$$

where ν_{xy} is a depth averaged turbulent exchange coefficient (m^2/sec), the magnitude of which is a function of the structure of the turbulence. For practical purposes, isotropic turbulence is often assumed, such that $\nu_{xx} = \nu_{xy} = \nu_{yx} = \nu_{yy} = \nu$, where$\nu$ is known as the eddy viscosity. For flow in open channels, a value in the order of:

$$\nu = (0.14 \pm 0.07)\, u_s H \qquad [2.8]$$

has been proposed (e. g. Fisher et al., 1979).

u_s is the shear velocity (m/sec) given by $u_s = \sqrt{gHS_f}$ where S_f is the friction slope in the principal flow direction.

The terms fV and $-fU$ in equations [2.2] and [2.3] represent the Coriolis forces, which are body forces due to the rotation of the earth. The Coriolis factor $f = 2\bar{\omega}\sin\lambda$,

where $\bar{\omega} = 7.29*10^{-5}\text{sec}^{-1}$ is the angular velocity of the earth's rotation, and λ is the latitude. Generally, the larger the water body, the more important the Coriolis forces become (Weiyan, 1992).

The shear stresses induced by the wind on the free surface in the x- and y-directions are represented by the terms τ_{a_x} and τ_{a_y}, respectively, given by $\tau_{a_x} = C_D \rho_a U \sqrt{U^2 + V^2}$, and $\tau_{a_y} = C_D \rho_a V \sqrt{U^2 + V^2}$, where C_D is a dimensionless drag coefficient (Weiyan, 1992), and ρ_a is the air density.

Equations [2.1] to [2.3] are a set of nonlinear, predominantly hyperbolic equations in the three independent variables H, q_x and q_y. One of the assumptions underlying the derivation of the above equations is that flow velocity does not vary in the vertical direction and that the vertical accelerations are negligible and therefore a hydrostatic pressure distribution exists. This implies that the depth averaged two-dimensional model can resolve flow details which are generally larger than the depth of flow. For example, considering the prediction of wave celerity, for a wavelength to depth ratio of 7, an error of 10% would be expected. This error would reduce to about 2% for a wavelength to depth ratio of 20 (Steffler and Jin, 1993). Clearly, flow phenomena of a three-dimensional nature such as the details of flow around a single rock can not be resolved and would require a three-dimensional model.

In the following derivation of the finite element formulation, the assumption is made that wind stresses and Coriolis forces are negligible. This assumption is generally acceptable for simulating flows in smaller domains such as streams and rivers, as these forces become important only when simulating larger water bodies such as big lakes and estuaries (Bertin, 1987). It should be mentioned that their inclusion does not add to the difficulty in solving the equations.

It is also assumed that no seepage inflows/outflows or rainfall occur (or are negligible) and that no scour or deposition takes place. Further, it is assumed that frictional resistance formulae for steady one-dimensional flow are applicable to unsteady two-dimensional flow. The bed slopes in the flow direction are assumed to be small, such that

$\sin\Theta \cong \tan\Theta$ (slope < 10%), where Θ is the angle the bed makes with the horizontal plane in the principal flow direction. Further, H, q_x and q_y should be continuous differentiable functions.

It should be noted that the non-symmetric conservative form of the equations is presented above. Hughes et al., (1986) used symmetric forms of the Euler and the Navier Stokes Equations to solve convection dominated flow problems using the SUPG method. They stated that stability would be guaranteed in finite element methods based upon this form of the equations. Hicks and Steffler, (1990), compared the symmetric form of the one-dimensional St. Venant equations to the non-symmetric (conservation) form. They reported inability of the symmetric form to conserve mass and momentum, especially in the presence of flow discontinuities. An error of about ten percent was observed in the momentum conservation for some test problems, whereas no error was observed when using the conservation form. Therefore, the non-symmetric conservation form of the equations is used in this work.

Equations [2.1] to [2.3] can be written in the conservative form:

$$\frac{\partial \phi}{\partial t} + \frac{\partial \mathbf{F_x}}{\partial x} + \frac{\partial \mathbf{F_y}}{\partial y} - \frac{\partial}{\partial x}\left(\nu H \frac{\partial}{\partial x}(\mathbf{C_{xx}} + \mathbf{C_{xy}})\right)$$

$$- \frac{\partial}{\partial y}\left(\nu H \frac{\partial}{\partial x}(\mathbf{C_{yx}} + \mathbf{C_{yy}})\right) + \mathbf{G} = 0 \qquad [2.9]$$

where:

$$\phi = (H \; q_x \; q_y)^T \qquad [2.10]$$

$$\mathbf{F_x} = \begin{pmatrix} q_x \\ Uq_x + g\frac{H^2}{2} \\ Uq_y \end{pmatrix} = \mathbf{M_x}\phi = \begin{bmatrix} 0 & 1 & 0 \\ g\frac{H}{2} & U & 0 \\ 0 & 0 & U \end{bmatrix}\phi \qquad [2.11]$$

$$\mathbf{F_y} = \begin{pmatrix} q_y \\ Vq_x \\ Vq_y + g\frac{H^2}{2} \end{pmatrix} = \mathbf{M_y}\phi = \begin{bmatrix} 0 & 0 & 1 \\ 0 & V & 0 \\ g\frac{H}{2} & 0 & V \end{bmatrix}\phi \qquad [2.12]$$

$$\mathbf{C_{xx}} = (0\ 2U\ V)^{\mathrm{T}} \qquad [2.13]$$

$$\mathbf{C_{xy}} = (0\ 0\ U)^{\mathrm{T}} \qquad [2.14]$$

$$\mathbf{C_{yx}} = (0\ V\ 0)^{\mathrm{T}} \qquad [2.15]$$

$$\mathbf{C_{yy}} = (0\ U\ 2V)^{\mathrm{T}} \qquad [2.16]$$

$$\mathbf{G} = \begin{pmatrix} 0 \\ q_x\sqrt{q_x^2 + q_y^2} - S_{o_x}gH \\ q_y\sqrt{q_x^2 + q_y^2} - S_{o_y}gH \end{pmatrix} \qquad [2.17]$$

A non-conservative form of equation [2.9] can be written as follows:

$$\frac{\partial\phi}{\partial t} + \mathbf{A_x}\frac{\partial\phi}{\partial x} + \mathbf{A_y}\frac{\partial\phi}{\partial y} - \frac{\partial}{\partial x}(\nu\mathbf{D_{xx}}\frac{\partial\phi}{\partial x} - \nu\mathbf{D_{xy}}\frac{\partial\phi}{\partial y})$$

$$-\frac{\partial}{\partial y}(\nu\mathbf{D_{yx}}\frac{\partial\phi}{\partial x} - \nu\mathbf{D_{yy}}\frac{\partial\phi}{\partial y}) + \mathbf{N}\phi = 0 \qquad [2.18]$$

$\mathbf{A_x}$ and $\mathbf{A_y}$ are known as the convection matrices, given by:

$$\mathbf{A_x} = \frac{\partial\mathbf{F_x}}{\partial\phi} = \begin{bmatrix} 0 & 1 & 0 \\ c^2 - U^2 & 2U & 0 \\ -UV & V & U \end{bmatrix} \qquad [2.19]$$

$$\mathbf{A_y} = \frac{\partial\mathbf{F_y}}{\partial\phi} = \begin{bmatrix} 0 & 0 & 1 \\ -UV & V & U \\ c^2 - V^2 & 0 & 2V \end{bmatrix} \qquad [2.20]$$

where c is the wave celerity given by $c = \sqrt{gH}$. The turbulent diffusion matrices $\mathbf{D_{xx}}$, $\mathbf{D_{xy}}$, $\mathbf{D_{yx}}$ and $\mathbf{D_{yy}}$ are given by:

$$\mathbf{D}_{xx} = \frac{\partial \mathbf{C}_{xx}}{\partial \phi} = \begin{bmatrix} 0 & 0 & 0 \\ -2U & 2 & 0 \\ -V & 0 & 1 \end{bmatrix} \quad [2.21]$$

$$\mathbf{D}_{xy} = \frac{\partial \mathbf{C}_{xy}}{\partial \phi} = \begin{bmatrix} 0 & 0 & 0 \\ 0 & 0 & 0 \\ -U & 1 & 0 \end{bmatrix} \quad [2.22]$$

$$\mathbf{D}_{yx} = \frac{\partial \mathbf{C}_{yx}}{\partial \phi} = \begin{bmatrix} 0 & 0 & 0 \\ -V & 0 & 1 \\ 0 & 0 & 0 \end{bmatrix} \quad [2.23]$$

$$\mathbf{D}_{yy} = \frac{\partial \mathbf{C}_{yy}}{\partial \phi} = \begin{bmatrix} 0 & 0 & 0 \\ -U & 1 & 0 \\ -2V & 0 & 2 \end{bmatrix} \quad [2.24]$$

$\mathbf{N}$ is the force matrix, such that $\mathbf{N}\phi = \mathbf{G}$, and is given by:

$$\mathbf{N} = \begin{bmatrix} 0 & 0 & 0 \\ -gS_{o_x} & \sqrt{q_x^2 + q_y^2}/(C_s^2 H^2) & 0 \\ -gS_{o_y} & 0 & \sqrt{q_x^2 + q_y^2}/(C_s^2 H^2) \end{bmatrix} \quad [2.25]$$

2.3 Boundary and Initial Conditions

Proper boundary and initial conditions are required to achieve a well posed problem. For a hyperbolic system of equations with real eigenvalues, as many initial conditions as unknowns are required (Hirsch, 1987). In most practical hydraulic problems, the exact values assigned to the variables as initial conditions are not of great importance, since their effect would be weakened by information continuously supplied from the boundaries at times $t > 0$. In addition, friction and turbulent diffusion terms soon attenuate errors in the initial data (Katopodes, 1977). Of course, this does not mean that completely erroneous values could be used, but generally any set of physically reasonable initial conditions should be adequate.

The interaction between the domain under consideration Ω and the surroundings is reflected in the external boundary conditions of the system, acting on the domain bound-

ary Γ. Usually different types of boundary conditions are specified over different segments of Γ. For the shallow water equations, these conditions can be classified as either no-flow boundaries such as rigid walls, or open boundaries such as an interface between Ω and an adjacent water body (Weiyan, 1992). The latter can be further divided into specified boundary conditions, which represent the influence of the surroundings on Ω, and non-reflective boundary conditions, which allow a wave to travel freely across the boundary. A combination of these latter two might sometimes be desirable. In this work, only no-flow and specified boundary conditions are implemented. The non-reflective type has not been attempted here, and the reader is referred to Hedstrom, (1979) or Verboom et al., (1982), for details on techniques adopted for these types of problems.

The type of boundary determines the number of boundary conditions that have to be specified on that boundary. A consideration of the characteristics of the system helps identifying that number (e.g. Daubert and Graffe, (1967), Hirsch, (1988) or Weiyan (1992)).

For the domain Ω with boundary Γ depicted in Figure 2.2, $\mathbf{n}$ is the unit inward normal to Γ at point P(x,y) $\in \Gamma$. The boundary condition is specified through the depth H and the normal and tangential discharge per unit width q_n and q_t, respectively. q_x and q_y are then related to q_n and q_t through:

$$q_x = -q_n \sin\alpha - q_t \cos\alpha \text{ , and } q_y = q_n \cos\alpha - q_t \sin\alpha \qquad [2.26]$$

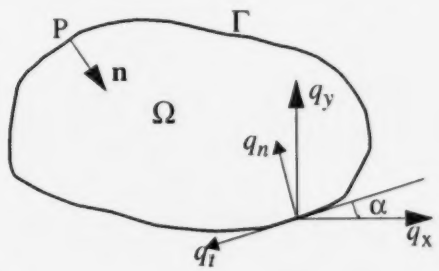

Figure 2.2 Boundary Condition Specification

The velocity vector at P is $\mathbf{W} = (U\ V)$. If:

$$\mathbf{W}\cdot\mathbf{n}\begin{cases} >0 \Rightarrow \text{inflow boundary} \\ <0 \Rightarrow \text{outflow boundary} \\ =0 \Rightarrow \text{no-flow boundary} \end{cases}$$

Further, defining the local Froude number in the two-dimensional domain as:

$$F_r = \frac{|\mathbf{W}|}{\sqrt{gH}} = \frac{\sqrt{U^2+V^2}}{\sqrt{gH}} \qquad [2.27]$$

the flow being subcritical for $F_r < 1$, supercritical for $F_r > 1$ and critical for $F_r = 1$, then the following possibilities exist:

2.3.1 No-Flow Boundary:

In this case, no flux crosses the boundary. Since for shallow water flow problems the resistance is mainly due to roughness distributed over the interior of the domain rather than from the boundary, a zero stress, slip boundary condition is assumed. Thus, a tangential velocity is allowed and computed at the boundary. A no-slip condition could also be specified. However, this condition could negatively affect the solution in the vicinity of the boundary, unless small enough elements are used to resolve the boundary layer.

2.3.2 Inflow Boundary:

1. *Subcritical*:

In this case, two characteristic curves enter the domain at the boundary, and thus two boundary conditions have to be specified. One possibility is to specify the stage and a zero tangential velocity at this boundary. Weiyan, (1992), states that such a specification could lead to virtual vortices in the vicinity of the boundary and disturbances added to the water surface. Another option would be to specify the two inflow depth averaged discharges q_n and q_t. Usually, the boundaries are selected such that q_t is zero. If the total discharge crossing the boundary is known, then the distribution of q_n over the boundary is based on the conveyance at each node, based on a uniform flow assumption. For some complex inflow boundaries, for example if the bed slope is very steep in part of the boundary and flat in another, instabilities may occur. In this case, an artificial entry reach can be used (about

one to two stream widths long), over which the inflow section changes gradually from rectangular to the natural shape.

When there is uncertainty about the distribution of discharge over the inflow boundary for simulating unmeasured flows, a cross-section further upstream could be added to the reach to allow the flow to adjust itself over a development length. Equating inertial and friction effects we get:

$$U\frac{\partial U}{\partial x} \approx gS_f \approx \frac{U^2}{C_s^2 H} \qquad [2.28]$$

or

$$\frac{U^2/2}{L_{US}} \sim \frac{U^2}{C_s^2 H} \qquad [2.29]$$

where L_{US} is the required upstream development length. The above gives

$$\frac{L_{US}}{H} \sim \frac{C_s^2}{2} \qquad [2.30]$$

Thus, for a C_s in the order of 10, L_{US} would be in the order of 50 stream depths.

2. *Supercritical*:

For this type of boundary, all three characteristic curves enter the domain with increasing time, and thus the three variables H, q_n and q_t are specified.

2.3.3 Outflow Boundary:

1. *Subcritical*:

Only one characteristic would be entering the domain for such a condition, and thus one boundary condition is specified. Usually, q_n and q_t are unknown, while a water level hydrograph is specified. If the outflow boundary is at a control section or a man made hydraulic structure, then a stage-discharge relation could be entered. If the downstream section can be located in a fairly straight long uniform reach of the stream, locally uniform flow could be assumed to estimate the downstream water elevation.

If uncertainty about the downstream boundary condition exists, it might be advisable to add some additional cross sections at the downstream end of the reach. From a consideration of the backwater effects introduced by an error in estimating the depth at the boundary, a conservative estimate of the additional reach length required (L_{DS}) would be

$$\frac{L_{DS}}{H} \sim \frac{1}{S_o} \qquad [2.31]$$

2. *Supercritical*:

In this case, all three characteristics are leaving the domain with increasing time, and thus no boundary conditions are specified.

2.4 Finite Element Formulation

The Streamline Upwind Petrov Galerkin (SUPG) Finite Element method is applied here to the system of equations [2.9]. The weight functions $\hat{\mathbf{B}}_i$ for the two-dimensional case have the form (Brooks and Hughes, 1982):

$$\hat{\mathbf{B}}_i = \mathbf{B}_i + \omega \Delta x \mathbf{W}_x \frac{\partial \mathbf{B}_i}{\partial x} + \omega \Delta y \mathbf{W}_y \frac{\partial \mathbf{B}_i}{\partial y} \qquad [2.32]$$

where $\mathbf{B}_i$ is the matrix of shape functions given by:

$$\mathbf{B}_i = \begin{bmatrix} b_i & 0 & 0 \\ 0 & b_i & 0 \\ 0 & 0 & b_i \end{bmatrix} \qquad [2.33]$$

where $i = 1$, NS; NS being the total number of shape functions b_i. In this thesis linear triangular and quadrilateral isoparametric elements are used.

The shape functions are functions of the space dimensions only, such that at any point $(x, y) \in \Omega$, $\phi \approx \sum_{j=1}^{NS} \mathbf{B}_j \Phi_j$, where Φ_j is the vector of nodal values of the unknowns and Ω is the solution domain. Figure 2.3 shows typical shape functions for node "A" of the linear triangular element ABC and for node "F" of the linear quadrilateral element

DEFG. The value of the shape function for a given node is described by a surface in the *x*-

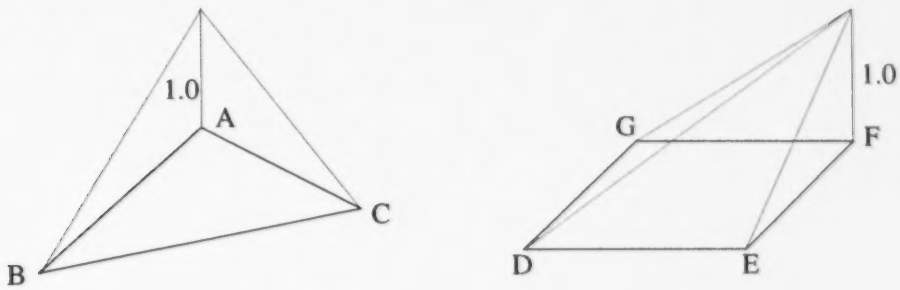

Figure 2.3 Shape Functions for Linear Elements

y-*z* space, *x* and *y* being the coordinates in the horizontal plane and the *z*-coordinate representing the value of the shape function at any point $P(x,y) \in \Omega$. As can be seen in Figure 2.3, the shape function has a value of 1.0 at that node and a value of 0.0 at all other nodes.

It is more convenient from a computational point of view to express the shape functions mathematically in terms of a local coordinate system *r*-*s* (Figure 2.4). For the trian-

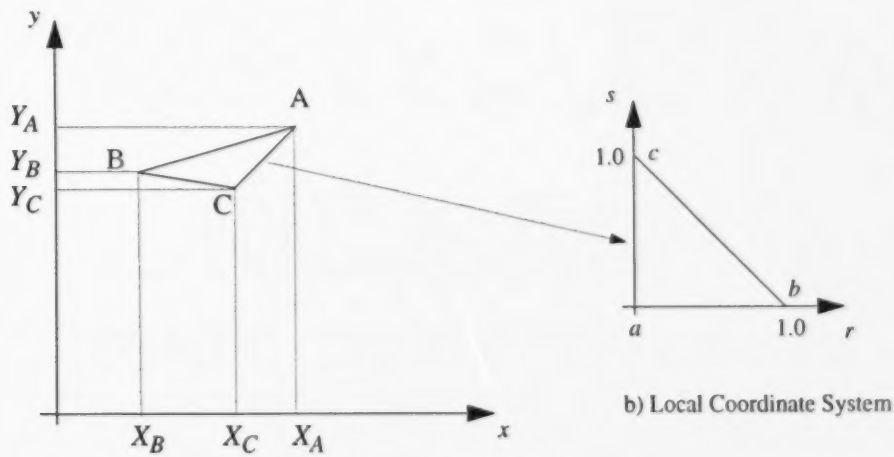

a) Global Coordinate System

b) Local Coordinate System

Figure 2.4 Elements in Local and Global Coordinate Systems

gular element depicted in Figure 2.4 b, the shape functions in terms of local coordinates for node "a" would be given by:

$$b(r,s) = \begin{bmatrix} 1-r-s \\ r \\ s \end{bmatrix} \qquad [2.34]$$

The differentials with respect to the local coordinates would then be:

$$\frac{\partial b}{\partial r} = \begin{bmatrix} -1 \\ 1 \\ 0 \end{bmatrix}, \text{and } \frac{\partial b}{\partial s} = \begin{bmatrix} -1 \\ 0 \\ 1 \end{bmatrix} \qquad [2.35]$$

In order to evaluate the weak statement, an expression in terms of global coordinates x and y is required, which is obtained through a transformation as follows:

Using isoparametric mapping, x and y can be expressed as:

$$x = \sum_{j=1}^{NS} b_j X_j, \quad y = \sum^{NS} b_j Y_j \qquad [2.36]$$

where X_j and Y_j are the nodal coordinates in the global coordinate system (Figure 2.4).

Using the chain rule for differentiation, the derivatives with respect to local and global coordinates can be related through:

$$\begin{bmatrix} \frac{\partial b_j}{\partial r} \\ \frac{\partial b_j}{\partial s} \end{bmatrix} = \begin{bmatrix} \frac{\partial x}{\partial r} & \frac{\partial y}{\partial r} \\ \frac{\partial x}{\partial s} & \frac{\partial y}{\partial s} \end{bmatrix} \begin{bmatrix} \frac{\partial b_j}{\partial x} \\ \frac{\partial b_j}{\partial y} \end{bmatrix} \qquad [2.37]$$

Making use of equation [2.36], the terms of the Jacobian matrix in equation [2.37] can be written as:

$$\hat{\mathbf{J}} = \begin{bmatrix} \frac{\partial x}{\partial r} & \frac{\partial y}{\partial r} \\ \frac{\partial x}{\partial s} & \frac{\partial y}{\partial s} \end{bmatrix} = \begin{bmatrix} \sum_{j=1}^{NS} \frac{\partial b_j}{\partial r} X_j & \sum_{j=1}^{NS} \frac{\partial b_j}{\partial r} Y_j \\ \sum_{j=1}^{NS} \frac{\partial b_j}{\partial r} X_j & \sum_{j=1}^{NS} \frac{\partial b_j}{\partial r} Y_j \end{bmatrix} \qquad [2.38]$$

Finally,

$$\begin{bmatrix} \frac{\partial b_j}{\partial x} \\ \frac{\partial b_j}{\partial y} \end{bmatrix} = \hat{\mathbf{J}}^{-1} \begin{bmatrix} \frac{\partial b_j}{\partial r} \\ \frac{\partial b_j}{\partial s} \end{bmatrix} \qquad [2.39]$$

In the Bubnov Galerkin FE method, weight functions equal to the basis functions are used. As this method results in a scheme equivalent to a centered FD scheme, it is not suitable for hyperbolic problems. The Petrov Galerkin Finite Element method uses modified weight functions as shown in equation [2.32]. It can be shown that the use of such weight functions introduces, through error cancelation between time and space derivatives, a third order accurate scheme (Hughes, 1982). This means that the leading error term would contain a fourth derivative, introducing highly selective artificial diffusion, which filters out undesirable short wavelengths and dies off quickly for longer wave lengths. Hicks and Steffler, (1992), through Fourier Analysis on the CDG application to the linearized St. Venant equations demonstrated this behavior for the one-dimensional case. Leonard, (1979), showed through numerical tests using the finite difference method in one and two dimensions the high accuracy that could be obtained with a third order scheme.

$\mathbf{W_x}$ and $\mathbf{W_y}$ are the upwinding matrices. Wang and Adeff, (1987), used the x-direction velocity U for the diagonal values of $\mathbf{W_x}$ and the y-direction velocity V for the diagonal values $\mathbf{W}_y$. The off-diagonal terms were set to zero. Katopodes, (1987), applied the Dissipative Galerkin (DG) method to the two-dimensional shallow water flow equations by setting $\mathbf{W_x} = \mathbf{A_x}/|U+c|$ and $\mathbf{W_y} = \mathbf{A_y}/|V+c|$. Hicks and Steffler, (1992), compared the Dissipative Galerkin (DG) formulation for the one dimensional St. Venant equations ($\mathbf{W} = \mathbf{A}/|U+c|$), to the CDG formulation in which $\mathbf{W} = \mathbf{A}/|\mathbf{A}|$, $\mathbf{A}$ being the convection matrix for the one-dimensional case. They showed through decomposition of $\mathbf{A}$ that in the DG scheme both wave components are scaled to the positive characteristic and thus the upwinding applied to the regressive wave might be too small. On the other hand, in the CDG method, both characteristics were scaled to their absolute values and thus proper upwinding could be assigned for each component. Hughes and Mallet (1986 b) presented the SUPG method for multidimensional advective diffusive systems. They

showed that by scaling the convection matrices by $\left(\sum_{i=1}^{d} \mathbf{A}_i^2\right)^{-1/2}$, d being the number of space dimensions, the resulting upwinding matrices possessed the properties of reducing correctly to the optimal one-dimensional system case. They also stated that other schemes such as Lax-Wendroff and Taylor-Galerkin methods are inferior for systems of equations because they cannot appropriately treat the independent modal components.

Thus for the two-dimensional system of equations under consideration, the two upwinding matrices are:

$$\mathbf{W}_x = \frac{\mathbf{A}_x}{\sqrt{\mathbf{A}_x^2 + \mathbf{A}_y^2}} \qquad [2.40]$$

$$\mathbf{W}_y = \frac{\mathbf{A}_y}{\sqrt{\mathbf{A}_x^2 + \mathbf{A}_y^2}} \qquad [2.41]$$

The inverse of the square root of the matrix is calculated directly using the Cayley-Hamilton theorem (Hoger and Carlson, 1984, see also Appendix C), thus avoiding the solution of the eigenproblem (Hughes and Mallet, 1986 b). The upwinding matrices are then obtained by premultiplying the convection matrices with the obtained matrix. Upwinding matrices of the form

$$\mathbf{W}_x = \mathbf{A}_x / |\mathbf{A}_x| \qquad [2.42]$$

$$\mathbf{W}_y = \mathbf{A}_y / |\mathbf{A}_y| \qquad [2.43]$$

are also examined in section 3.7.4 and their performance is tested and compared to the matrices of [2.40] and [2.41]. For the parameters Δx and Δy in equation [2.32], Hughes and Mallet, (1986 a), suggested for quadrilateral elements to use the maximum of the length of the two diagonals + $\sqrt{2}$. Hicks and Steffler, (1992), used a value of half the element length for the one-dimensional St. Venant equations. Katopodes, (1987), used parameters equal to $\Delta x = \sqrt{\left(\frac{\partial x}{\partial r}\right)^2 + \left(\frac{\partial x}{\partial s}\right)^2}$ and $\Delta y = \sqrt{\left(\frac{\partial y}{\partial r}\right)^2 + \left(\frac{\partial y}{\partial s}\right)^2}$, where r and s are the local coordinates. As the element shape for the problems under consideration is not too

distorted, a simple expression $\Delta x = \Delta y = \frac{\sqrt{A}}{2}$ is used, A being the element area. For more distorted elements, a direction dependent expression such as the one used by Katopodes might be advisable. The parameter ω has also been investigated by several authors. Hicks and Steffler, (1992 b), reviewed the literature in that regard. They also presented a Fourier Analysis, showing the effect of ω and also other parameters such as the Courant Number (C_r), and the implicitness factor θ on the scheme behavior for solving the one-dimensional St. Venant Equations. Because the Fourier Analysis is performed for a linearized form of the equations, and because the equations under consideration are for two-dimensional flow, the results serve only as indicators of model behavior. An extension to two dimensions would be useful, has however not been attempted in this work. A set of carefully selected numerical experiments can give good insight into the stability and convergence aspects of the scheme (Lee and Froehlich, 1986). For the numerical experiments presented in section 3.7, values of ω ranging from 0.25 to 1.0 were tested. It was found that results are generally not very sensitive to the exact values of ω, but best results were obtained for values of ω of 0.25 for transient problems and of 0.5 for steady problems.

Applying the Galerkin FE approach with weight functions given by [2.32] to the system of equations [2.9], making use of equations [2.10] to [2.25], yields:

$$\int_{\Omega} \hat{\mathbf{B}}_i \left(\frac{\partial \phi}{\partial t} + \frac{\partial}{\partial x}(\mathbf{M}_x \phi) + \frac{\partial}{\partial y}(\mathbf{M}_y \phi) - \frac{\partial}{\partial x}\left(\nu \mathbf{D}_{xx} \frac{\partial \phi}{\partial x} - \nu \mathbf{D}_{xy} \frac{\partial \phi}{\partial y}\right) \right.$$

$$\left. - \frac{\partial}{\partial y}\left(\nu \mathbf{D}_{yx} \frac{\partial \phi}{\partial x} - \nu \mathbf{D}_{yy} \frac{\partial \phi}{\partial y}\right) + \mathbf{N}\phi \right) d\Omega = 0 \qquad [2.44]$$

Substituting for test functions and basis functions and multiplying through, we obtain:

$$\int_{\Omega} (\hat{\mathbf{B}}_i \mathbf{B}_j \frac{\partial \Phi_j}{\partial t} + \mathbf{B}_i (\underline{\frac{\partial}{\partial x} (\mathbf{M}_x \mathbf{B}_j \Phi_j)} + \underline{\frac{\partial}{\partial y} (\mathbf{M}_y \mathbf{B}_j \Phi_j)}$$

$$\underline{-\frac{\partial}{\partial x} \nu (\mathbf{D}_{xx} \frac{\partial \mathbf{B}_j}{\partial x} \Phi_j + \mathbf{D}_{xy} \frac{\partial \mathbf{B}_j}{\partial y} \Phi_j)} \underline{-\frac{\partial}{\partial y} \nu (\mathbf{D}_{yx} \frac{\partial \mathbf{B}_j}{\partial x} \Phi_j + \mathbf{D}_{yy} \frac{\partial \mathbf{B}_j}{\partial y} \Phi_j)} + \mathbf{N}\mathbf{B}_j \Phi_j)$$

$$+ \omega \Delta x (\mathbf{W}_x \frac{\partial \mathbf{B}_i}{\partial x} + \mathbf{W}_y \frac{\partial \mathbf{B}_i}{\partial y}) (\mathbf{A}_x \frac{\partial \mathbf{B}_j}{\partial x} \Phi_j + \mathbf{A}_y \frac{\partial \mathbf{B}_j}{\partial y} \Phi_j - \frac{\partial}{\partial x} \nu (\mathbf{D}_{xx} \frac{\partial \mathbf{B}_j}{\partial x} \Phi_j - \mathbf{D}_{xy} \frac{\partial \mathbf{B}_j}{\partial y} \Phi_j)$$

$$- \frac{\partial}{\partial y} \nu (\mathbf{D}_{yx} \frac{\partial \mathbf{B}_j}{\partial x} \Phi_j + \mathbf{D}_{yy} \frac{\partial \mathbf{B}_j}{\partial y} \Phi_j) + \mathbf{N}\mathbf{B}_j \Phi_j)) d\Omega = 0 \qquad [2.45]$$

Integrating the underlined terms (Bubnov Galerkin components of convection and diffusion) by parts yields:

$$\int_{\Omega} (\hat{\mathbf{B}}_i \mathbf{B}_j \frac{\partial \Phi_j}{\partial t} - \frac{\partial \mathbf{B}_i}{\partial x} \mathbf{M}_x \mathbf{B}_j \Phi_j - \frac{\partial \mathbf{B}_i}{\partial y} \mathbf{M}_y \mathbf{B}_j \Phi_j$$

$$+ \frac{\partial \mathbf{B}_i}{\partial x} \nu (\mathbf{D}_{xx} \frac{\partial \mathbf{B}_j}{\partial x} \Phi_j + \mathbf{D}_{xy} \frac{\partial \mathbf{B}_j}{\partial y} \Phi_j)$$

$$+ \frac{\partial \mathbf{B}_i}{\partial y} \nu (\mathbf{D}_{yx} \frac{\partial \mathbf{B}_j}{\partial x} \Phi_j + \mathbf{D}_{yy} \frac{\partial \mathbf{B}_j}{\partial y} \Phi_j) + \mathbf{B}_i \mathbf{N}\mathbf{B}_j \Phi_j$$

$$+ \omega (\Delta x \mathbf{W}_x \frac{\partial \mathbf{B}_i}{\partial x} + \Delta y \mathbf{W}_y \frac{\partial \mathbf{B}_i}{\partial y}) (\mathbf{A}_x \frac{\partial \mathbf{B}_j}{\partial x} \Phi_j + \mathbf{A}_y \frac{\partial \mathbf{B}_j}{\partial y} \Phi_j$$

$$- \frac{\partial}{\partial x} \nu (\mathbf{D}_{xx} \frac{\partial \mathbf{B}_j}{\partial x} \Phi_j - \mathbf{D}_{xy} \frac{\partial \mathbf{B}_j}{\partial y} \Phi_j) - \frac{\partial}{\partial y} \nu (\mathbf{D}_{yx} \frac{\partial \mathbf{B}_j}{\partial x} \Phi_j + \mathbf{D}_{yy} \frac{\partial \mathbf{B}_j}{\partial y} \Phi_j)$$

$$+ \mathbf{N}\mathbf{B}_j \Phi_j)) d\Omega + \int_{\Gamma} (\mathbf{B}_i \mathbf{M}_x \mathbf{B}_j \Phi_j) d\Gamma$$

$$+ \int_{\Gamma} (\mathbf{B}_i \nu (\mathbf{D}_{xx} \frac{\partial \mathbf{B}_j}{\partial x} \Phi_j + \mathbf{D}_{xy} \frac{\partial \mathbf{B}_j}{\partial y} \Phi_j + \mathbf{D}_{yx} \frac{\partial \mathbf{B}_j}{\partial x} \Phi_j + \mathbf{D}_{yy} \frac{\partial \mathbf{B}_j}{\partial y} \Phi_j)) d\Gamma = 0 \qquad [2.46]$$

In the above, the Petrov-Galerkin components are not integrated by parts, as this would necessitate the use of higher order elements. The last two integrals in [2.46] are integrals on the domain boundary Γ, which result from the integration by parts of the Bub-

nov convection and diffusion components, respectively. It can be seen that these terms are natural convective and diffusive fluxes across the boundary. This provides an accurate and easy means for specifying natural boundary conditions. For example, to specify a no-flow boundary condition, the two terms are set equal to zero. A zero stress (slip) boundary is assumed, thus eliminating the contribution from the diffusive terms on the boundary integral.

It should be mentioned here that spurious oscillations perpendicular to no-flow boundaries in the vicinity of shocks are observed, unless the upwinding is set to zero perpendicular to the domain boundaries. The reason for this could be that the upwinding terms are not integrated by parts, and thus do not contribute to the boundary integrals.

Since the Φ_j are functions of time only, the partial time derivative in [2.46] can be replaced by an ordinary derivative. The equation can be rearranged to be written in the form:

$$\mathbf{S}_{ij}\frac{d}{dt}\Phi_j + (\mathbf{K}_{ij} + \overline{\mathbf{BK}}_{ij}\overline{\mathbf{CBC}})\,\Phi_j + \overline{\mathbf{BK}}_{ij}\overline{\mathbf{BC}}\,\hat{\Phi}_j = 0 \qquad [2.47]$$

where $\hat{\Phi}_j$ is the vector of known boundary values $\hat{H}$, $\hat{q}_x$ and $\hat{q}_y$. The matrix $\overline{\mathbf{BK}}_{ij}$ results from the boundary integral. The matrix $\overline{\mathbf{BC}}$ is a diagonal matrix with a one on the diagonal corresponding to a known and a zero to an unknown value of the variables on the boundary. The matrix $\overline{\mathbf{CBC}} = \mathbf{I} - \overline{\mathbf{BC}}$, $\mathbf{I}$ being the identity matrix. For example for the case of a subcritical inflow boundary (section 2.3.2), where q_x and q_y are known and H is unknown, the matrix $\overline{\mathbf{BC}}$ would be equal to:

$$\overline{\mathbf{BC}} = \begin{bmatrix} 0 & 0 & 0 \\ 0 & 1 & 0 \\ 0 & 0 & 1 \end{bmatrix} \qquad [2.48]$$

while $\overline{\mathbf{CBC}}$ would equal:

$$\overline{\mathbf{CBC}} = \begin{bmatrix} 1 & 0 & 0 \\ 0 & 0 & 0 \\ 0 & 0 & 0 \end{bmatrix} \qquad [2.49]$$

The above implementation of boundary conditions facilitates the use of the boundary integral flux terms directly as shown below, resulting in excellent conservation properties.

Further,

$$\mathbf{S}_{ij} = \int_{\Omega} \hat{\mathbf{B}}_i \mathbf{B}_j d\Omega \qquad [2.50]$$

$$\begin{aligned}
\mathbf{K}_{ij} = \int_{\Omega} \Big(& -\frac{\partial \mathbf{B}_i}{\partial x} \mathbf{M}_x \mathbf{B}_j - \frac{\partial \mathbf{B}_i}{\partial y} \mathbf{M}_y \mathbf{B}_j \\
& + \frac{\partial \mathbf{B}_i}{\partial x} \nu \left(\mathbf{D}_{xx} \frac{\partial \mathbf{B}_j}{\partial x} + \mathbf{D}_{xy} \frac{\partial \mathbf{B}_j}{\partial y} \right) \\
& + \frac{\partial \mathbf{B}_i}{\partial y} \nu \left(\mathbf{D}_{yx} \frac{\partial \mathbf{B}_j}{\partial x} + \mathbf{D}_{yy} \frac{\partial \mathbf{B}_j}{\partial y} \right) + \mathbf{B}_i \mathbf{N} \mathbf{B}_j \\
& + \omega \left(\Delta x \mathbf{W}_x \frac{\partial \mathbf{B}_i}{\partial x} + \Delta y \mathbf{W}_y \frac{\partial \mathbf{B}_i}{\partial y} \right) \left(\mathbf{A}_x \frac{\partial \mathbf{B}_j}{\partial x} + \mathbf{A}_y \frac{\partial \mathbf{B}_j}{\partial y} \right. \\
& - \frac{\partial}{\partial x} \nu \left(\mathbf{D}_{xx} \frac{\partial \mathbf{B}_j}{\partial x} - \mathbf{D}_{xy} \frac{\partial \mathbf{B}_j}{\partial y} \right) - \frac{\partial}{\partial y} \nu \left(\mathbf{D}_{yx} \frac{\partial \mathbf{B}_j}{\partial x} + \mathbf{D}_{yy} \frac{\partial \mathbf{B}_j}{\partial y} \right) \\
& \left. + \mathbf{N} \mathbf{B}_j \right) \Big) d\Omega
\end{aligned} \qquad [2.51]$$

$$\begin{aligned}
\overline{\mathbf{BK}}_{ij} = \int_{\Gamma} \Big(& \mathbf{B}_i \mathbf{M}_x \mathbf{B}_j \\
& + \mathbf{B}_i \nu \left(\mathbf{D}_{xx} \frac{\partial \mathbf{B}_j}{\partial x} + \mathbf{D}_{xy} \frac{\partial \mathbf{B}_j}{\partial y} + \mathbf{D}_{yx} \frac{\partial \mathbf{B}_j}{\partial x} + \mathbf{D}_{yy} \frac{\partial \mathbf{B}_j}{\partial y} \right) \Big) d\Gamma
\end{aligned} \qquad [2.52]$$

Gaussian numerical integration is used to evaluate the above integrals. The use of one integration point for the linear triangular elements was found to lead to stability problems due to poor solution matrices. This problem was overcome by using three integration points. For the linear quadrilateral elements, four integration points are used. Coordinates and weights as well as corresponding accuracy for the different Gauss points can be found in Burnett, (1987).

Applying a finite difference discretization to the time derivative by means of the implicitness operator $\theta \in [0, 1]$, with $\theta = 0$ for explicit and $\theta = 1$ for fully implicit solution, yields:

$$\mathbf{S}_{ij}\frac{(\Phi_j^{n+1} - \Phi_j^n)}{\Delta t} + \theta\left[(\mathbf{K}_{ij} + \overline{\mathbf{BK}}_{ij}\overline{\mathbf{CBC}})\,\Phi_j + \overline{\mathbf{BK}}_{ij}\overline{\mathbf{BC}}\,\hat{\Phi}_j\right]^{n+1}$$

$$+ (1-\theta)\left[(\mathbf{K}_{ij} + \overline{\mathbf{BK}}_{ij}\overline{\mathbf{CBC}})\,\Phi_j + \overline{\mathbf{BK}}_{ij}\overline{\mathbf{BC}}\,\hat{\Phi}_j\right]^{n} = 0 \qquad [2.53]$$

where n denotes the n^{th} time step. Rewriting:

$$\{\mathbf{S}_{ij} + \theta\Delta t\,[\mathbf{K}_{ij} + \overline{\mathbf{BK}}_{ij}\overline{\mathbf{CBC}}]\}^{n+1}\Phi_j^{n+1} + \theta\Delta t\,[\overline{\mathbf{BK}}_{ij}\overline{\mathbf{BC}}]^{n+1}\hat{\Phi}_j^{n+1}$$

$$= \{\mathbf{S}_{ij} - (1-\theta)\,\Delta t\,[\mathbf{K}_{ij} + \overline{\mathbf{BK}}_{ij}\overline{\mathbf{CBC}}]\}\,\Phi_j^n - (1-\theta)\,\Delta t\,[\overline{\mathbf{BK}}_{ij}\overline{\mathbf{BC}}]^n\hat{\Phi}_j^n \qquad [2.54]$$

or

$$\overline{\mathbf{K}}_{ij}^{n+1}\Phi_j^{n+1} + \theta\Delta t\overline{\mathbf{BK}}_{ij}^{n+1}\overline{\mathbf{BC}}^{n+1}\hat{\Phi}_j^{n+1} = \overline{\mathbf{F}}_i^n \qquad [2.55]$$

or

$$\overline{\mathbf{K}}_{ij}^{n+1}\Phi_j^{n+1} + \theta\Delta t\overline{\mathbf{BK}}_{ij}^{n+1}\overline{\mathbf{BC}}^{n+1}\hat{\Phi}_j^{n+1} - \overline{\mathbf{F}}_i^n = 0 \qquad [2.56]$$

Applying the Newton-Raphson technique to the above system of nonlinear equations, the residual $\mathbf{R}_i$ at the m^{th} iteration is given by:

$$\mathbf{R}_i^{n+1,m} = \overline{\mathbf{K}}_{ij}^{n+1,m}\Phi_j^{n+1,m} + \theta\Delta t\overline{\mathbf{BK}}_{ij}^{n+1,m}\overline{\mathbf{BC}}^{n+1,m}\hat{\Phi}_j^{n+1,m} - \overline{\mathbf{F}}_i^{n,m} \qquad [2.57]$$

and the corrections vector $\delta\Phi_k^{n+1,m+1}$ equals:

$$\delta\Phi_k^{n+1,m+1} = [\mathbf{J}_{ik}^{n+1,m}]^{-1}(-\mathbf{R}_i^{n+1,m}) \qquad [2.58]$$

where $\mathbf{J}_{ik}^{n+1,m}$ is the Jacobian matrix given by:

$$\mathbf{J}_{ij}^{n+1,m} = \frac{\partial}{\partial\Phi_j^{n+1,m}}\mathbf{R}_i^{n+1,m} \qquad [2.59]$$

The above yields a system of linear equations in $\delta\Phi_j^{n+1,m+1}$:

$$\mathbf{J}_{ij}^{n+1,m}\delta\Phi_j^{n+1,m+1} = -\mathbf{R}_i^{n+1,m} \qquad [2.60]$$

After each iteration, the values of the variables are updated through:

$$\Phi_j^{n+1,m+1} = \Phi_j^{n+1,m} + \delta\Phi_j^{n+1,m+1} \qquad [2.61]$$

Finally, when the error norm $\varepsilon = \sqrt{\frac{\sum[(\delta\Phi)^2]}{\sum\Phi^2}} \leq$ tolerance, the solution proceeds to the next time step.

2.5 Dry Elements

2.5.1 General

Among the challenging problems facing the developers of two-dimensional models, is the treatment of wetting and drying domain areas. In this case negative or even very small depths, if not properly accounted for, lead to stability problems and make a solution impossible. This situation is encountered in most practical river and coastal engineering problems, such as flood propagation, dam break analysis, tidal processes etc. Even when attempting a steady state solution of flow in a natural river or stream for a given discharge, the distribution of the water surface elevations over the domain are not known a priori, and usually parts of the domain are found to be wet and other parts dry.

Generally, two options exist for the treatment of this problem, either to solve the equations everywhere regardless of wet or dry, or to remove dry areas from the solution domain. In the first method, special treatments are required for the dry and partially dry elements. The second approach, might require the definition of new meshes and renumbering of the unknowns, resulting in considerable computational effort at every time step. Further, mass conservation cannot be ensured and propagation of flood waves would be limited by the process of activating dry elements (Hervonet and Janin, 1994).

Akanbi and Katopodes, (1988), developed a moving grid finite element model to simulate flood propagation over initially dry land. Although the moving grid eliminated

the need for redundant computations on dry areas, a significant portion of computational time was devoted to the regeneration of the grid and tracking of the wave front, and thus the overall computational efficiency was limited (Akanbi and Katopodes, 1988). Also, the presented model was restricted to horizontal bathymetry.

Leclerc et al., (1990), presented a model based on the mixed interpolation FE method. For wet elements, the full dynamic shallow water flow equations were solved. For dry elements, velocities were set equal to zero, while for partially wet elements, reduced momentum equations (through neglecting the pressure terms) were introduced. They had to resort to artificial values of turbulent diffusion to achieve a stable solution, and recommended a judicious choice for the diffusion parameter. Further, they stated that this approach would be inappropriate for simulating rapid boundary movements produced, for example, by dam breaks or short frontal tidal waves.

Tchamen and Kahawita, (1994), proposed a technique to simulate wetting and drying areas using Riemann solvers with the FV method. They presented the results for a one-dimensional approach, but stated that the same techniques had been extended to a two-dimensional model. The technique applied well to the case of horizontal bed. However, in the case of varying bathymetry, problems of evaluating bathymetry and friction source terms arose, and artificial techniques had to be introduced. They stated that these techniques gave good results for a linear bed slope. For concave bed slopes, reasonable results could only be obtained with "sufficiently close" grid spacing. No practical guidelines were provided for the selection of this spacing. In the case of concave bed slopes, existence of a solution could not be guaranteed altogether. As bathymetry in natural water bodies is usually not restricted to a monotone curvature, the possible non-existence of a solution could be generalized to almost any practical flow situation.

Hervonet and Janin, (1994), used a two-dimensional Finite Element model (TELEMAC-2D), developed and implemented by Laboratoire National d'Hydraulique (LNH), France, to simulate flood propagation over initially dry beds. They chose a non-conservative form of the equations to reduce stability problems related to shallow depths. The SUPG Finite Element Technique (Brooks and Hughes, 1982) was used for the continuity equation and the Method of Characteristics for the momentum equations. The θ implicit treatment of the time derivative allowed stable (but not necessarily accurate) solu-

tions for Courant Numbers up to 50. They included two options in the code regarding the treatment of dry areas: either solving the equations everywhere, or removing the drying zones from the computational domain. In the first approach, they assumed that the water surface coincided with the dry bed (Figure 2.5). This produced a gradient and driving

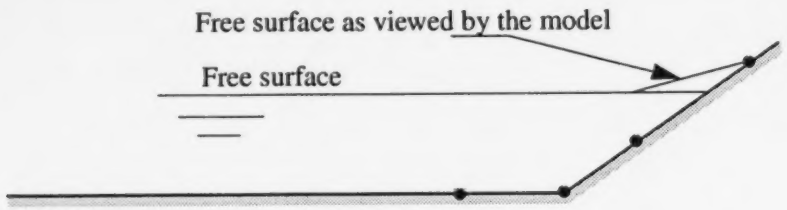

Figure 2.5 Partially Dry Elements (Hervonet and Janin, 1994)

force from the dry to the wet region in the momentum equations and corrections were required. They found that the final results greatly depended on the method with which the corrections were applied and on the algorithms used to detect the half wet/half dry elements. They also reported problems in areas of steep slopes. They concluded that neither of the two methods was fully satisfactory, and that further research was required on this topic.

2.5.2 Treatment of Domains with Partially Dry Beds

A technique has been developed here to allow the inclusion of dry areas in the solution domain. At each iteration, a test is made for each element to check whether any of its nodes is dry. If the element is found to be totally dry, equations [2.1] to [2.3] are replaced by:

$$S\frac{\partial H}{\partial t} + \frac{\partial q_x}{\partial x} + \frac{\partial q_y}{\partial y} = 0 \qquad [2.62]$$

$$\frac{\partial H}{\partial x} + \frac{1}{T}q_x - S_{o_x} = 0 \qquad [2.63]$$

$$\frac{\partial H}{\partial y} + \frac{1}{T}q_y - S_{o_y} = 0 \qquad [2.64]$$

These equations can be viewed as analogous to the equations describing the groundwater flow in the aquifer adjacent to the river depicted in Figure 2.6. S is the aquifer storativity

and T is the aquifer transmissivity (m^2/sec), which is equal to the product of the aquifer permeability and aquifer thickness.

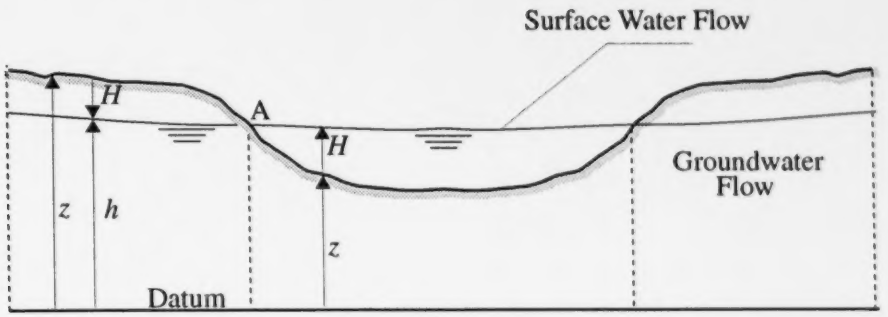

Figure 2.6 Wet and Dry Subdomains (right and left of point A respectively)

In the above figure, z and h are the elevations of the ground surface and the free water surface above a horizontal datum, taken here as the bottom of the aquifer, respectively. Thus h is equal to the aquifer thickness. In all the tests considered, a no flow boundary condition has been specified for all the external aquifer boundaries.

Considering the stream and adjacent aquifer depicted in Figure 2.6, we can arrive at a rough estimate for the ratio between the amount of groundwater flow and the amount of surface water flow through the simulation domain. This analysis would help minimizing the groundwater flow if we are only interested in the surface water flow. Assuming a steady uniform flow through the stream, then the discharge per unit width of the stream q_s would be approximately equal to:

$$q_s = C_s H^{3/2} S_f^{1/2} \qquad [2.65]$$

For the aquifer, making use of equation [2.63], and assuming that the longitudinal water surface slope in the stream is equal to the longitudinal water surface slope in the aquifer, the discharge per unit width in the aquifer q_a would equal

$$q_a = T\frac{\partial h}{\partial x} = TS_f \qquad [2.66]$$

Combining equations [2.65] and [2.66] yields:

$$q_a = \frac{T q_s^2}{C_s^2 H^3} \qquad [2.67]$$

or

$$\frac{q_a}{q_s} = \frac{T q_s}{C_s^2 H^3} \qquad [2.68]$$

Now, assuming a depth of flow in the stream of the order of 1 m, a Chezy C_s of the order of 10, and a flow velocity in the stream of around 1 m/sec, and assuming the width of the simulated portion of the aquifer being approximately equal to the stream width, then an aquifer transmissivity of 1 m^2/sec would result in a discharge flowing through the aquifer around 1% of the discharge in the stream.

The solution for the flow proceeds as follows. During the solution process, a check is made on the value of depth over all elements. If an element is found to be partially dry (for example element ABC in Figure 2.7), the line of depth $H = H_{min}$ is found. H_{min} is a minimum value of positive depth, below which the groundwater flow equations are applied. It is important to specify an $H_{min} > 0.0$, to avoid stability problems with the shallow water equations related to vanishing depth values. The coordinates of the Gauss integration points of the element are then calculated for the two resulting polygons ADEC and BED separately, and the weight is assigned proportional to the relative area (Figure 2.7). Then, equations [2.1] to [2.3] are used to calculate the contribution from BED to the stiffness matrix, whereas equations [2.62] to [2.64] are used for ADEC.

Considering triangle ABC in Figure 2.7, and examining equation [2.67], it can be seen that the discharge value at point B (surface water flow) would usually be much larger than the values at A and C (groundwater flow). As the two different types of equations are integrated over the same element ABC, the finite element solution will attempt to produce the best representative values over the domain, which might lead to local inaccuracy in computed discharges. It was however found that these inaccuracies remain very localized and do hardly affect the wave propagation speed for unsteady simulations (section 3.7) or the overall solution (Chapter 4). Perhaps one way to overcome this problem could be to

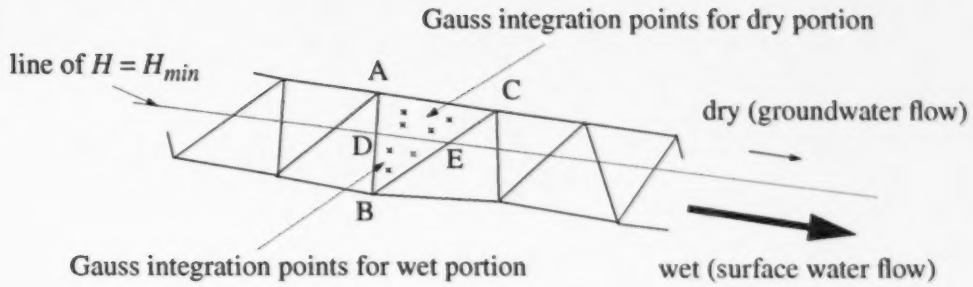

Figure 2.7 Dividing the Domain into Dry and Wet Regions

compute the water surface and identify areas of wet and dry over the solution domain. Then, the nodal coordinates of the vertices on either side of the mixed elements (either the dry or the wet nodes, possibly the ones which give the minimum overall shift) can be shifted to coincide with the line of $H = H_{min}$, and then a final solution could be obtained with this new node layout. This modification has not been attempted in this work.

The values of H_{min} and T could be related using a simplified argument. This is done by equating the conveyance of the aquifer with the conveyance of the stream in the vicinity of the aquifer, to prevent retarded response between the two water bodies. If we write the x-direction momentum equation for steady zero-inertia surface flow as:

$$\frac{g}{2}\frac{\partial}{\partial x}H^2 + gHS_{f_x} - gHS_{o_x} = 0, \qquad [2.69]$$

then, substituting for S_{f_x}, simplifying and comparing to equation [2.63], we obtain:

$$T = \frac{C_s^2 g H^3}{\sqrt{q_x^2 + q_y^2}} = \frac{C_s^2 g H^3}{q} \qquad [2.70]$$

which provides a relation between T and H (which would be H_{min} in this case). For example, if H_{min} is selected as 0.01 m, then assuming a q in the vicinity of the wet dry interface of the order of 0.001 m^2/sec, $C_s \sim 10$ and $g \approx 10$ m^2/sec, then T would be of the order of 1.0 m^2/sec.

The value of S can pose a constraint on the time step for unsteady problems. This can be seen from the analysis below, by considering the one-dimensional form of equation [2.62]:

$$S\frac{\partial H}{\partial t} + \frac{\partial q_x}{\partial x} = 0 \qquad [2.71]$$

From the one-dimensional form of equation [2.63] we obtain:

$$q_x = T(S_o - \frac{\partial H}{\partial x}) \qquad [2.72]$$

substituting [2.72] in [2.71] and assuming a constant slope S_o:

$$\frac{\partial H}{\partial t} = \frac{T}{S}\frac{\partial^2 H}{\partial x^2} = D\frac{\partial^2 H}{\partial x^2} \qquad [2.73]$$

Equation [2.73] is a diffusion equation in H, $D = \frac{T}{S}$ being the diffusion parameter. The dimensionless diffusion number r_D is defined as:

$$r_D = \frac{D\Delta t}{\Delta x^2} \qquad [2.74]$$

where Δt and Δx are the time step and spatial discretization, respectively. A truncation error analysis suggests a value of r_D equal to 1/6 for highest accuracy for an explicit centered space forward time scheme. A Fourier stability analysis specifies a minimum value of r_D of 1/2. It also indicates that the scheme would be unconditionally stable for $\theta \geq 0.5$. Thus, if we choose for transient problems using a semi-implicit scheme a value of r_D in the order of 1.0, we obtain the following relation which computes the time step given the spatial discretization and aquifer characteristics:

$$\Delta t = \Delta x^2 \frac{S}{T} \qquad [2.75]$$

On the other hand, if we are only interested in the surface water flow, the parameters S and T can be chosen to enhance numerical stability by choosing a larger value for S (not greater than unity) and a smaller value for T. As can be seen from equation [2.67], choos-

ing a smaller value for T will reduce the flow through the aquifer, which would be desirable in this case.

For the limited number of tests performed, a value of $T = 1$ m^2/sec was found to give stable and accurate solutions. Values of $T = 0.1$ m^2/sec and 0.01 m2/sec were also tried for the tests in Chapter 4. The impact on the simulated surface water flow predictions was found to be minimal. The value of S was chosen equal to unity. Changing the value of S to 0.1 in the trapezoidal channel test with dry side slopes (section 3.8) resulted in a slightly faster rate of drawdown of the water table in the aquifer during the unsteady phase, did however not affect the final steady state solution.

Generally, if we are not interested in simulating flow in the aquifer, then the choice of the parameters can be as follows. First, a value of H_{min} equal to about 1% of the average depth of flow in the stream can be selected. The aquifer transmissivity can then be calculated from equation [2.70]. Equation [2.75] then provides a guideline for the choice of aquifer storativity S based on the time and space discretizations. Chapters 3 and 4 contain examples of the choice of aquifer parameters for different test cases.

2.6 Mesh generation

2.6.1 Introduction

An important aspect of a finite element simulation, especially in multi-dimensions, is the generation of a proper mesh. This can be done either manually or automatically. In the case of 2-D flow problems, manual mesh generation is achieved by discretizing the domain under consideration into polygonal elements by hand, and then estimating the values for the different parameters such as roughness and bed elevation at all the generated nodes. The nodes and elements have then to be numbered by the user and tables of nodal connectivities have to be prepared for each element. Since the horizontal extent of the flow domain in natural streams usually changes with changes in water levels, a new mesh might be required whenever the flow varies. This process requires many hours of office work. An alternative to this is automated mesh generation, in which the finite element program develops its own mesh based on geometric information supplied by the user. Extensive

research has been done in that field and it is now considered by many developers as an integral part of the finite element simulation.

2.6.2 Unstructured Mesh Generation

The following properties are desirable in a mesh generation routine:

1. Make use of all available data in order to develop the mesh that best represents these data.
2. Minimize the effort required for preparing input files, by allowing the use of the same input files used to run widely used 1-D programs such as HEC-2 or IFG-4 directly.
3. Take advantage of any scattered measurements available.
4. Discretize any complex geometry (having islands, boundary irregularities, branches, etc.) in an efficient and reliable manner.
5. Perform calculations and storage allocation in a computationally efficient way.
6. Perform smoothing on a generated mesh to obtain more regular triangles.
7. Renumber nodes to minimize band width.

2.6.3 Description of the mesh generation routine

An automatic mesh generation routine has been developed, which generates an unstructured triangular element mesh inside the study reach. The process of mesh generation can be summarized in the following steps:

1. Preparation of input file (manual or automatic).
2. Placement of boundary and internal nodes
3. Triangulation
4. Smoothing
5. Renumbering
6. Interpolation

A description of each of the above topics follows. Chapter 4 shows examples of the different stages of the generation of an unstructured mesh for a natural river domain.

2.6.3.1 Preparation of input file

The mesh generation routine requires two input files. The first one is used to generate the finite element calculation mesh. The file contains information about the element type (either 3 or 6-node triangular elements), the number of loops 'nloops' (each closed boundary is considered as a loop), and information about the starting front for node reordering. This is followed by the nodal information (node number and x- and y-coordinate) of the external boundary, and then by the nodal information of the (nloops -1) internal boundaries. At the end is information about the fixed internal nodes.

The second input file, which contains the x- and y-coordinates, elevation, and roughness height values of the field data points, is required to generate the interpolation mesh. This mesh is used to interpolate data from given data points to find properties such as bed elevation and friction coefficients for the calculation mesh.

A preprocessor has been developed to generate the above two input files automatically from the one-dimensional IFG-4 input file (used in the Physical Habitat Simulation System (PHABSIM) program). The preprocessor reads in cross-section data as well as discharge and water levels. The preprocessor outputs the proper boundary conditions and initial conditions as well as information for the reordering routine. Because the only available information about the layout of cross-sections is the spacing between each two consecutive sections, the assumption is made that the centerline (based on the two extreme data points for each cross-section) is straight. More detailed information describing river meanders can be readily included in the model once they are available.

2.6.3.2 Placement of boundary and interior nodes

The generation of a calculation mesh starts by reading in the calculation mesh input file. Then, the nodes are placed along internal and external boundary segments according to a spacing specified by the user. After that, internal nodes are placed by slicing through the domain and placing nodes in the interior of the domain along horizontal lines. A check is made to prevent generating a node too close to an already existing node. Other criteria could be specified for placing the nodes, for example along bed contours.

2.6.3.3 Triangulation

The element generation uses the advancing front method (Lo. 1985). At the beginning of the process, the advancing front coincides with the external boundary of the domain. A front segment is the segment lying between two neighboring nodes on the front. While the given domain boundary remains always the same, the generation front changes continuously throughout the process and has to be updated whenever a new element is formed. The triangulation is initiated by selecting the last segment AB of the front. The goal is to determine a node C, such that node C lies to the left of the directed segment AB and that Δ ABC is in some sense optimal (Figure 2.8). In order to accomplish this, the two closest nodes C_1 and C_2 are chosen, and the node C is chosen which gives the best triangle shape. Then the front is updated by replacing segment AB by segments AC and CB. CB would now be the active front segment. The process of triangulation is terminated once the advancing front is reduced to zero.

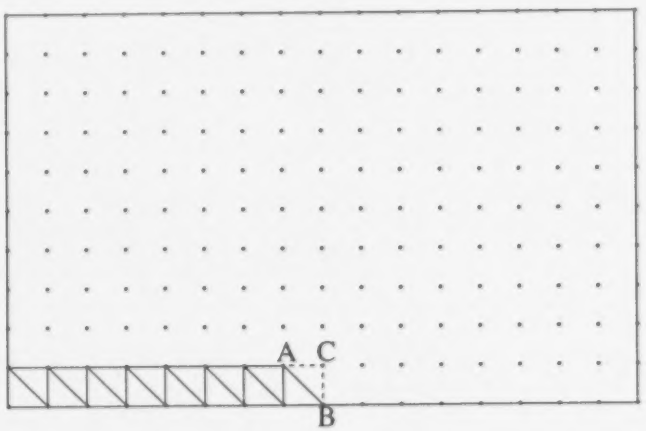

Figure 2.8 Element Generation Using the Advancing Front Method

2.6.3.4 Smoothing

A smoothing routine is applied to the node coordinates of the generated mesh to improve the element shape. The criterion chosen for smoothing is that each node is moved to the average coordinate of all its neighboring nodes. A neighboring node is any node that is connected to the node under consideration by an element side. Internal and external

boundary nodes as well as prespecified data nodes are not moved during the smoothing process. Other criteria could be chosen for smoothing to achieve different mesh shapes by applying some weight functions to the nodal coordinates as required. For example, higher weight could be assigned to nodes in locations showing rapid changes in topography.

2.6.3.5 Renumbering

The original numbering of the nodes is inconvenient from a computational point of view, as it would result in a large front/band width. A routine has been developed, which renumbers the nodes to reduce this width. This is achieved by moving a front across the domain and numbering the nodes as the front proceeds. The user has to specify the initial corner nodes that include the ordering front. (As mentioned above, the IFG4 preprocessor automatically includes this information in the calculation mesh input file.) The front advances into the domain, its ends always connected to and moving along the external boundary of the domain, until all nodes have been passed by the front and renumbered. As for typical river reaches the width is smaller than the length of the domain, the starting points for the renumbering front are usually specified as the two extreme nodes of the inflow boundary.

2.6.3.6 Interpolation

A routine has been developed which can make use of any available scattered data points to find nodal values at the nodes of the calculation mesh. First, a mesh is generated by the same triangulation routine described in 2.6.3.3, to connect the given data points by the most suitable triangles for the purpose of interpolation. For the present layout of the available data points (for example Figure 4.4), the best triangle shape would be as close as possible to isosceles, as triangles would extend in the longitudinal direction of the stream. When the same criterion as the one used in the above element generation routine was used to select nodes to form triangles (choosing the two closest nodes to the front segment), some triangles appeared which extended from one bank of the stream to the other bank. To overcome this problem, the criterion was changed to choosing the two nodes closest to each edge of the front segment under consideration. After the interpolation mesh is developed, the location of each node of the calculation mesh is determined with respect to the interpolation triangles. Then, areal interpolation is applied to obtain the nodal values. For

example for point "A" of the figure below, a weight equal to the area of triangle BCP divided by the area of triangle ABC is assigned.

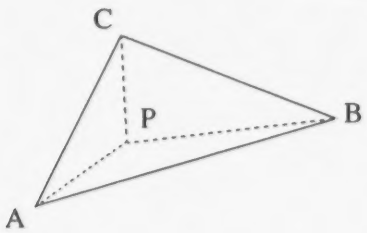

Figure 2.9 Interpolation Procedure Using Areal Interpolation

It should be mentioned that the use of data collected for a one-dimensional model does usually not give the best representation of the study reach. An example of this is the layout of data points for the Waterton River study as shown in Figure 4.4. It can be seen that the resolution is generally too fine at cross sections and too coarse in between cross sections. Further, actual channel alignment is not represented in the one-dimensional data file. Therefore, a scattered data point layout would be more appropriate for the two-dimensional model.

2.7 Summary

In this chapter, the two-dimensional shallow water flow equations describing free surface flow in the horizontal plane have been presented together with the underlying assumptions and limitations. The appropriate boundary and initial conditions have been discussed. The Characteristic-Dissipative-Galerkin (CDG) finite element formulation has been presented, and a new technique to simulate fully dynamic flow on a partly dry domain has been proposed. Finally, the generation of an unstructured computational mesh for natural streams has been discussed. In the coming two chapters, the two-dimensional model is subjected to a number of hypothetical and real test cases to evaluate the different aspects of the numerical scheme.

Chapter 3

Model Evaluation

3.1 Introduction

Several numerical experiments are presented in this chapter, which examine the performance of the two-dimensional scheme. The first test simulates the standing waves resulting from supercritical flow through a channel constriction. The computed results compare reasonably well to measurements taken by Ippen and Dawson, 1951. The second test (section 3.3) simulates the break of a hypothetical circular dam. Different element types are tried with this test to examine the effect of element shape on the obtained solution. The test in section 3.4 simulates the partial failure of a hypothetical dam. This test, proposed by Fennema and Chaudhry in 1990, has been used by several authors to examine two-dimensional schemes. In section 3.5, the directional dependency is examined through a hydraulic jump and a one-dimensional dambreak problem. The stability range with regard to the implicitness factor θ is examined in section 3.6. Finally, the performance of the dry bed simulation routine is tested in sections 3.7 and 3.8.

3.2 Supercritical Flow Through a Channel Contraction

This test demonstrates the ability of the method to simulate supercritical flow and to predict the locations and heights of the standing waves resulting from a channel constriction. It also shows the limitations of the shallow water flow equations used. Calculated values are compared to laboratory measurements taken by Ippen and Dawson (1951). The flume has a straight entry length, then changes width from 0.6096 m (2 ft.) to 0.3048 m (1 ft.) over a length of 1.26 m (4.13 ft.), the contraction angle being 6.9°. The flow enters the flume at a discharge of 0.0669 m^3/sec (1.44 $ft.^3$/sec), with a depth of 0.0305 m (0.1 ft.) and a velocity of 2.19 m/sec (7.15 ft./sec), resulting in a Froude number of 4.0. The contraction results in oblique standing waves as described in Ippen and Dawson (1951). The simulation is performed using a finite element mesh composed of linear quadrilateral elements (Figure 3.1).

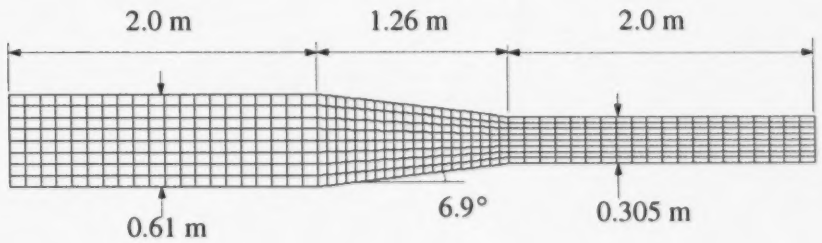

Figure 3.1 Finite Element Mesh

The contraction section is described by eight elements across and twenty along the channel. The boundary conditions are specified as supercritical inflow and outflow conditions and no-flow side walls. The simulation is performed by running an unsteady simulation using a time step of 0.05 seconds ($C_r \approx 2$) until a steady state is reached. The initial conditions are prescribed as a $H = 0.03$ m, $q_x = 0.0669$ m^3/sec and $q_y = 0.0$ throughout. A steady state solution is obtained after 100 steps (convergence criteria $\varepsilon = 10^{-10}$). Figure 3.2 and Figure 3.3 compare measured depth contours (Ippen and Dawson 1951) to the simulated contours. The overall agreement is not bad, however some discrepancy can be observed between the measured and simulated 6.0 and 7.5 cm contours. This is probably because the shallow water equations are not able to account for the small wavelength to

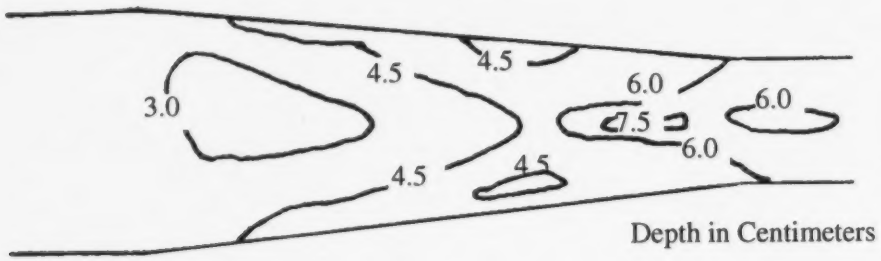

Figure 3.2 Measured Depth Contours
(Reproduced from Ippen and Dawson, 1951)

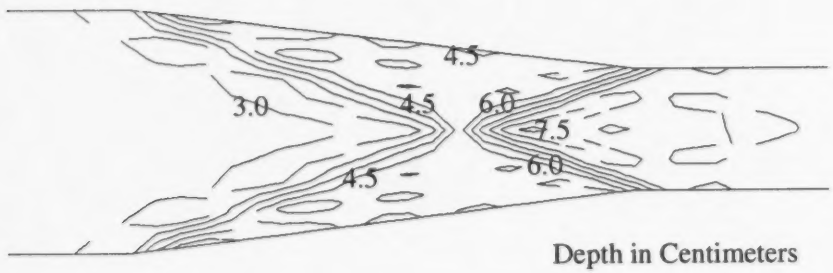

Figure 3.3 Simulated Depth Contours

depth ratio found in this vicinity, and it is unlikely that refining the mesh would be able to produce much improvement. Other governing equations which account for vertical velocity components and non-hydrostatic pressure distributions would be needed to resolve such flow details.

Conservation was checked by comparing the total discharges entering through the inflow boundary to the total discharge leaving through the outflow boundary at steady state. The two were found to be exactly equal.

3.3 Circular Dam Break Problem

This test simulates the flow resulting from the break of a hypothetical circular dam, 25 m in diameter (Alcrudo and Garcia-Navarro, 1993). The main objective of the test is to examine the effect of different element shapes and directional dependence on the obtained solution.

Initially, the depth of water inside the dam is 10 m, and 1 m outside, with zero velocity throughout (Figure 3.4). The domain is square 50 x 50 m. A no-flow boundary condi-

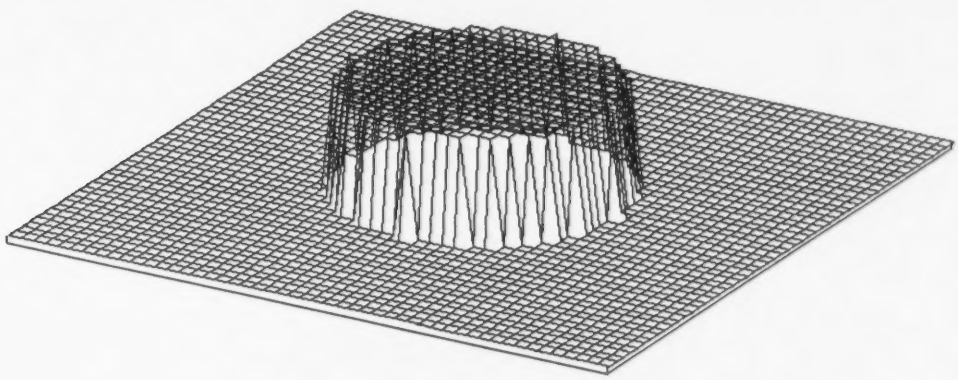

Figure 3.4 Circular Dam Break: Initial Water Surface

tion is specified on the boundary of the domain. High velocities and supercritical flows result from this dam break, which make it an interesting challenge for a numerical scheme. In addition, the simulated flow can give an indication of mesh dependency of the model. Three meshes are tested, one having linear quadrilateral elements, one having 90° triangles and one having equilateral triangles (Figure 3.5 to Figure 3.7).

The simulation is performed for 30 time steps of 0.023 seconds (maximum $C_r \approx 0.4$). Depth contours and velocity vectors obtained from the three meshes are plotted in Figure 3.8 to Figure 3.13. A three-dimensional plot of depth contours obtained from the quadrilateral element mesh is shown in Figure 3.14.

Generally, all meshes introduce some distortion to the solution. From examining the figures, it can be seen that the least distortion is obtained by using the equilateral or the square elements. It can be seen that the 90° triangles have one preferred direction (perpendicular to the hypotenuse), the quadrilaterals have two preferred directions (in the direc-

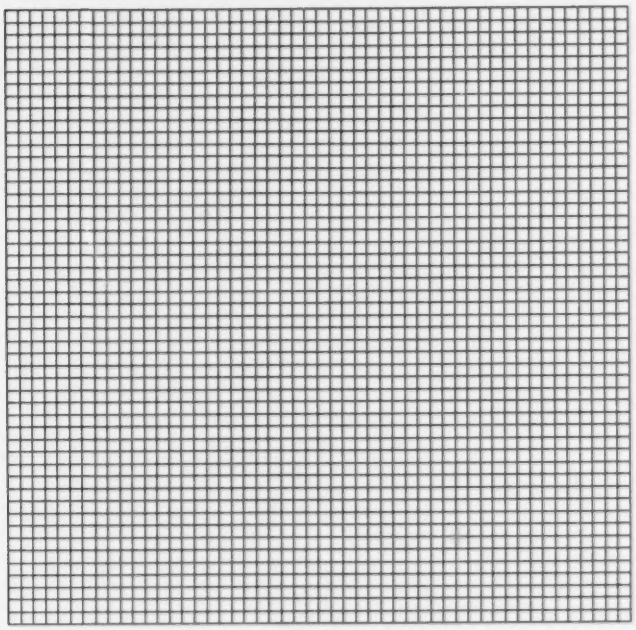

Figure 3.5 Finite Element Mesh (Quadrilaterals)

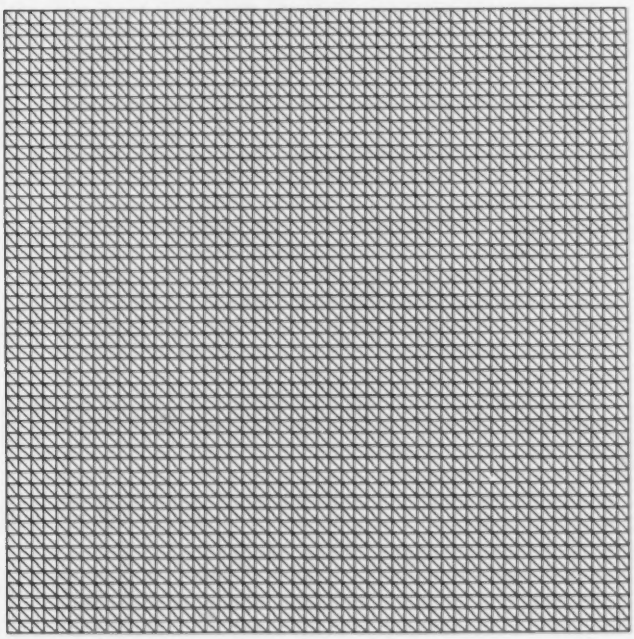

Figure 3.6 Finite Element Mesh (90° Triangles)

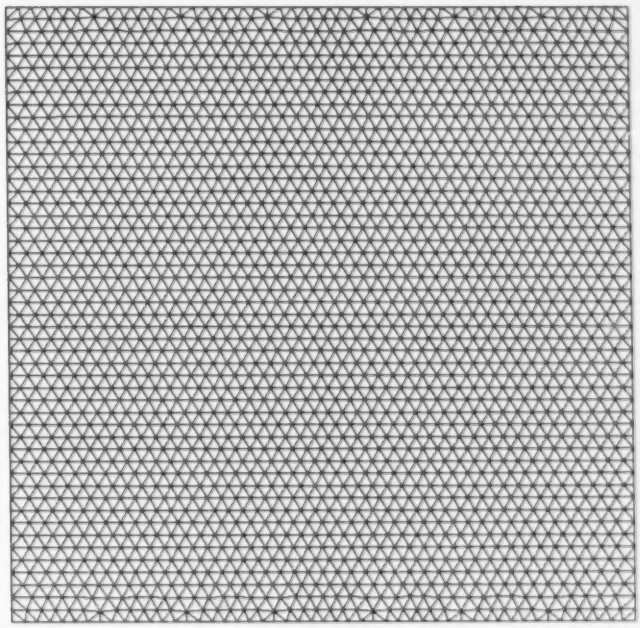

Figure 3.7 Finite Element Mesh (Equilateral Triangles)

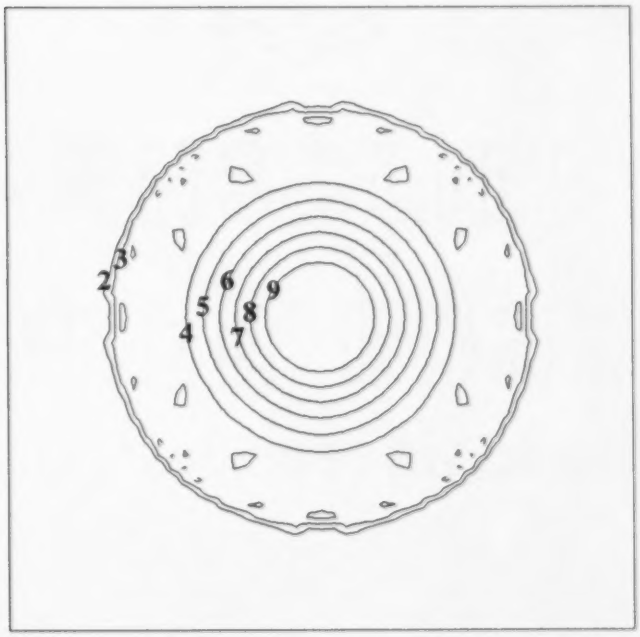

Figure 3.8 Depth Contours (Quadrilateral Elements) at t = 0.69 sec

tion of the two diagonals), whereas the equilateral triangles have three preferred

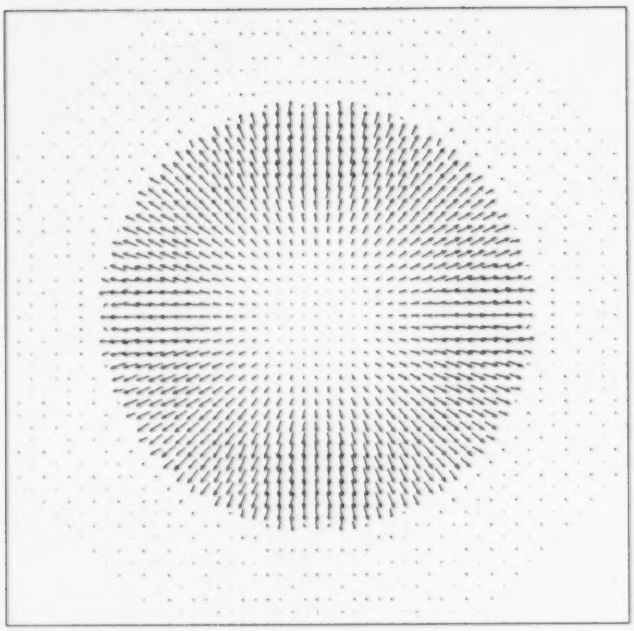

Figure 3.9 Velocity Vectors (Quadrilateral Elements) at t = 0.69 sec

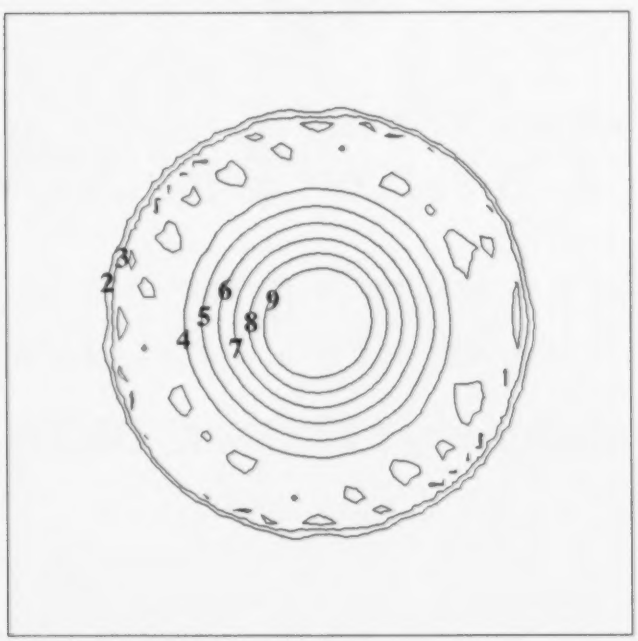

Figure 3.10 Depth Contours (90° Triangular Elements) at t = 0.69 sec

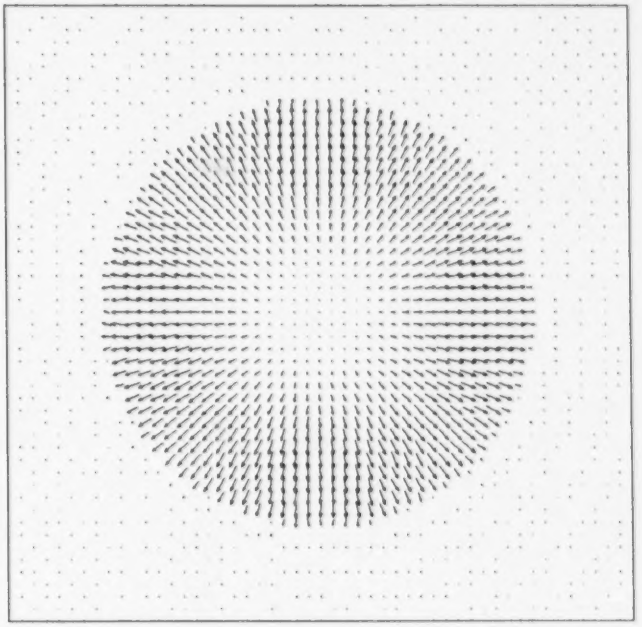

Figure 3.11 Velocity Vectors (90° Triangular Elements) at t = 0.69 sec

Figure 3.12 Depth Contours (Equilateral Triangular Elements)
at t = 0.69 sec

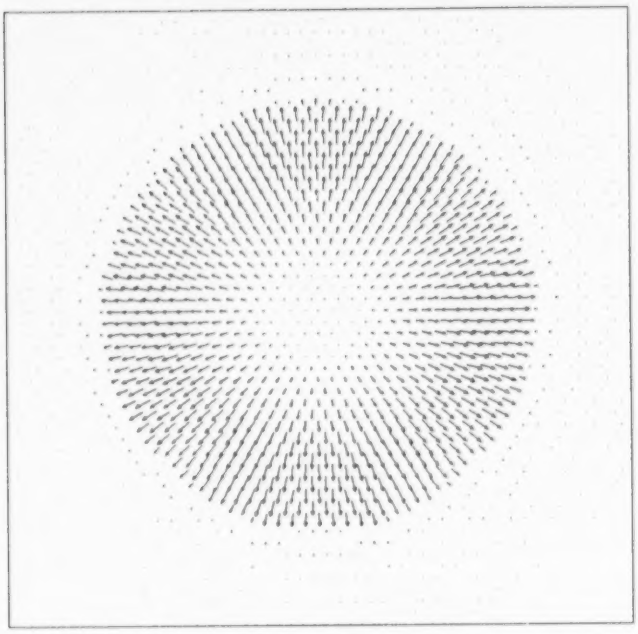

Figure 3.13 Velocity Vectors (Equilateral Triangular Elements)
at t = 0.69 sec

directions. The convergence characteristic of the equilateral triangles mesh are slightly superior to the other meshes. For the specified tolerance of 10^{-5}, the quadrilaterals and the 90° triangles meshes converge in 5 to 6 iterations per time step, whereas the equilateral triangles mesh converges in 5 iteration per step throughout the simulation.

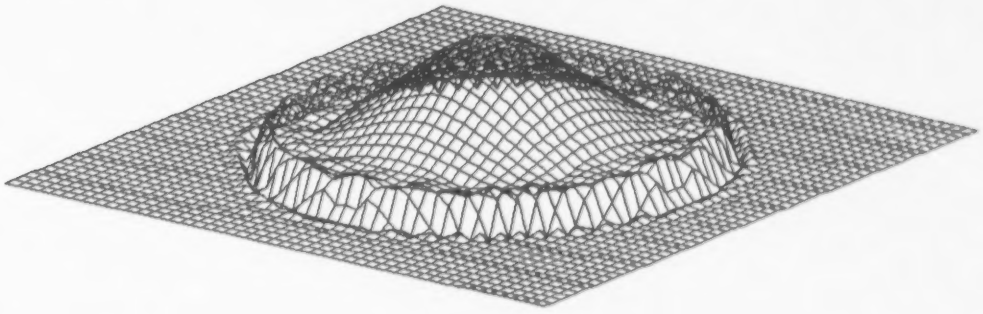

Figure 3.14 Computed Water Surface (quadrilateral mesh)
at time t = 0.69 sec

3.4 Partial Dam Failure

This test was first introduced by Fennema and Chaudhry, 1990, to test the two-dimensional McCormack and Gabutti schemes. It has been used later by other authors to test different two-dimensional models (e. g. Alcrudo and Garcia-Navarro, 1993, and Zhou et. al., 1994). The test domain is 200x200 m square, with a 10 m thick dam towards the middle (Figure 3.15). Initially, the water depth is 10 m upstream of the dam and 5 m on the downstream side, with zero velocity everywhere. An unsymmetrical breach occurs in the dam at time t=0.0 (Figure 3.16).

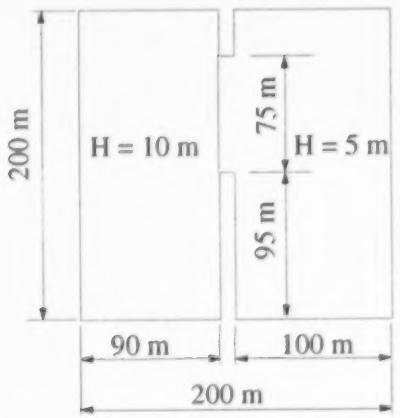

Figure 3.15 Partial Dam Failure: Definition Sketch

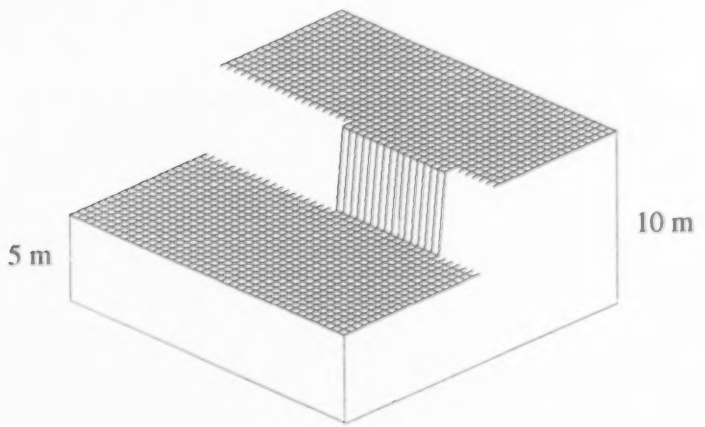

Figure 3.16 Initial Water Surface

The discontinuous initial conditions and the 90° corners impose severe computational difficulties, and most numerical schemes fail under such conditions (Fennema and Chaudhry, 1990). The bed is assumed frictionless. Linear quadrilateral elements of 5m x 5m are used to develop the finite element mesh (Figure 3.17).

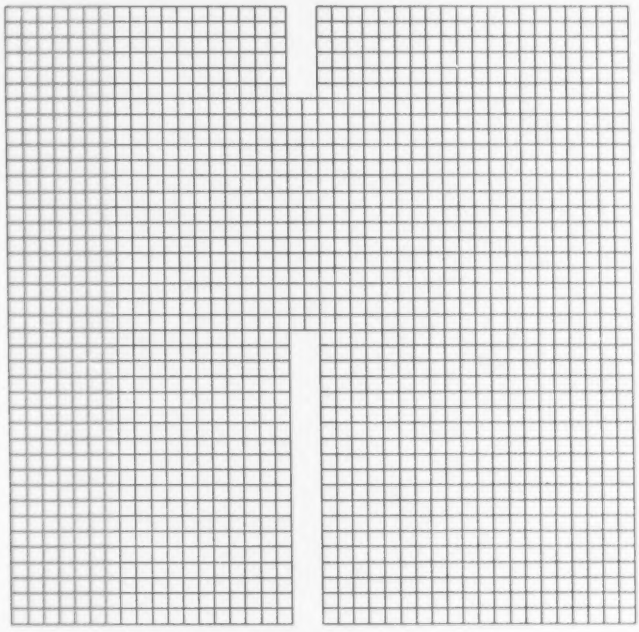

Figure 3.17 Finite Element Mesh

A time step of 0.355 seconds is chosen, which results in a maximum Courant Number in the order of 1.0 based on the progressive wave speed. Results are presented at the end of 20 time steps (t=7.1 seconds), when the progressive and regressive wave fronts are close to the downstream and upstream domain boundaries and the side wave front has reached one side-wall of the channel. Figure 3.18 shows the depth contours and Figure 3.19 shows the velocity vectors. The three-dimensional water surface is shown in Figure 3.20. Figure 3.21 compares results of the CDG scheme to other numerical schemes (results of other schemes digitized from Figure 14 in Fennema and Chaudhry, 1990). It can be seen that the results of the CDG scheme show more details on the negative wave side and a steeper front for the progressive wave, however, as no measurements are available for this test, no conclusions can be drawn regarding the accuracy of this or the other schemes. Mass conservation is checked by comparing the volume of water at the begin-

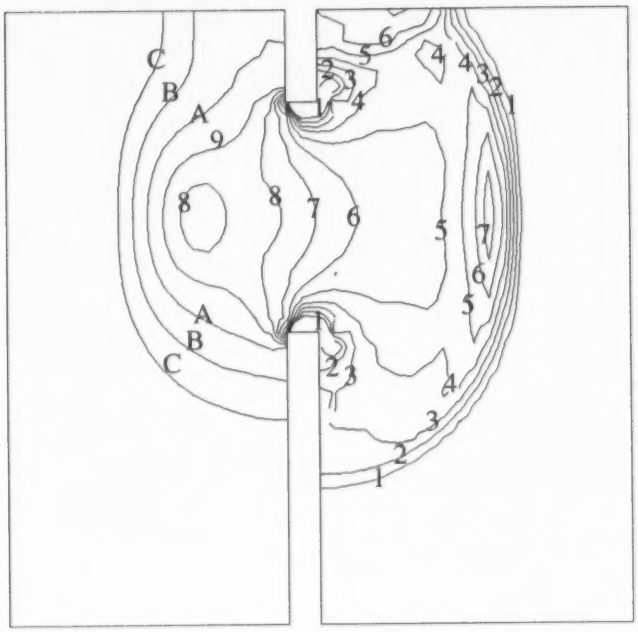

Figure 3.18 Computed Depth Contours

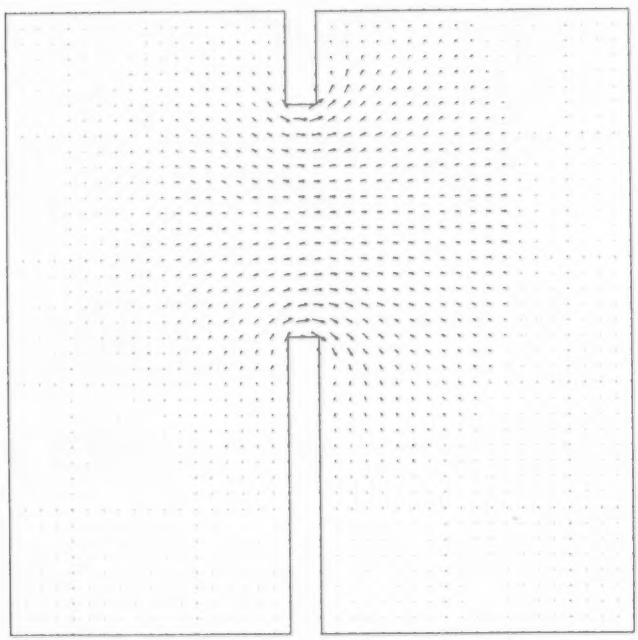

Figure 3.19 Velocity Vectors at time t = 7.1 seconds

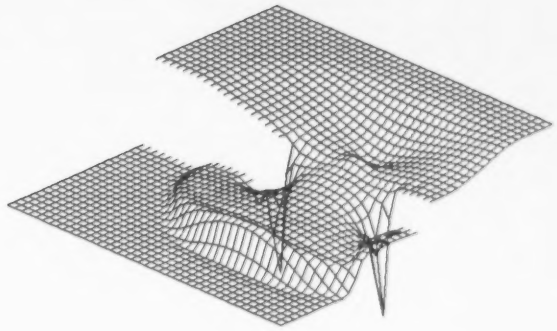

Figure 3.20 Water Surface at time t = 7.1 seconds

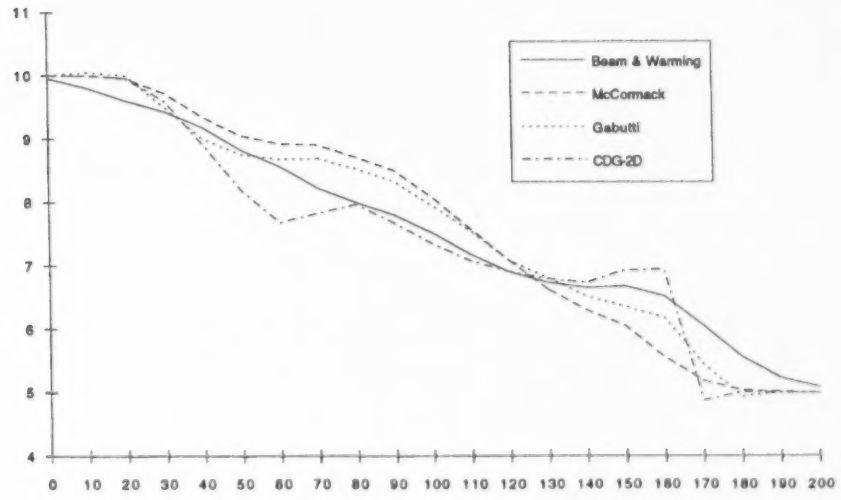

Figure 3.21 Comparison Between Computed Water Surface Profiles at t = 7.1 seconds, y = 140 m

ning to the volume of water at the end of the simulation. The two volumes are exactly equal.

3.5 Directional Dependency of Upwinding

Two tests are conducted to test and compare the CDG and the one dimensional CDG (equations [2.42] and [2.43]) schemes. In each test, two situations are compared; First, with the flow direction aligning with the x-axis, and then at 45° with the coordinate axes. In this way, the directional dependency of the schemes is examined.

3.5.1 Hydraulic Jump

This test simulates a hydraulic jump in a frictionless horizontal channel. The reach is 150 m long and 15 m wide. The flow enters at a discharge per unit width of 4.07172 $m^2/(sec\ )$ and a depth of 1.0 m resulting in a Froude number of 1.3. This results in a supercritical flow in the main flow direction, whereas when run at 45°, the Froude numbers based on the x and y velocity components are less than unity. The downstream boundary condition is specified as a subcritical outflow boundary with a depth of 1.40526 m, which is the conjugate depth for the given supercritical flow conditions. It should be noted that since the channel is frictionless, it is important to specify the values of the variables to a high degree of accuracy in order to be able to achieve convergence. The initial conditions place the jump at the middle of the channel (75 m downstream). The finite element mesh is composed of square linear elements of 5 m side length. An upwinding parameter ω of 1.0 and a θ of 1.0 (fully implicit) are used for this test. A starting time step of 0.25 seconds is used, which is magnified every time step by a factor of 1.05, resulting in a time step of 30 seconds ($C_r = 45$) at the end of 100 steps.

For the CDG scheme, it is found that results are independent of the mesh orientation. Results obtained for the mesh in the *x*-direction coincide with those at 45°. Results at the end of 100 time steps are shown in Figure 3.22. No convergence could be obtained for the one-dimensional CDG method for either orientation.

3.5.2 Dambreak Problem

Here, a dambreak problem in a horizontal frictionless channel is simulated (Fennema et al., 1987). The reach is 2000 m long and 75 m wide, with the dam located in the middle of the reach. Initially, water depth is 10 m to the left of the dam and 5 m to the

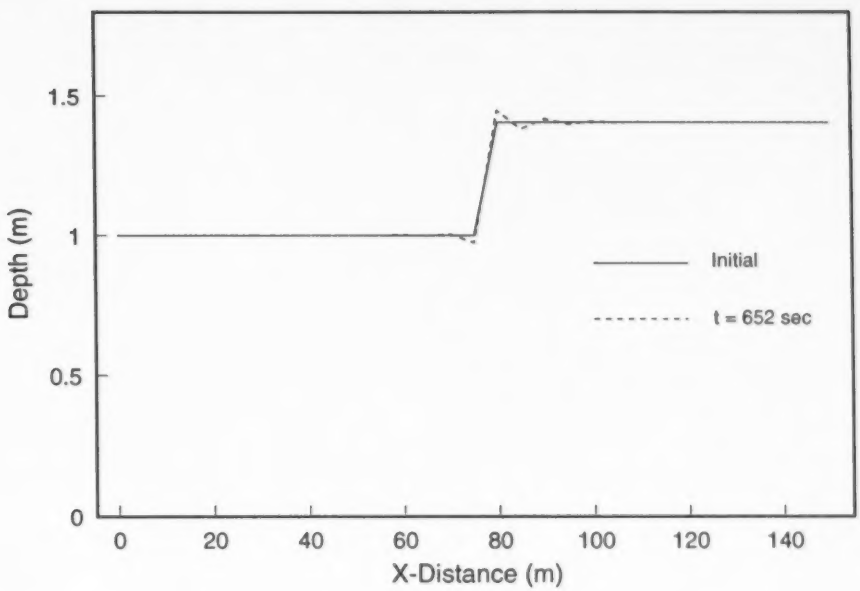

Figure 3.22 Hydraulic Jump Initially and after 100 Time Steps in the x-Direction and at 45° Using the CDG method

right, velocity being zero throughout. No-flow boundary conditions are specified on all boundaries. The mesh is composed of linear square elements of 25 m side length. A time step of 1.25 seconds is used, resulting in a C_r of 0.6 based on the progressive wave speed. θ is set equal to 0.5 and an ω of 0.25 is used. The water surface is plotted at the end of 48 time steps (t=60 seconds). Results for the x-direction flow simulation are shown in Figure 3.23 and Figure 3.24.

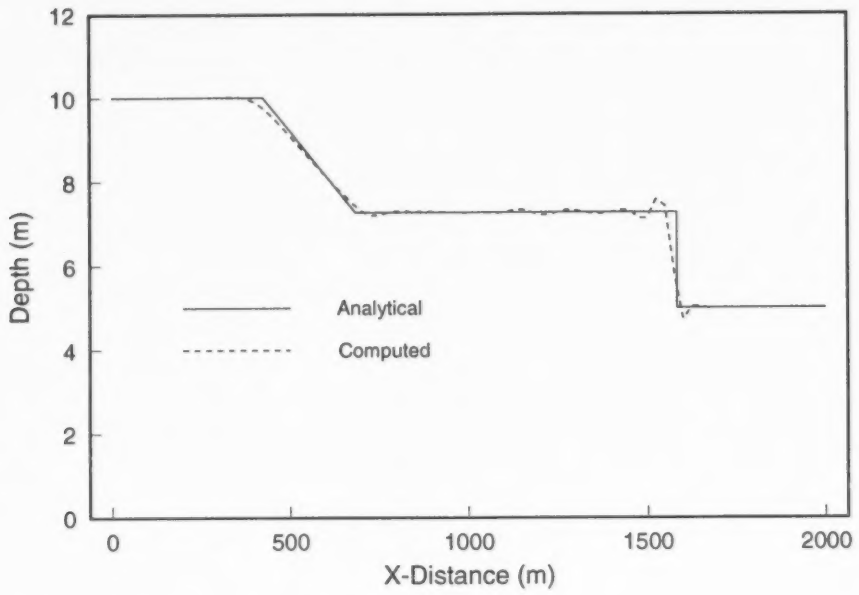

Figure 3.23 Water Surface After 60 seconds from Dam Break, Flow in the x-direction (one-dimensional CDG-method).

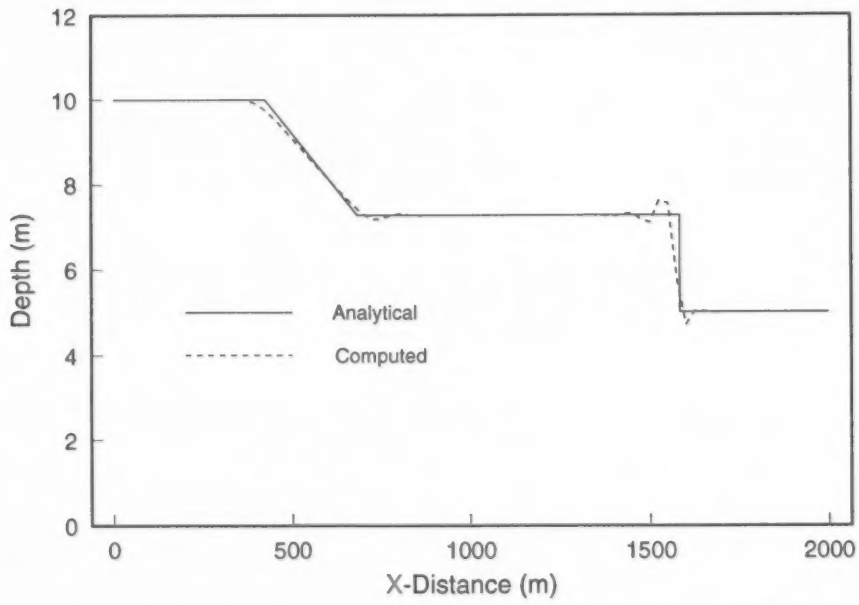

Figure 3.24 Water Surface After 60 seconds from Dam Break, Flow in the x-direction and at 45° (CDG-solution)

It can be seen that the one-dimensional CDG solution shows spurious oscillations. Also, cross oscillations in water surface and discharge, which are strongest in the vicinity of the advancing front, are observed. The CDG solution appears more accurate, with no cross-oscillations. When the mesh is set at 45° to the x-axis, it is found that the CDG results are not affected. Interestingly, the one-dimensional CDG results at 45° are found to be almost identical to the CDG results, with no cross-oscillations occurring.

The above tests confirm the directional independence of the CDG method as stated by Hughes and Mallet, (1986 b). Further, the tests show the directional dependency of the one-dimensional CDG scheme, with optimal performance obtained for flow at 45° to the coordinate directions.

3.6 Stability Range

This test examines the effect of the implicitness factor θ on the stability of the solution. The test simulates a stationary hydraulic jump on a frictionless horizontal prismatic channel, 150 m long and 15 m wide (Katopodes, 1984). Square linear quadrilateral elements of side length 5 m are used to construct the finite element mesh. A constant time step of 0.3 seconds is used (C_r = 0.5 based on the supercritical flow velocity). The flow enters the channel at a depth of 1.00829 m and a discharge per unit width of 5 m^2/sec (F_r = 1.58). The conjugate depth corresponding to this supercritical flow is 1.80 m, and is specified as the downstream boundary condition. The initial conditions place the hydraulic jump at the middle of the reach (75 m downstream). The test is run for values of θ ranging from 0.5 to 1.0 (at 0.05 interval) for an extended period of time (10,000 time steps), and the minimum value of θ which provides a stable solution is found.

It is found that the solution is stable for a value of θ equal to or greater than 0.65. Figure 3.25 shows the computed water surface at the end of the 10,000 time steps (t = 3,000 secs) for θ = 0.65.

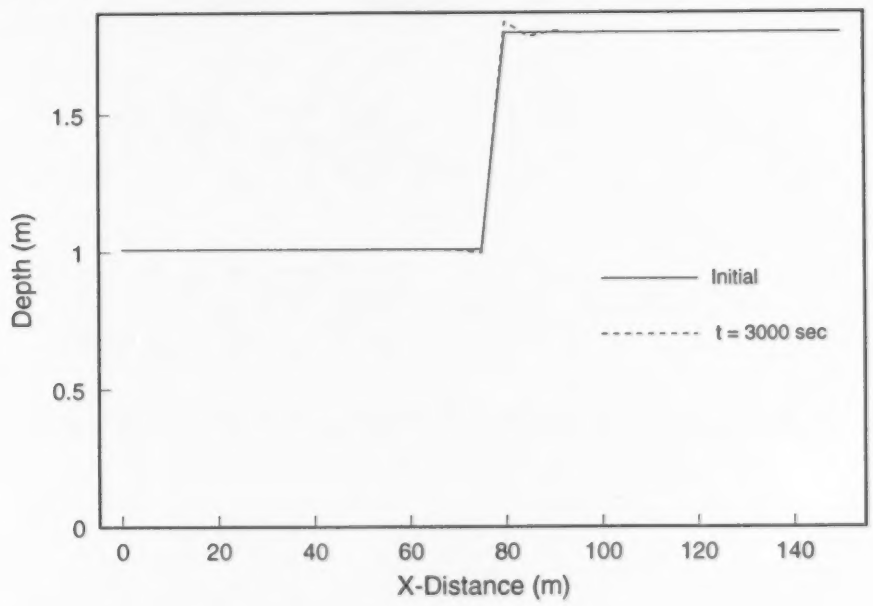

Figure 3.25 Initial and Final Water Surface (at 10,000 steps) for θ = 0.65

At a θ of 0.60, spurious waves of wavelength 3 to 5 Δ (element side length) appear on the subcritical reach after about 1,000 time steps. They grow with time and eventually

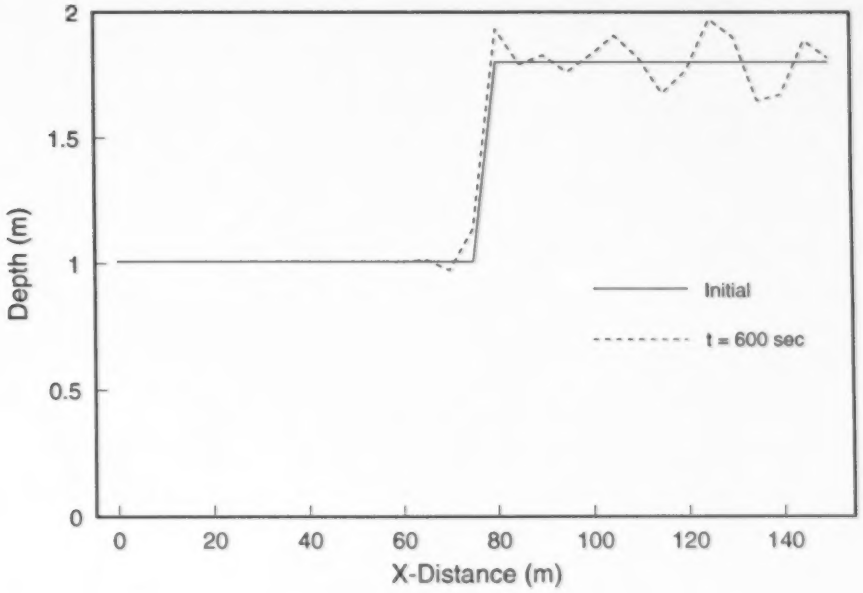

Figure 3.26 Water Surface after 2000 time steps for θ = 0.6

destroy the solution after about 3,200 steps. Figure 3.26 shows the wave shape after 2000 time steps.

3.7 Dambreak on Dry Bed

This test examines the ability of the dry-element simulation routine to simulate unsteady flow over a dry bed. The experimental data are obtained from Schoklitsch (1917). He performed a number of lab and field experiments, in which he measured the water surface profile for different dambreak problems. In the test under consideration, he ran a dambreak problem in a laboratory flume made of smoothed wood, 0.096 m wide and 0.08 m high. At time t = 0, a wall located at the middle of the flume and separating a 0.074 m deep water body from the dry downstream side was swiftly removed. Water surface profiles were recorded at times t = 3.75 sec and t = 9.4 sec.

The finite element mesh uses square linear quadrilateral elements of 0.2 m side length. No-flow boundary conditions are specified at all boundaries. For the roughness height of smooth wood, Streeter and Wylie, 1981, suggest a value in the range from 0.18 to 0.90 mm. A value of 0.50 mm is thus chosen for this test. The test is run once with a time step of 0.0625 seconds (maximum $C_r \approx 0.4$ based on the progressive wave speed) for 60 steps (i.e. $t = 3.75$ sec), and a second time for a time step of 0.1 seconds (maximum $C_r \approx 0.6$ based on the progressive wave speed) for 94 steps ($t = 9.4$ sec). The choice of different time steps for the two tests is just to produce results at the exact times measurements were taken. Measured and computed water surface profiles are shown in Figure 3.27. A small wiggle producing negative depth can be observed at the wave front. However, this wiggle does not result in any computational instability as the program simply simulates it as a groundwater flow in that region.

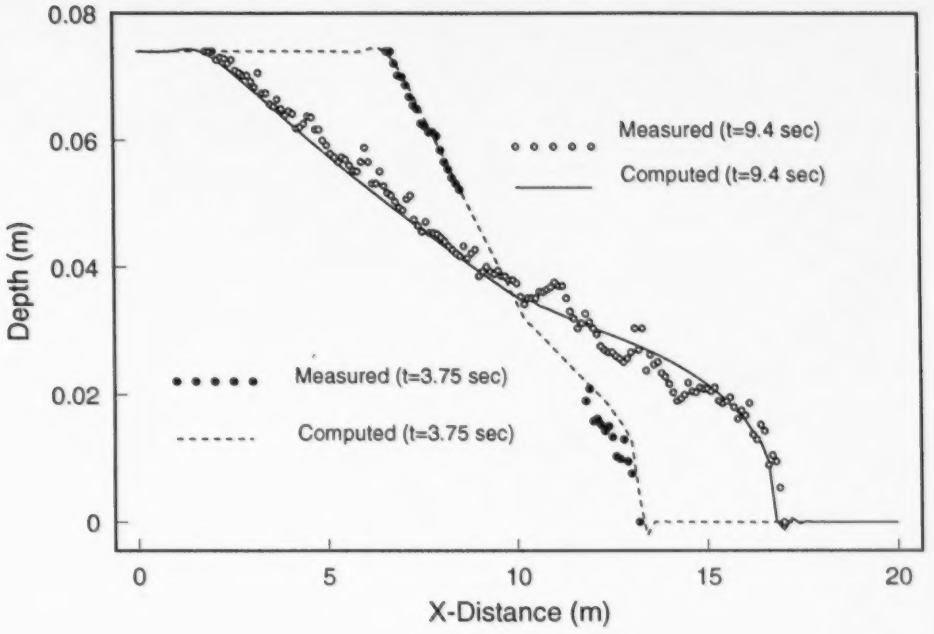

Figure 3.27 Measured and Simulated Water Surfaces for Dambreak on Dry Bed
(Measured Data from Schoklitsch, 1917)

3.8 Flow in a Trapezoidal Channel With Partly Dry Side Slopes

This test solves for a steady state flow in a hypothetical trapezoidal channel, 5 m bed width and 7.5 to 1 side slopes. The channel has a total length of 300 m, with 100 m transition lengths from rectangular to trapezoidal at the upstream end, and from trapezoidal to rectangular at the downstream end. The longitudinal bed slope is 0.0013, and the roughness height is 0.2 m, resulting in a normal depth of about 2.5 m at a discharge of $80\ m^3/sec$. The turbulent diffusion coefficient is set equal to zero to increase the computational challenge. A subcritical inflow boundary condition with a total inflow discharge of $80\ m^3/sec$ is specified. Initial conditions set the water depth at 2.5 m throughout the channel. The downstream boundary condition specifies a depth of 1.0 m, slightly higher than the critical depth of 0.81 m. Thus, the water surface is drawn down with time, exposing dry nodes and elements on the trapezoidal reach slopes.

The finite element mesh is composed of square linear quadrilateral elements, 5 m side length. A θ of 0.5 is used and the time step is chosen as 0.5 seconds, resulting in a maximum C_r of 0.6. T is chosen as $1.0\ m^2/sec$, and H_{min} is taken equal to 0.01 m. A storativity of 1.0 is used. The test is run for 1000 steps, at the end of which $\varepsilon = 10^{-5}$. Figure 3.28 shows the longitudinal water surface profiles at times $t = 0.0$, 10.0, 100.0 and 500.0 seconds. Figure 3.29 shows a cross section at $x = 200$ m and Figure 3.30 shows depth contours for the steady state solution (t = 500 seconds). Figure 3.31 shows the computed

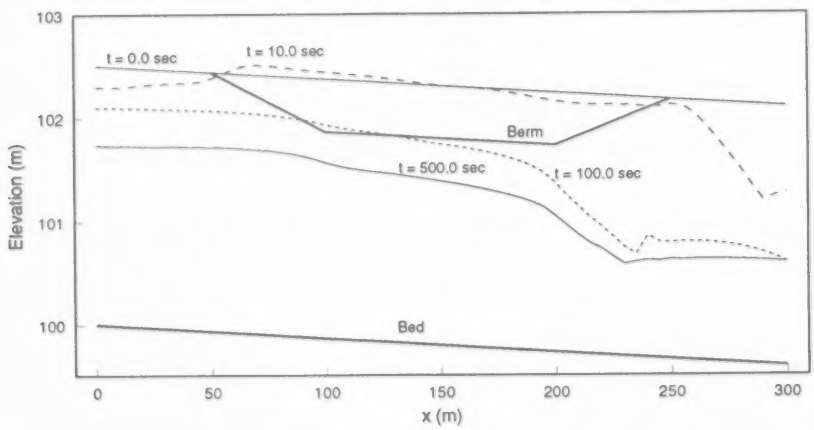

Figure 3.28 Computed Longitudinal Water Surface Profiles at y = 15 m

steady state velocity vectors.

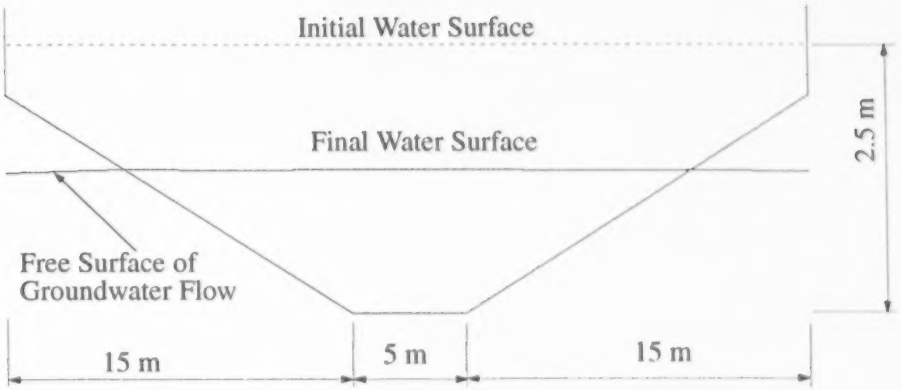

Figure 3.29 Cross Section at x = 200 m after 500 seconds, Showing Wet and Dry Areas

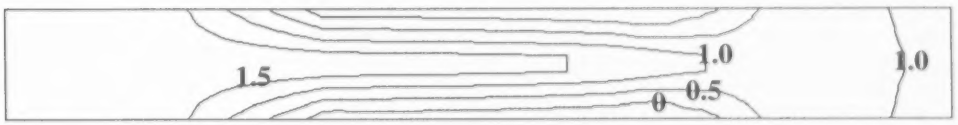

Figure 3.30 Depth Contours at Steady State (t = 500 seconds)

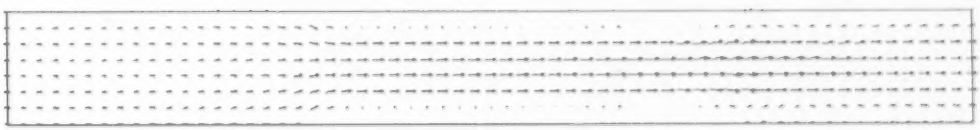

Figure 3.31 Steady State Velocity Vectors

The sensitivity of the results to S were examined. Using a value of S of 0.1 resulted in a slightly faster rate of drawdown of the groundwater table during the unsteady phase (about 5% difference in the calculated minimum depth at t = 100 seconds), but did not affect the final steady state.

3.9 Summary

Several numerical experiments were presented in this chapter, which examined the performance of the two-dimensional scheme. The first test simulated supercritical flow through a channel constriction. The computed results compared reasonably well to measurements taken by Ippen and Dawson, 1951. The second test (section 3.3) simulated the break of a hypothetical circular dam to examine the effect of element shape on the obtained solution. The test in section 3.4 simulated the partial failure of a hypothetical dam. In section 3.5, two tests, a hydraulic jump and a one-dimensional dambreak problem, were carried out to test the directional dependency of the upwinding scheme. The stability range with regard to the implicitness factor θ was examined in section 3.6. Finally, the performance of the dry bed simulation routine was tested in sections 3.7 and 3.8.

Chapter 4

Simulation of Flow in Physical Fish Habitat

4.1 Introduction

In this chapter, the developed two-dimensional hydraulic model is applied to flow situations in physical fish habitat. Two test studies are examined, which compare the performance of the two-dimensional approach to the zero/one-dimensional approach found in the widely used IFN assessment methods[1]. The first deals with flow over a side bar in a hypothetical reach. The test is run for two different discharges, and results using the two approaches are compared. The second test examines flow in an actual fish habitat reach of the Waterton River, Alberta, Canada. First, a high flow of 14.6 m3/sec is simulated using both the one-dimensional and the two-dimensional approaches. The test intends to evaluate the performance of the two approaches in the absence of velocity measurements. Based on the arguments presented in Appendix B regarding the difficulty, and sometimes impossibility, of collecting the extensive velocity measurements required for the zero/one-dimensional model, this test appears to provide a valid comparison for certain flow situations. Then, a low flow of 1.52 m^3/sec is simulated. At this flow, portions of the bed become exposed. Therefore, this case serves as a test for the dry bed simulation routine.

1. Appendix B gives an overview of these methods

4.2 Hypothetical Test Case: Flow over a Side Bar

A test problem of flow over a side bar in a straight channel is presented here. Results using a one-dimensional approach similar to the one used in PHABSIM are compared to results of the two-dimensional model. The domain consists of a straight channel 60 m wide and 720 m long with a roughness height of 0.20 m. At the middle of the reach exists a side bar 120 m long (Figure 4.1). The longitudinal bed slope is 0.0002, which results in a normal depth of 3.0 m at a discharge of 180 m^3/sec.

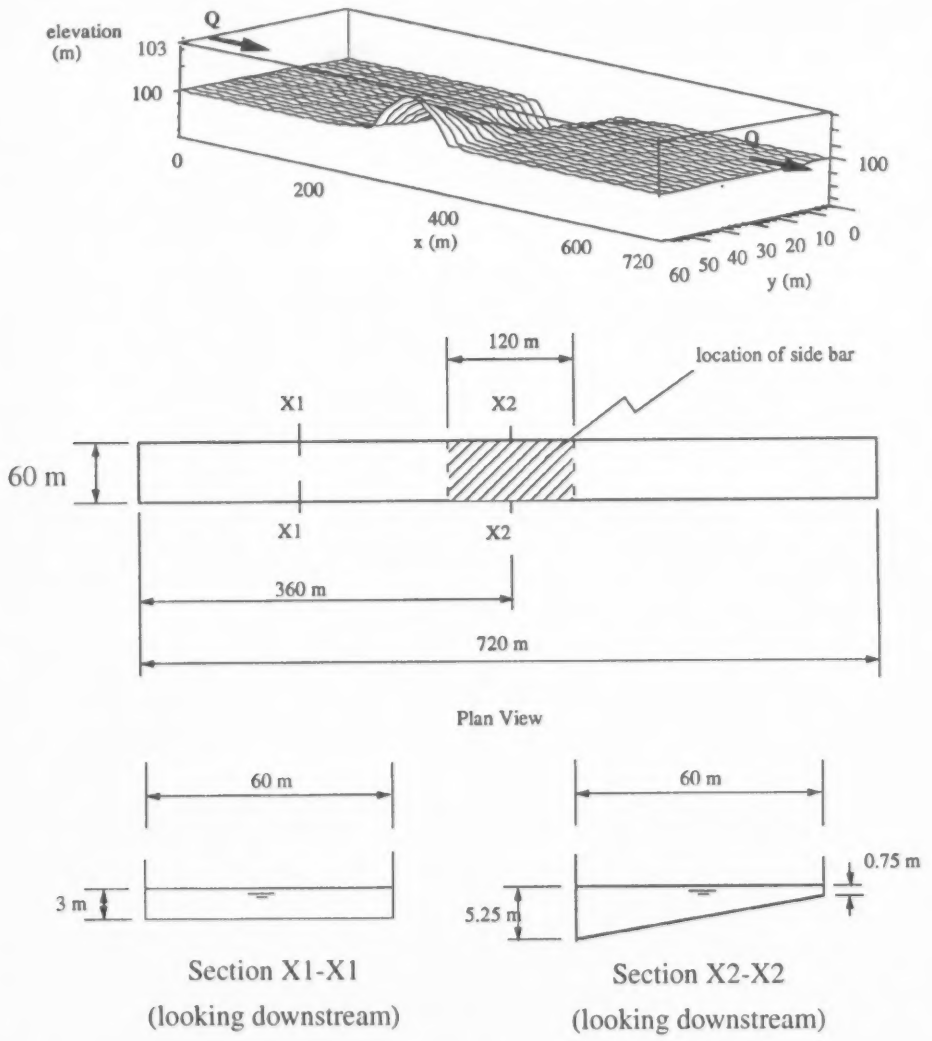

Figure 4.1 Flow Over a Side Bar

First, it is assumed that no velocity calibration data are available for the one-dimensional model. The friction coefficients are calculated based on the roughness height. A simulation is performed using both approaches for a discharge of 180 m^3/sec. The results are shown in Figure 4.2. Since the one-dimensional model scales the velocity to the local depth, it thus predicts the minimum velocity (about 0.4 m/sec) to occur on the shallow side. On the other hand, the two-dimensional model considers the redistribution of momentum, and accordingly predicts a higher velocity on the shallow side (about 1.1 m/sec) than on the deep side, as would be expected.

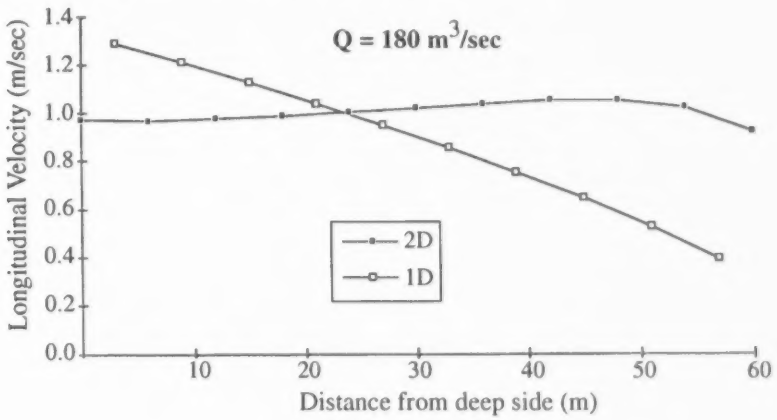

Figure 4.2 Transverse Distribution of Longitudinal Velocity at Sec. X2-X2
Q = 180 m^3/sec

In the second test, it is assumed that one full depth and velocity calibration data set for the one-dimensional model are available at a discharge of 180 m^3/s. This set is obtained from the results of the two-dimensional model for the same discharge. Then the calibrated model is run to simulate flow at a discharge of 1800 m^3/s, and compared to two-dimensional simulation results (Figure 4.3). In this case, the one-dimensional model builds the calculation of the velocity distribution on conveyance values that are based on the low discharge, and in which the effect of the bump is very pronounced, and thus predicts a high value of velocity (about 4.6 m/s) on the shallow side. However, for this large discharge a large depth of flow (about 11 m) will occur, and the effect of the bump will be minor. Thus a more uniform velocity distribution would be expected, as predicted by the two-dimensional model (approximately constant value of 2.5 m/s).

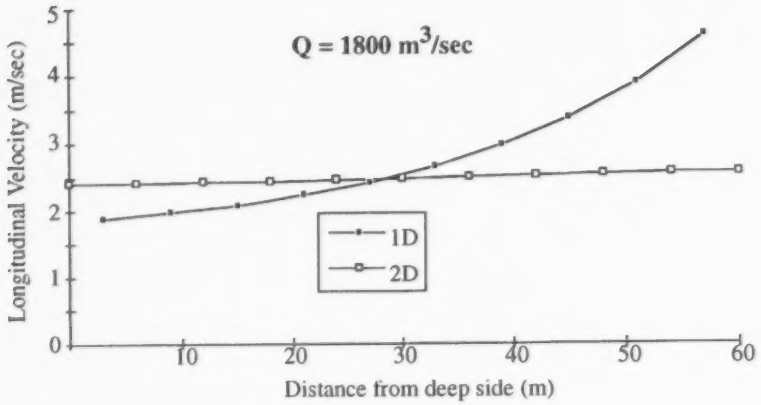

Figure 4.3 Transverse Distribution of Longitudinal Velocity at Section X2-X2
$Q = 1800\ m^3/sec$

As no experimental or analytical data are available to compare the results to, this test serves mainly to indicate that a significant difference between the two approaches can exist for certain flow situations. Flows where inertia forces are dominant, such as in the case when rapid changes occur in bed topography, are examples of such. Although the results of the two-dimensional model appear more reasonable from a hydraulic point of view, this test cannot be used as conclusive evidence for the superiority of either approach.

4.3 Real Test Case: Simulation of Flow in a Fish Habitat

As an example for simulating flow in a real fish habitat, a reach of the Waterton River near Glenwood, Alberta, Canada, has been chosen. The flow is simulated for a high flow of 14.6 m^3/sec and for a low flow of 1.52 m^3/sec. For the high flow, the river reach has an average width of 50 m. An island, which is submerged at the high flow, becomes exposed at the low flow, a good test for the dry element simulation routine. The average longitudinal slope is 0.003. The reach has a length of 245 m and is described by 12 cross sections. Figure 4.4 shows the cross section layout and the distribution of field data points. The mesh generation routine was utilized to develop the two-dimensional finite element mesh from the one-dimensional IFG-4 input file. As no information about river meander or channel alignment is available in such an input file (as it would be irrelevant for the one-dimensional model), the shown cross-section alignment has been assumed by the mesh generation routine. If information about section alignment were available (for example distance between cross-sections along left and right bank and one diagonal distance), it could be readily used to get a better picture of the stream and to account for the effect of channel alignment on the distribution of the flow. The interpolation mesh developed from the data points is shown in Figure 4.5. The developed finite element calculation mesh has 853 nodes and 1516 elements (Figure 4.6). The interpolated bed contours are shown in Figure 4.7. The reach contains some interesting features such as a submerged island, a riffle and a pool.

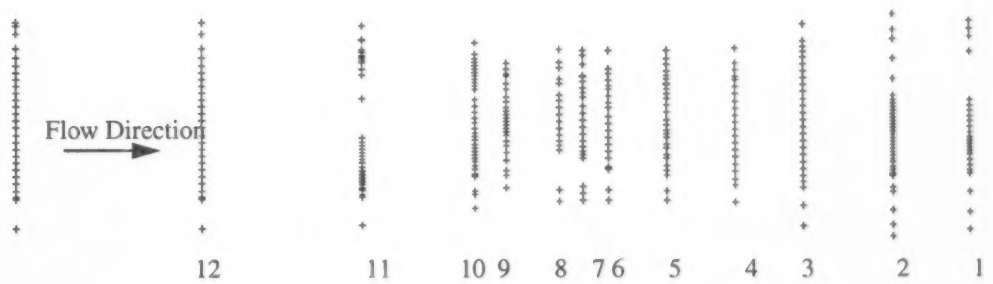

Figure 4.4 Layout of Cross-Section Data Points and Cross-Section Numbers
Waterton River

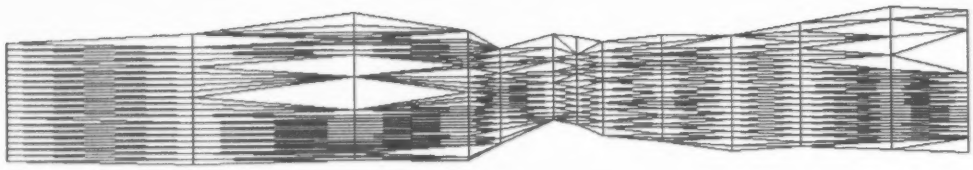

Figure 4.5 Interpolation Mesh (Waterton River)

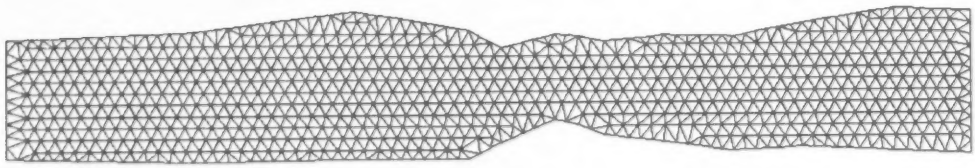

Figure 4.6 Finite Element Calculation Mesh (Waterton River)

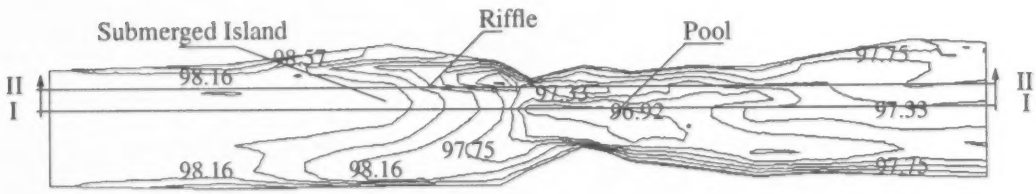

Figure 4.7 Interpolated Bed Contours, Waterton River

4.3.1 Simulation of High Flow

The simulation discharge was 14.6 m^3/sec. No velocity measurements were used to calibrate the two models. A constant roughness height (k_s) of 0.15 m was assumed throughout the domain, as no roughness data were provided in the IFG-4 input file. This value of k_s was found to give best agreement with the measured water surface when using the two-dimensional model. It should be mentioned that the results of the two-dimensional model were found to be not very sensitive to exact roughness values. For example the use

of a k_s of 0.3 m (i.e. a 100% increase), resulted in about 8% increase in calculated water depths. This can be attributed to the relatively short length and dynamic topography of typical fish habitat sites, which make roughness only of secondary importance as compared to a proper geometric description. This shows the weakness in the zero-dimensional "Manning's equation" approach, which bases the analyses on roughness and disregards inertia.

For the one-dimensional model, the depth and roughness data were used to calculate cell conveyances, which were then used to calculate the velocity distribution across the river. For the two-dimensional model, the simulation was performed by considering only the topographic features of the domain together with the assumed constant roughness height. A value of $0.07 u_s H$ m^2/sec was used for the turbulent exchange coefficient ν. The sensitivity of the results towards this variable was also tested and was found to be minor as long as ν was kept *within physically reasonable values*. For example, increasing ν to $0.14 u_s H$ m^2/sec (100% increase) resulted in variations in depths and velocities of less than 1%.

Depths and velocities were then calculated using the two-dimensional model. Figure 4.8 to Figure 4.10 present results of the two-dimensional model at steady state. Figure 4.8 and Figure 4.9 show simulated longitudinal cross sections at steady state, and Figure 4.10 shows the computed velocity vectors. Figure 4.11 and Figure 4.12 compare measured to simulated velocity values at cross sections 11 and 10 respectively. Cross section 11 is on the submerged island just upstream of cross section 10, which is downstream of the island.

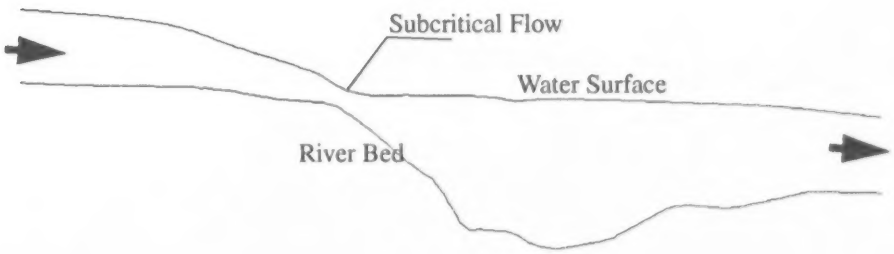

Figure 4.8 Longitudinal Section I-I

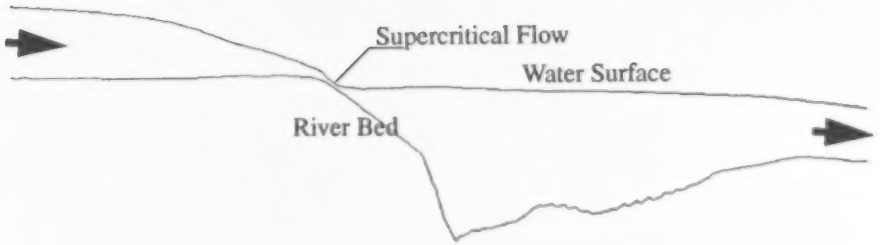

Figure 4.9 Longitudinal Section II-II

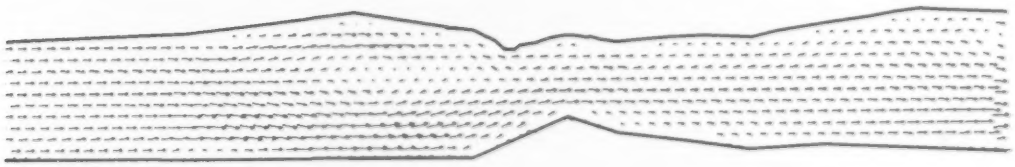

Figure 4.10 Computed Steady State Velocity Vectors

In Figure 4.11 it can be seen that both models perform reasonably well, the two-dimensional model performing slightly better. However Figure 4.12 shows a much better performance of the two-dimensional model. From the measured velocity data in Figure 4.12 it can be seen that a lower velocity exists in the deeper part of the cross section. This can be explained by the presence of the submerged island just upstream of that location. It can be seen that the two-dimensional model correctly predicts a lower velocity in this region. The one-dimensional model, however, predicts a higher value based on the higher conveyance. The results of the two-dimensional model could be further improved through a better distribution of the data points over the domain (i.e. less data points at and more in between cross-sections, to describe any interesting topographic features present between the sections), and through knowledge of the actual river alignment.

Conservation has been checked by comparing the values of total discharge entering the reach at the upstream section and leaving the reach at the downstream section. The difference was found to be less than 0.001%.

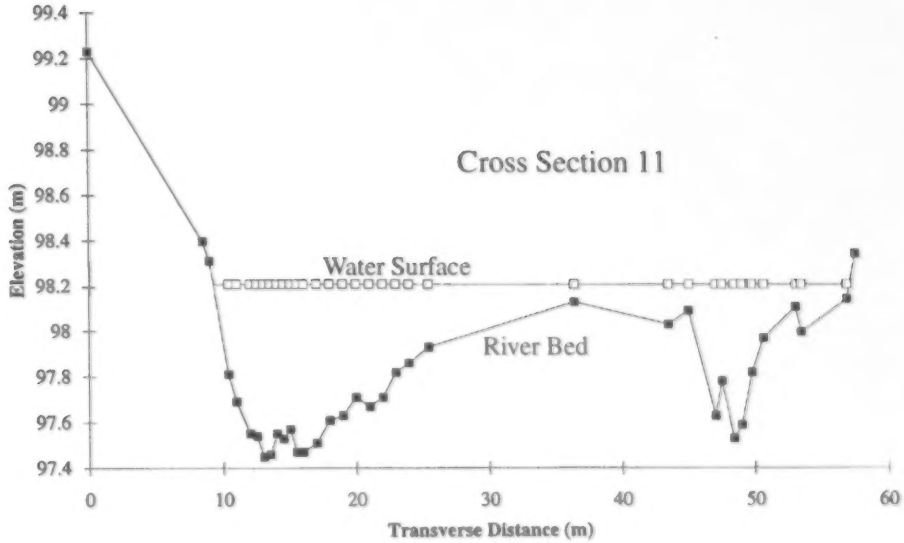

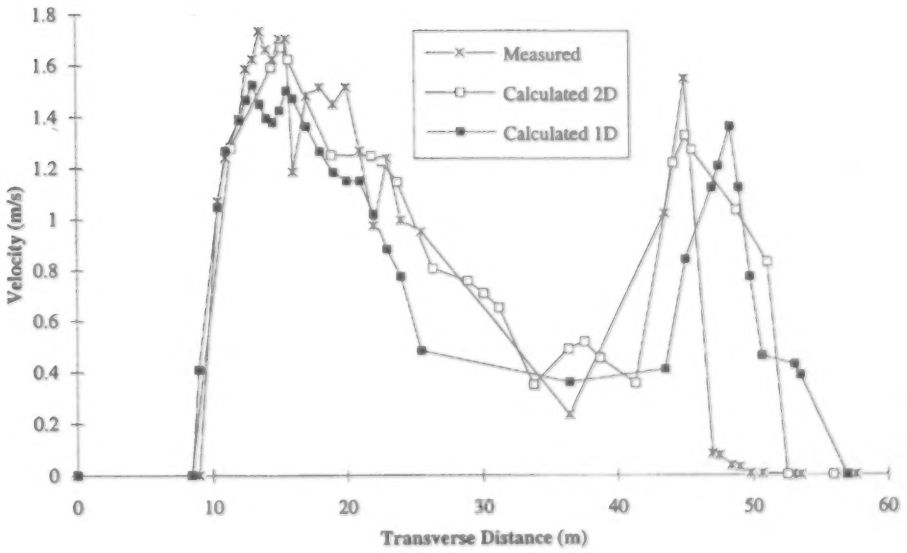

Figure 4.11 Comparison Between Measured and Simulated Velocities
Cross Section 11 (Refer to Figure 4.4 for Cross Section Number)

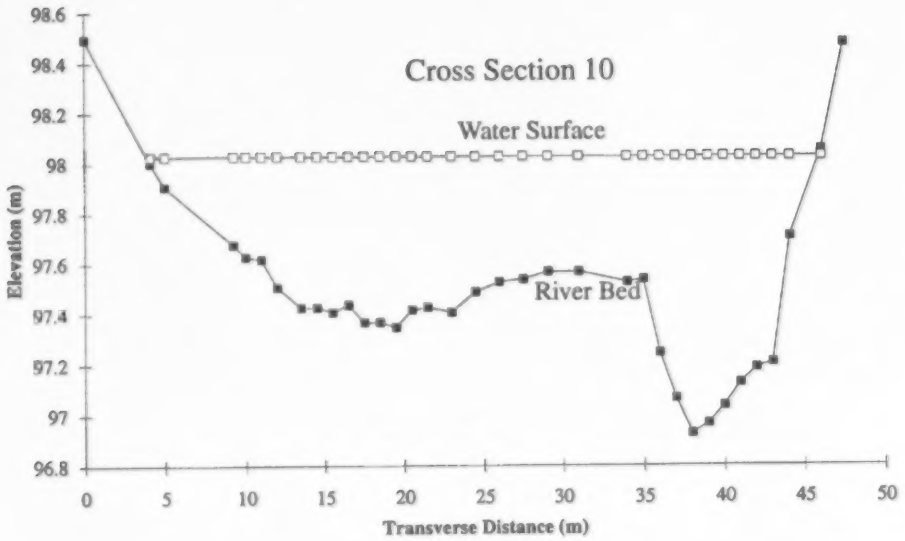

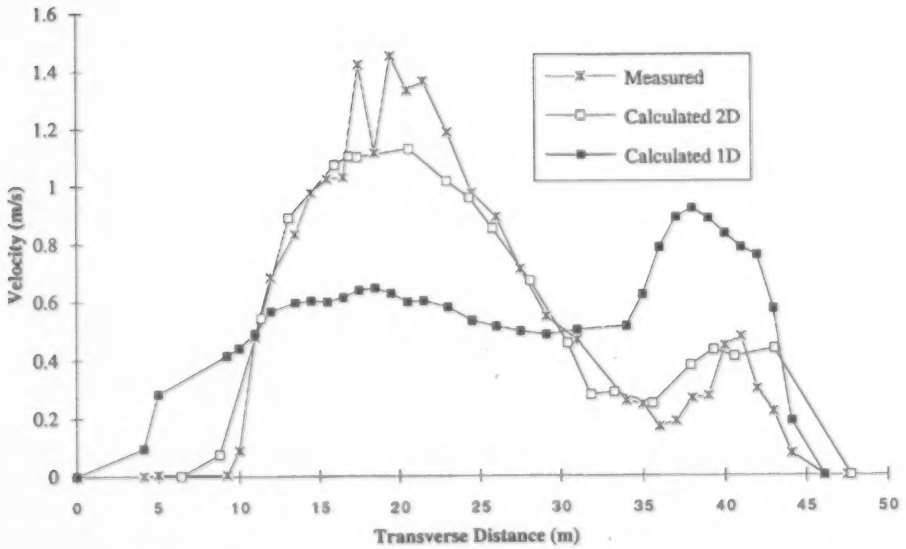

Figure 4.12 Comparison Between Measured and Simulated Velocities
Cross Section 10 (Refer to Figure 4.4 for Cross Section Numbers)

4.3.2 Simulation of Low Flow

At the low flow of 1.52 m^3/sec, the island becomes exposed. The same values of roughness height and turbulent exchange coefficient as for the high flow simulation were used. Figure 4.13 shows the calculated depth contours at a low flow of 1.52 m^3/sec. It can

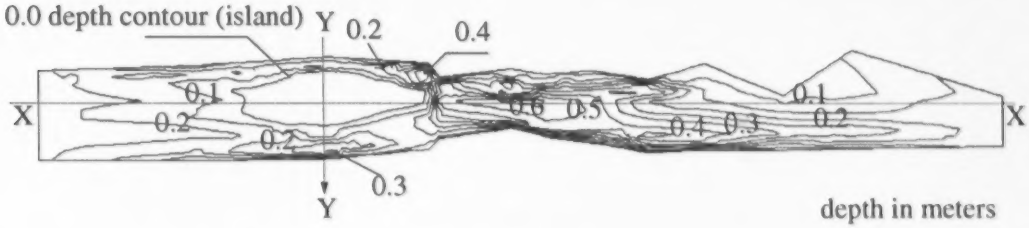

Figure 4.13 Depth Contours at Low Flow (Q = 1.52 m^3/sec)

be seen that the width of the river is now smaller and that the island is exposed. Figure 4.14 shows longitudinal cross section (X-X) through the island. Regions of ground- and

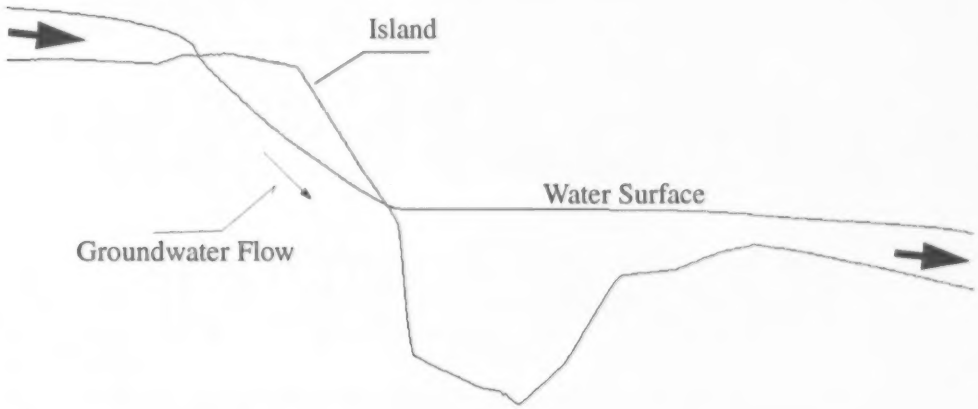

Figure 4.14 Longitudinal Section X-X

surface water flow can be seen. Figure 4.15 shows cross-section Y-Y through the island. It can be seen that the water surface on the right side of the island is slightly higher than on the left side, and therefore, a slight transverse groundwater flow is observed as shown. In Figure 4.16 the predicted velocity vectors are plotted. Figure 4.17 and Figure 4.18 com-

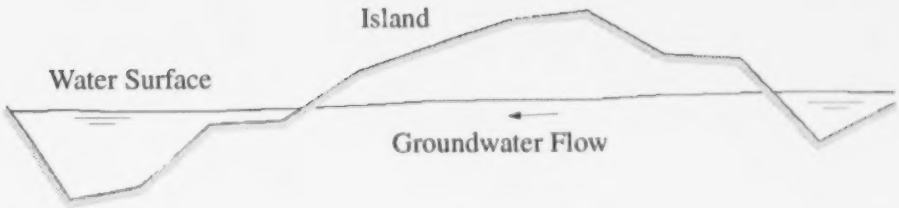

Figure 4.15 Cross-Section Y-Y Through the Island

Figure 4.16 Velocity Vectors at Low Flow (Q = 1.52 m^3/sec)

pare measured to simulated velocity values at cross-sections 11 and 10 respectively (cross-section numbers are shown in Figure 4.4). Considering that at this low flow the average depth of flow is about 0.30 m, and considering the large spacing between cross-sections (e.g. 40.0 m between sections 10 and 11, i.e. a longitudinal spacing between data points larger than 100 times the depth), it can be expected that topographic details in between cross-sections, which might have been insignificant at high flows, could become important for simulating low flows. Therefore, it can be seen that the match between measured and calculated velocities is not as good as for the high flow (Figure 4.11 and Figure 4.12). Hence, when selecting field data points for the two-dimensional model, even when measuring at high flow, the lowest flow to be simulated, and the corresponding small depths, should always be kept in mind.

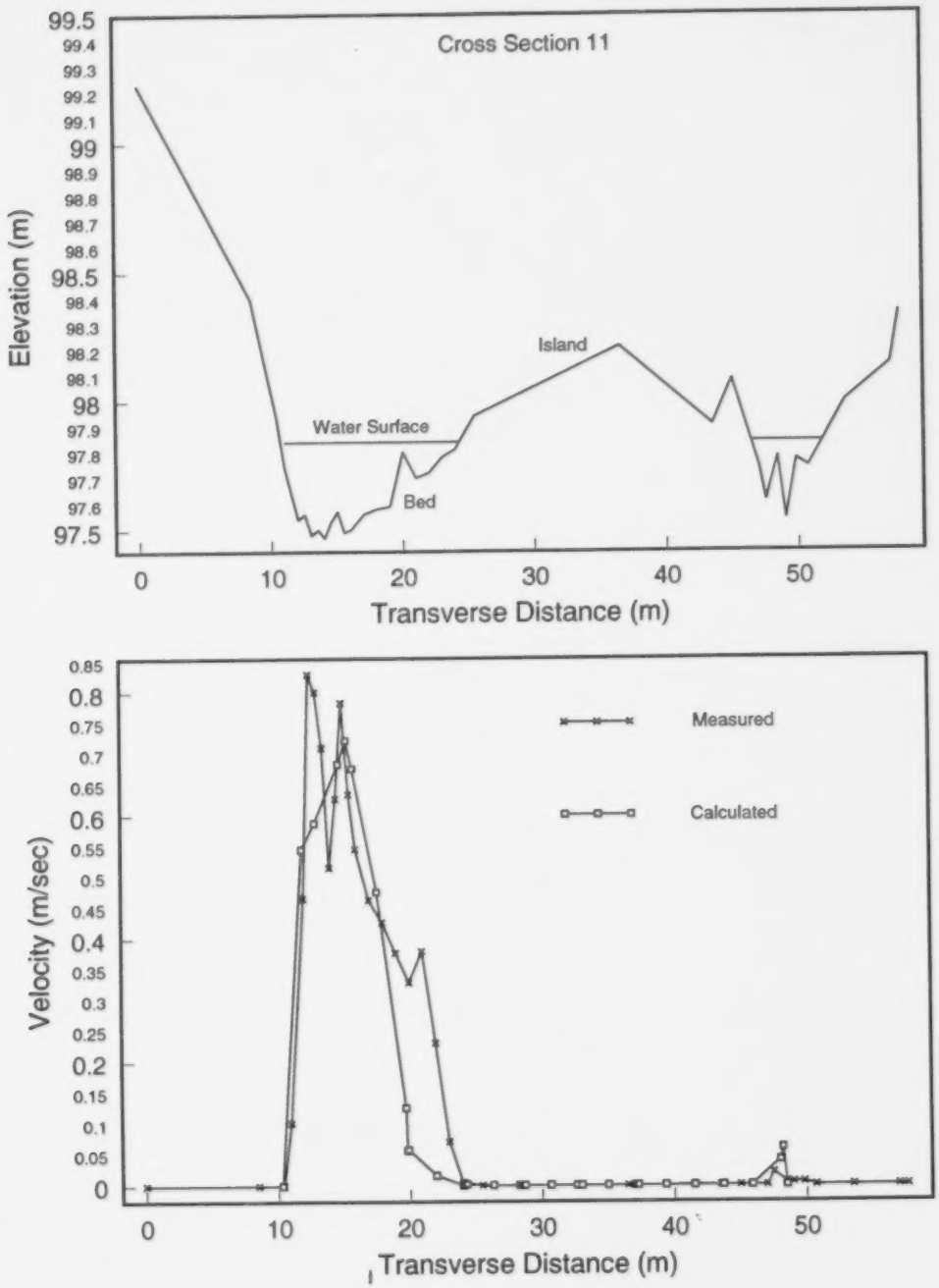

Figure 4.17 Comparison Between Measured and Simulated Velocities at Low Flow (Cross-Section 11)

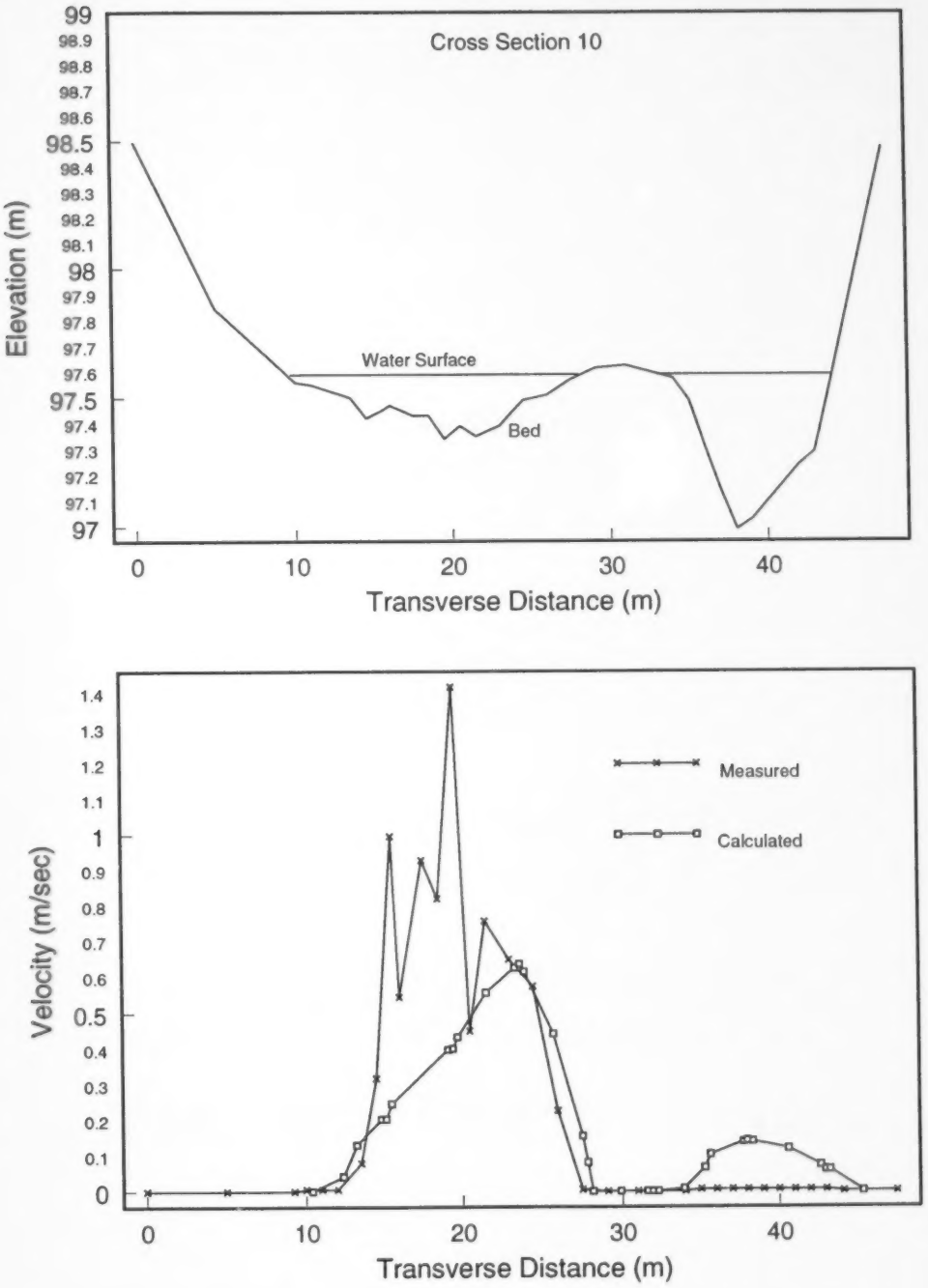

Figure 4.18 Comparison Between Measured and Simulated Velocities at Low Flow (Cross-Section 10)

Chapter 5

Summary and Conclusions

The main purpose of the present research was to develop an accurate and robust two-dimensional finite element flow simulation model. Several shortcomings in the presently available two-dimensional computer models have been pointed out in Chapter 1, such as the need for excessive artificial diffusion, cross-wind diffusion, poor conservation properties and difficulty to simulate complex flow phenomena such as shocks, domains containing variations between super- and subcritical flows, and partially dry bed conditions.

The Finite Element method has been chosen for this work because of its consistency, generality and ability to conform well to complex domains. Several features have been implemented in the model and tested through hypothetical and real flow situations. The presented Characteristic-Dissipative-Galerkin technique is stable and accurate in simulating shocks and domains containing variations of super- and subcritical flow. The upwinding is third order accurate, and thus preserves the interesting flow features. Comparison between laboratory measurements and simulation of standing waves resulting from supercritical flow in a channel constriction showed satisfactory agreement. Numerical tests of simulating a hydraulic jump and a dambreak problem first with the mesh aligned with the x-coordinate axis and then at 45° with the coordinate axes showed that the selected

upwinding matrices have the property of reducing correctly to the optimal one-dimensional system case.

The integration by parts of the governing equations facilitated a natural implementation of boundary conditions. The application of the different types of boundary conditions has been extensively tested and showed satisfactory performance. As the conservation form of the shallow water flow equations is used, the model possesses excellent conservation properties (sections 3.2 and 3.4).

A technique has been proposed to simulate flow in wet/dry domains. Simulation of a dambreak problem on an initially dry bed compared well to measurements taken by Schoklitsch (1917). Other hypothetical and real tests confirmed the robustness of the technique for any degree of geometric complexity (sections 3.8 and 4.3). This is an important feature when simulating flow in natural rivers and fish habitats, especially at the low flows which usually result in limiting conditions for fish. Further, it facilitates the simulation of other complex flow phenomena such as flow from the main channel to the floodplain and tidal processes.

The model has been applied to simulate flow in a natural fish habitat and showed good agreement with field measurements. The model can utilize cross section field data collected for a one-dimensional model to automatically develop a two-dimensional finite element mesh.

The numerical properties of the developed two-dimensional model make it a good tool for simulation the complex flow in natural fish habitat. As the presently used one-dimensional models require extensive velocity measurements at each cross section for different discharges, using a two-dimensional model would result in a substantial reduction in total project time and cost. This would be particularly useful when studying non-wadable rivers, where it would be difficult to obtain the extensive velocity measurements required for the one-dimensional model.

The two-dimensional model would give a better representation of the flow, as it accounts for the two-dimensional flow features resulting usually from islands, meanders, water projects, etc., and thus would be able to simulate complex flow patterns such as recirculation, vortices (horizontal velocity components only) and transverse water surface

slopes. The model would also be able to account for unsteady flow and simulate sub- and supercritical flows and localized shocks. The two-dimensional model gives more flexibility in collecting the data points, thus allowing to collect less data along the transects and more data along the stream at locations which are interesting from a biological point of view. The need for cross-section weighting factors, which involve subjectivity in their determination, would be eliminated. Further, the two-dimensional model would help in answering questions about other uses of the river such as recreational activities, riparian vegetation, slope stability, releases from power stations, safe ramping rates etc.

As the two-dimensional model provides a good representation of the flow field and possesses good conservation properties, it could be further developed to simulate transport phenomena and flow under ice cover. The finite element mesh could be utilized directly to integrate habitat quality parameters over the simulation domain.

References

Abbott, M.B., 1979. Computational Hydraulics - Elements of the Theory of Free Surface Flows. Pitman Publishing Company, London, England.

Akanbi, A. A., and Katopodes, N. D., 1988. Model for Flood Propagation on Initially Dry Land. Journal of Hydraulic Engineering, ASCE, Vol. 114, No. 7, pp. 689-706.

Alcrudo, F. and Garcia-Navarro, P., 1993. A High-Resolution Godunov-Type Scheme in Finite Volumes for the 2D Shallow-Water Equations. International Journal for Numerical Methods in Fluids, Vol. 16, pp. 489-505.

ASCE Task Committee on Turbulence Models in Hydraulic Computations, 1988. Turbulence Modeling of Surface Water Flow and Transport. Journal of Hydraulic Engineering, ASCE, Vol. 114, No. 9.

Bates, P. D., Malcolm, G. A., Baird, L., Walling, D. E. and Simm, D., 1992. Modeling Floodplain Flows Using a Two-Dimensional Finite Element Model. Earth Surface Processes and Landforms, Vol. 17, pp. 575-588.

Bechara, J. A., Leclerc, M., Belzile, L., and Boudreau, P., 1994. A Numerical Method for Modeling the Dynamics of the Spawning Habitat of Landlocked Salmon. Proceedings of the First International Symposium on Habitat Hydraulics, The Norwegian Institute of Technology, Trondheim, Norway, pp. 170-185.

Benque, J. P., Cunge, J. A., Feuillet, J., Hauguel, A. and Holly, F. M., 1982. New Method for Tidal Current Computation. Journal of the Waterway, Port, Coastal and Ocean Division, ASCE, Vol. 108, No. WW3, pp. 396-417.

Bertin, J. J., 1987. Engineering Fluid Mechanics. 2nd ed. Englewood Cliffs, N.J., Prentice-Hall.

Bietz F. B., Martin, J. A. and Englert, J., 1985. Instream Flow Needs for Fish in Alberta: A Users Guide to Assessment Methods. Alberta Energy and Natural Resources, Fish and Wildlife Division, Edmonton, Alberta.

Bilodeau, L., 1991. Two-Dimensional Modeling of a Submergence Flow over a Rugged Topography. Colloque International sur La Modelisation des Ondes de Submersion, Montreal.

Binns, N.A. and Eiserman, F. M., 1979. Quantification of Fluvial Trout Habitat in Wyoming. Transactions of the American Fisheries Society, Vol. 108, pp. 215-228.

Boss Corporation and Brigham Young University, 1992. Boss FASTTABS, User's Manu-

al.

Bovee, K. D. and Milhous, R. T., 1978. Hydraulic Simulation in Instream Flow Studies: Theory and Techniques. Instream Flow Information Paper No. 5. U.S. Fish and Wildlife Service. FWS/OBS-78/33

Bovee, K.D., 1982. A Guide to Stream Habitat Analysis Using the Instream Flow Incremental Methodology. Instream Flow Information Paper No. 12. U.S. Fish and Wildlife Service. FWS/OBS-82/26

Bovee, K.D., 1986. Development and Evaluation of Habitat Suitability Criteria for Use in the Instream Flow Incremental Methodology. Instream Flow Information Paper No. 21. U.S. Fish and Wildlife Service. Biol. Rep. 86(7).

Bowlby, J.N. and Roff, J.C., 1986. Trout Biomass and Habitat Relationships in Southern Ontario Streams. Transactions of the American Fisheries Society, Vol. 115, pp 503-514.

Brooks, A. N. and Hughes, T. J. R., 1982 Streamline Upwind Petrov Galerkin Formulations for Convection Dominated Flows with Particular Emphasis on the Incompressible Navier-Stokes Equations. Computer Methods in Applied Mechanics and Engineering, Vol. 32, pp. 199-259.

Burnett, D. S., 1987. Finite Element Analysis. Addison-Wesley Publishing Company, Don Mills, Canada.

Chaudhry, M. H., 1993. Open-Channel Flow. Prentice Hall, New Jersey.

Chow, V.T., 1959. Open-Channel Hydraulics. McGraw-Hill Book Co., New York.

Cuplin, P. and Van Haveren, B., 1979. Instream Flow Guidelines. U.S. Bureau of Land Management, Washington D.C.

Daubert, A. and Graffe O., 1967. Quelques Aspects des Ecoulements presque Horizontaux a Deux Dimensions en Plan et Non Permanants Application aux Estuaires. La Houille Blanche, No. 8, pp. 847-860.

Fennema, R. J. and Chaudhry, M. H., 1990. Explicit Methods for 2-D Transient Free-Surface Flows. Journal of Hydraulic Engineering, ASCE, Vol. 116, No. 8, pp. 1013-1034.

Fernett, D., 1992. Instream Flow Incremental Methodology (IFIM) - Applications in Western Canada. Oral Presentation at IFN Seminar, Edmonton, Alberta, April 14th, 1992.

Finnie, J. I., 1992. Solving Turbulent Flows Using Finite Elements. Journal of Hydraulic Engineering, ASCE, Vol. 117, No. 11, pp. 1513-1530.

French, R.H., 1986. Open-Channel Hydraulics. McGraw-Hill Book Co., New York.

Fritz, E.S., 1980. Potential Impacts of low PH on Fish and Fish Populations. U.S. Fish and Wildlife Service, Biological Services Program, National Power Plant Team.

Froehlich, D. C., 1989. Finite Element Surface Water Modeling System: Two-dimensional Flow in a Horizontal Plane, Users Manual. U. S. Federal Highway Administration, Report No. FHWA-RD-88-177.

Gee, M. D., Anderson, M. G., and Baird, L., 1990. Two-Dimensional Floodplain Modeling. US Army Corps of Engineers, Hydrologic Engineering Center. Technical Paper No. 128.

Geer, W. H., 1980. Evaluation of Five Instream Needs Methodologies and Water Quantity Needs of Three Utah Trout Streams. U.S. Fish and Wildlife Service, Ft. Collins, CO. Publication W/IFG-80/W91.

Ghanem, A. H., and Hicks, F.E. (1992) A Review of the Hydraulic Models Used in Instream Flow Needs Assessment Methods. Water Resources Engineering Report No. 92-4, Department of Civil Engineering, University of Alberta, Canada.

Gray, W. G. and Lynch, D. R., 1979. On the Control of Noise in Finite Element Tidal Computations: A Semi-Implicit Approach. Computers and Fluids, Vol. 7, pp. 47-67.

Gresho, P. and Lee, R. L., 1979. Don't Suppress the Wiggles-They're Telling You Something. In: Finite Element Methods for Convection Dominated Flows, AMD Vol. 34, ASME, pp. 37-62.

HEC-2, 1990. Water Surface Profiles: Users Manual. Hydrologic Engineering Center, U.S. Army Corps of Engineers, Davis, CA.

Hedstrom, G. W., 1979. Nonreflecting Boundary Conditions for Nonlinear Hyperbolic Systems, Journal of Computational Physics, Vol. 31, pp. 222-237.

Heinrich, J. C., Huyakorn, P. S., Zienkiewicz O. C. and Mitchell, A. R., 1977. An 'upwind' Finite Element Scheme for Two-Dimensional Convective Transport Equation. International Journal for Numerical Methods in Engineering, Vol. 11, pp. 134-143.

Henderson, F. M., 1966. Open Channel Hydraulics. Mcmillan Series in Civil Engineering, New York.

Hervouet, J. M. and Janin, J. M., 1994. Finite Element Algorithms for Modeling Flood Propagation. Modeling of Flood Propagation over Initially Dry Areas, Proceedings of the Specialty Conference co-sponsored by ASCE-CNR/GNDCI-ENEL spa, pp. 102-113.

Hicks, F. E. and Steffler, P. M., 1990. Finite Element Modeling of Open Channel Flow. Department of Civil Engineering, University of Alberta, Technical Report (WRE 90-

6).

Hicks, F. E. and Steffler, P. M., 1992. Characteristic Dissipative Galerkin Scheme for Open-Channel Flow. Journal of Hydraulic Engineering, ASCE, Vol. 118, No. 2, pp. 337-352.

Hirsch, C., 1988. Numerical Computation of Internal and External Flows. John Wiley and Sons. Vol. 1 and 2.

Hogan, D. L. and Church, M., 1989. Hydraulic Geometry in Small Coastal Streams: Progress Toward Quantification of Salmonid Habitat. Canadian Journal of Fisheries and Aquatic Sciences, Vol. 46, pp 844-852.

Hoger, A. and Carlson, D. E., 1984. Determination of the Stretch and Rotation in the Polar Decomposition of the Deformation Gradient. Quarterly of Applied Mathematics. Vol. 42, No. 1, pp. 113-117.

Hoppe, R. A., 1975. Minimum Streamflows for Fish. Soils-Hydrology Workshop, U.S. Forest Service, Montana State University, Bozeman.

Hughes, T. J. R. and Brooks, A. N., 1979. A Multi-Dimensional Upwind Scheme with no Crosswind Diffusion. In: Finite Element Methods for Convection Dominated Flows, AMD Vol. 34, ASME, pp. 19-35.

Hughes, T. J. R. and Mallet, M., 1986 a. A New Finite Element Formulation for Computational Fluid Dynamics: III. The Generalized Streamline Operator for Multidimensional Advective-Diffusive Systems. Computer Methods in Applied Mechanics and Engineering, Vol. 58, pp. 305-328.

Hughes, T. J. R. and Mallet, M., 1986 b. A New Finite Element Formulation for Computational Fluid Dynamics: IV. A Discontinuity-Capturing Operator for Multidimensional Advective-Diffusive Systems. Computer Methods in Applied Mechanics and Engineering, Vol. 58, pp. 329-336.

Hughes, T. J. R., Franca, L. P. and Mallet, M., 1986. A New Finite Element Formulation for Computational Fluid Dynamics: I. Symmetric Forms of the Compressible Euler and Navier-Stokes Equations and the Second Law of Thermodynamics. Computer Methods in Applied Mechanics and Engineering, Vol. 54, pp. 223-234.

Hughes, T. J. R., Mallet, M. and Mizukami, A., 1986. A New Finite Element Formulation for Computational Fluid Dynamics: II. Beyond SUPG. Computer Methods in Applied Mechanics and Engineering, Vol. 54, pp. 341-355.

Ippen, A. T. and Dawson, J. H., 1951. Design of Channel Contractions. Transactions of the American Society of Civil Engineers, Vol. 116, pp. 326-346.

Katopodes, N. and Strelkoff, T., 1978. Computing Two-Dimensional Dam-Break Flood

Waves. Journal of Hydraulic Engineering, ASCE, Vol. 104, No. 9, pp. 1268-1288.

Katopodes, N. D. and Strelkoff, T., 1979. Two-Dimensional Shallow Water Wave Models. Journal of the Engineering Mechanics Division, ASCE, Vol. 105., No. EM2, pp. 317-334.

Katopodes, N. D., 1977. Two-Dimensional Unsteady Flow through a Breached Dam by the Method of Characteristics. Ph. D. Thesis, University of California, Davis, pp. 157.

Katopodes, N. D., 1984. A Dissipative Galerkin Scheme for Open-Channel Flow. Journal of Hydraulic Engineering, Vol. 110, No. 4, pp. 450-466.

King, I. P. and Norton, W. R., 1986. Finite Element Model for Two-Dimensional Depth Averaged Flow, RMA-2V, Version 3.3b. Resource Management Associates, Lafayette, CA.

Lai, C., 1986. Numerical Modeling of Unsteady Open Channel Flow. Advances in Hydroscience, Vol. 14.

Layher, W. G., 1983. Habitat Suitability for Selected Adult Fishes in Prairie Streams. Ph.D. dissertation, Oklahoma State University, Stillwater.

Leclerc, M., Bellemare, J., Dumas, G., and Dhatt, G., 1990. A Finite Element Model of Estuarian and River Flows with Moving Boundaries. Advances in Water Resources, Vol. 13, No. 4, pp. 158-168.

Lee, J. K. and Froehlich, D. C., 1986. Review of Literature on the Finite-Element Solution of the Equations of Two-Dimensional Surface-Water Flow in the Horizontal Plane. U. S. Geological Survey, Circular 1009.

Leonard, B. P., 1979. A Survey of Finite Differences of Opinion on Numerical Muddling of the Incomprehensible Defective Confusion Equation. In: Finite Element Methods for Convection Dominated Flows, AMD Vol. 34, ASME, pp. 1-18.

Ligget, J. A., 1974. Equations of Unsteady Flow. Unsteady Flow in Open Channels, ed. Mahmood K. and Yevjevich V., Vol. 1, pp. 29-62.

Lo, S.H., 1985. A New Mesh Generation Scheme for Arbitrary Planar Domains. *International Journal for Numerical Methods in Engineering*, 21, pp. 1403-1426.

Milhous, R. T., Wegner, D. L. and Waddle, T., 1981. Physical Habitat Simulation System (PHABSIM). Instream Flow Information Paper No. 11. U.S. Fish and Wildlife Service. FWS/OBS-81/43 Revised.

Milhous, R.T., Updike, M.A., and Schneider, D.M., 1989. Physical Habitat Simulation System (PHABSIM) Reference Manual-Version II. Instream Flow Information Paper No. 26. U.S. Fish and Wildlife Service. Biol. Rep. 89 (16)

Morhardt, J.E., 1986. Instream Flow Methodologies. Electric Power Research Institute, Palo Alto, Ca. Research Project 2194-2.

Nelson, F.A., 1984. Guidelines for Using the Wetted Perimeter (WETP) Computer Program. Montana Department of Fish, Wildlife and Parks, Bozeman, Montana.

Northern Great Plains Resource Program, 1974. Instream Needs Subgroup Report: Work Group C.

Orth, D.J. and Maughan, O.E., 1982. Evaluation of the Incremental Methodology for Recommending Instream Flows for Fishes. Transactions of the American Fisheries Society, Vol. 111, pp 413-445.

Rabern, D. A., 1984. Development of Habitat Based Models for Predicting Standing Crops of Nine Species of Riverine Fishes in Georgia. M.Sc. Thesis, University of Georgia, Athens.

Randolph, C. L. and White, R. G., 1984. Validity of the Wetted Perimeter Method for Recommending Instream Flows for Salmonids in Small Streams. Montana Water Resources Research Center, Bozeman.

Reiser, D. 1992. Instream Flow Needs Methods - Applications in North America. Oral Presentation at IFN Seminar, Edmonton, Alberta, April 14th, 1992.

Rodi, W., 1984. Turbulence Models and their Application in Hydraulics - A State of the Art Review, 2nd ed. IAHR, Delft.

Samuels, P. G., 1983. Two-Dimensional Modeling of Flood Flows using the Finite Element Method. International Conference on the Hydraulic Aspects of Floods and Flood Control, London, England, pp. 229-240.

Schoklitsch, A., 1917. Ueber Dammbruchwellen. Sitzungsberichte der Kaiserlichen Akademie der Wissenschaften, Vienna, Vol. 126, pp. 1489-1514.

Shakib, F., Hughes, T. J. R. and Johan, Z., 1991. A New Finite Element Formulation for Computational Fluid Dynamics: X. The Compressible Euler and Navier-Stokes Equations. Computer Methods in Applied Mechanics and Engineering, Vol. 89, pp. 141-219.

Soulis, J. V., 1992. Computation of Two-Dimensional Dam-Break Flood Flows. International Journal for Numerical Methods in Fluids, Vol. 14, pp. 631-664.

Steffler, P. M. and Jin, Y. C., 1993. Depth Averaged and Moment Equations for Moderately Shallow Free Surface Flow. Journal of Hydraulic Research, IAHR, Vol. 31, No. 1, pp. 5-17.

Streeter, V. L. and Wylie, E. B., 1981. Fluid Mechanics. McGraw-Hill Ryerson Limited.

Swank, G. W. and, Phillips, R. W., 1976. Instream Flow Methodology for the Forest Service in the Pacific Northwest Region. Proceedings of the Symposium and Specialty Conference on Instream Flow Needs, American Fisheries Society, Vol. II, pp 334-343.

Swift, C. H., 1976. Estimates of Stream Discharges Preferred by Steelhead Trout for Spawning and Rearing in Western Washington. USGS Open File Report 75-155. U.S. Geological Survey, Tacoma, WA.

Tchamen, G. W. and Kahawita, R., 1994. The Numerical Simulation of Wetting and Drying Areas Using Riemann Solvers. Modeling of Flood Propagation over Initially Dry Areas, Proceedings of the Specialty Conference co-sponsored by ASCE-CNR/GNDCI-ENEL spa, pp. 127-140.

Tennant, S. A., 1976. Instream Flow Regimes for Fish, Wildlife, Recreation and Related Environmental Resources. Proceedings of the Symposium and Specialty Conference on Instream Flow Needs, American Fisheries Society, Vol. II, pp 359-373.

Thacker, W. C., 1978. Comparison of Finite Element and Finite Difference Schemes. Part I: One-Dimensional Gravity Wave Motion. Journal of Physical Oceanography, Vol. 8, pp. 676-679.

Thacker, W. C., 1978. Comparison of Finite Element and Finite Difference Schemes. Part II: Two-Dimensional Gravity Wave Motion. Journal of Physical Oceanography, Vol. 8, pp. 680-689.

Van Rijn, L. C., 1990. Principles of Fluid Flow and Surface Waves in Rivers, Estuaries, Seas, and Oceans. Aqua Publications, Amsterdam, The Netherlands.

Verboom, G. K., Stelling, G. S. and Officier, M. J., 1982. Boundary Conditions for the Shallow Water Equations, in Engineering Applications of Computational Hydraulics, Vol. 1, (Abbott, M. B. and Cunge, J. A. ed), Pitman, pp. 230-262.

Walters, R. A. and Carey, G. F., 1983. Analysis of Spurious Oscillation Modes for the Shallow Water and Navier-Stokes Equations. Computer and Fluids, Vol. 11, No. 1, pp. 51-68.

Walters, R. A. and Cheng, T., 1980. Accuracy of an Estuarine Hydrodynamic Model Using Smooth Elements. Water Resources Research, Vol. 16, No. 1, pp. 187-195.

Walters, R. A., 1983. Numerically Induced Oscillations in Finite Element Approximations to the Shallow Water Equations. International Journal for Numerical Methods in Fluids, Vol. 3, pp. 591-604.

Walters, R. A., and Carey G.F., 1984. Numerical Noise in Ocean and Estuarine Models. Advances in Water Resources, Vol. 7, pp. 15-20.

Waters, B. F., 1976. A Methodology for Evaluating the Effects of Different Streamflows on Salmonid Habitat. Proceedings of the Symposium and Specialty Conference on Instream Flow Needs, American Fisheries Society, Vol. II, pp 254-266.

Weiyan, T., 1992. Shallow Water Hydrodynamics. Elsevier Oceanography Series, 55. Elsevier, Amsterdam.

Wesche, T. A. and Rechard, P.A., 1980. A Summary of Instream Flow Methods for Fisheries and Related Research Needs. Water Resources Research Institute, University of Wyoming, Laramie.

White, R. J. and Brynildson, O. M., 1967. Guidelines for Management of Trout Stream Habitat in Wisconsin. Wisconsin Department of National Research Technology, Bull. 39.

White, R. J., Hansen, E. A. and G. R. Alexander, 1976. Relationship of Trout Abundance to Stream Flow in Midwestern Streams. Proceedings of the Symposium and Specialty Conference on Instream Flow Needs, American Fisheries Society, Vol. II, pp 376-399.

Zhao, D. H., Shen, H. W., Tabios, G. Q., Lai, J. S., and Tan, W. Y., 1994. Finite Volume Two-Dimensional Unsteady-Flow Model for River Basins. Journal of Hydraulic Engineering, ASCE, Vol. 120, No. 7, pp. 863-883.

Zienkiewicz, O. C., 1977, The Finite Element Method. McGraw-Hill Book Company, UK.

Appendix A

Field Data Collection for Two-dimensional Flow Simulation of Fish Habitat

The two-dimensional model can directly utilize data collected for a one-dimensional model to generate a two-dimensional finite element mesh. It should be noted however, that for a one-dimensional model, strict specifications exist for the spacing between data points along the transect, whereas many interesting and important details between transects can be lost, as no data are taken (or could be utilized) in between transects for the one-dimensional model. A data point in the one-dimensional model represents a very narrow and long rectangle (cell), over which stream characteristics are assumed to be constant. This same cell is used later in the habitat simulation model. On the other hand, the two-dimensional model can make use of any information anywhere in the stream, with a data point representing the stream characteristics at its exact location. Linear interpolation is then applied to predict properties between data points, resulting in a continuous representation of the stream topography. Therefore, to make better use of the modeling capabilities of the two-dimensional model, the following should be taken into consideration while collecting field data:

1. It should be noted that the two-dimensional model does not require that the data be collected by cross sections (except at the inflow and outflow sections, where it would be useful to have cross section information for specification of boundary conditions). Any available data describing the topography of the domain (e.g. relative location and elevation of each data point) can be readily read in and used to develop the two-dimensional finite element mesh. When collecting field data for the two-dimensional model it should be kept in mind that it is intended to predict flow phenomena such as recirculation, separation, flow around islands and obstructions etc. Hence, data points should be placed to adequately represent topographic features such as islands, riffles, pools, bars, dunes, and obstructions, or man-made features such as river training works and mitigation structures. If a reach does not show much variation, then a large spacing between data points would be allowed, maybe up to 10 times the average water depth or one quarter of the average stream width, whichever is less. It should be noted that in this case it would still be possible to adequately simulate and predict velocities and depths at locations where field data points were not placed, as long as the stream characteristics between these data points vary linearly.

2. Velocity measurements are not necessarily required for a two-dimensional model. However, for the purpose of comparing the performance of the one- and two-dimensional models, velocity measurements taken for the one-dimensional model calibration should be sufficient. Also, depth measurements are not necessary, but are useful for verifying roughness heights and checking the model performance. Preferably (but not necessarily), a few depth measurements should be taken at a higher flow. If a one-dimensional model is to be used as well (e.g. in order to compare results), then the data requirements for the one-dimensional model should be consulted and will generally be limiting.

3. For each data point, get an estimate of the "roughness height". For a gravel bed river this might be the average particle size. For fine substrate rivers with bedforms (ripples), the roughness height would be the average ripple height. If there are large bedforms (e.g. dunes or sandbars) which have a wavelength larger than about 5 to 7 times the depth of flow, then the bedforms should be captured as topographic features (e.g. by

placing data points at the extremities and the crest), while the roughness height would be equal to the average grain size. For rivers with vegetation, a description of type and size of vegetation would be useful.

4. Measure as high as possible over islands and on the overbanks to facilitate modeling of high flows. Information about vegetation (roughness) would be required here as well.

5. As river meanders are a two-dimensional feature of the stream, it would also be useful to have a measure of the stream sinuosity. If data points are all related to a global x- and y-coordinate system, then the shape of the river meanders would be directly represented by the data points. However, if data are collected at cross sections, then, in addition to distances along the left and right banks, another piece of information, such as the diagonal distance between each two cross sections, would be required (as illustrated below).

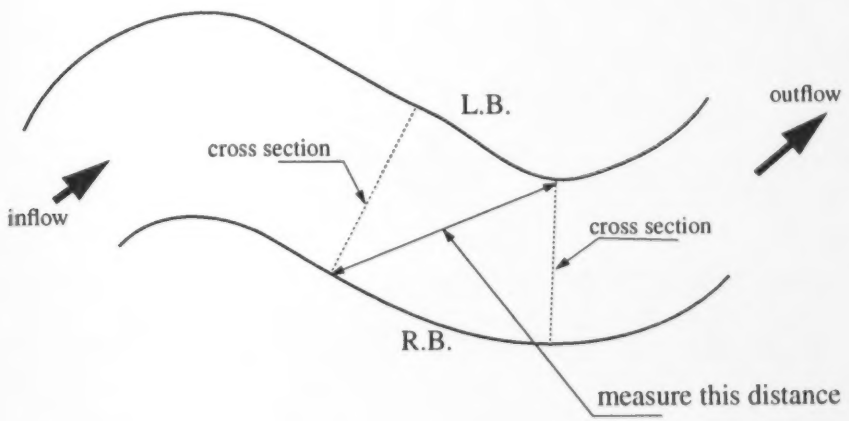

6. The boundaries (first and last cross sections) should be located at points along the stream where the stage-discharge relationship can be readily defined. For example, at gauge sites, weirs, rapids or approximately uniform flow reaches. In the absence of a well defined stage-discharge relationship, additional cross sections upstream and downstream of the study area would be helpful. It is important to note that this is a requirement of any hydraulic model (one-dimensional or two-dimensional).

7. Any information that would aid in completing the picture of the flow domain is valuable. Photographs, sketches, field notes, maps, GIS type information and description of vegetation and/or exposed bedforms could be utilized to develop and/or improve the simulation mesh.

8. The degree of accuracy required for measurements depends on many factors such as the depth of flow, width of river, type of flow, size of reach etc. As a rough guideline, the accuracy in measuring bed elevations should be of the order of 2 to 5 cm, whereas for longitudinal distances it could be within 20 to 50 cm.

Appendix B

Hydraulic Modeling in Instream Flow Needs Assessment Methods

B.1 Introduction

River engineering projects such as bridges, culverts, dams, weirs, water intake structures and channel modifications can potentially present harmful environmental conditions to fish, either by interrupting their migration routes or through changes to their natural habitat. Instream Flow Needs (IFN) studies are used to provide a means of assessing the adverse effects of different hydrotechnical projects on fisheries resources in order to provide guidelines for planners and designers.

Numerous Instream Flow Needs (IFN) assessment techniques have been developed during the last three decades. While some of these methods have found widespread use, others have only been applied successfully by their developers. In this chapter, a number of common IFN methods are presented. Although the methods described do not encompass every single method ever developed, an attempt has been made to consider methods which have gained wide acceptance in North America.

In this thesis, IFN techniques are classified based on the number of input variables. As the name implies, *Single Variable Methods* rely on a single input variable, usually

hydraulic or hydrologic, to recommend a minimum acceptable flow required to assure an adequate fish habitat. *Multi-variable Methods* are more comprehensive in that they consider the effects of several variables on the habitat condition or fish biomass. Among these are the empirical methods, which are developed through statistical analyses of variables known to be limiting to some stage of fish life. The alternative is the deterministic approach such as that used in the Instream Flow Incremental Methodology (IFIM), which considers relationships between streamflow and usable habitat area for different life stages of fish species.

Aside from the suitability of each model to the purpose of defining adequate fish habitat conditions, a topic beyond the scope of this thesis, there are two key criteria for assessing the hydraulic component of each model. The first is related to the ability of a given model to adequately represent the physics of the flow and the second is the way in which these hydraulic models are implemented and their results interpreted. Therefore, the discussion presented focuses on the theoretical strengths or weaknesses of the hydraulic components, as well as identifying any potential errors in their implementation.

B.2 Single Variable Methods

B.2.1 Introduction

Single Variable Methods base the recommendation for Instream Flow Needs assessments on a single variable which in turn provides a recommended minimum acceptable streamflow for planning purposes, in an attempt to assure adequate fish habitat. Although these methods are relatively simple to use, they cannot quantify changes in available habitat as a result of proposed modifications to the stream channel. Single Variable Methods may be broadly grouped into two categories: those based on a representative discharge and those based on channel hydraulic characteristics.

B.2.2 Discharge Methods

B.2.2.1 General

Discharge methods are particularly suited to preliminary feasibility studies as they are entirely based on readily available data from water survey stations and, therefore,

require no field data collection. The fundamental concept underlying these methods is that the minimum discharge required to ensure adequate fish habitat can be related to some representative streamflow, such as the mean annual flow (Bietz et al., 1985).

B.2.2.2 Tennant's Method (Montana Method)

Tennant (1976) presented the results of numerous field studies conducted over several years and which involved 11 streams in Montana, Nebraska and Wyoming, U.S.A. Based on this data, Tennant concluded that the conditions of the aquatic habitat is remarkably similar on most streams carrying the same portion of the average flow and consequently proposed the following qualitative relation between habitat quality and mean annual flow (MAF) as a guideline for IFN assessment studies:

% of Mean Annual Flow	Description
10	minimum instantaneous flow recommended to sustain short-term survival habitat
30	base flow recommended to sustain good survival habitat
60	base flow recommended to provide excellent to outstanding survival habitat

Tennant (1976) observed that width, depth, and velocity all changed more rapidly from no flow to a flow of 10% of the average, than in any range thereafter, as, on average, 10% of the MAF was found to cover about 60% of the maximum wetted perimeter. He also observed that depths averaged 1 foot (0.30 m) and velocities averaged 0.75 ft/sec (0.23 m/sec) at 10% of the MAF, which he states have been shown to be at the lower limit of acceptable values, based on other studies. He further concluded that 30% of the MAF would sustain good survival habitat for most aquatic life forms as this would be reflected in satisfactory widths, depths and velocities and because most of the shallow riffle and shoal areas would be covered with water allowing large fish to move. For the 60% flow, Tennant expected that most of the channel substrate would be covered with water including shallow riffle and shoal areas. The majority of banks would serve as cover for fish. Therefore, Tennant concluded that 60% of the MAF would provide excellent to outstanding habitat conditions. Tennant also stated that these recommendations have been sub-

stantiated through "Analyses of hundreds of additional flow regimens near U.S.G.S. gages in 21 different states..." during the period from 1959 to 1976 (Tennant, 1976).

B.2.2.3 Other Discharge Methods

Although a number of other discharge methods have been proposed, few have gained the wide acceptance that Tennant's method enjoys (Bietz et al., 1985). Morhardt (1986) provided a detailed comparison of these other methods which forms the basis of the following discussion. Hoppe (1975) based his recommendations for minimum acceptable flow on the daily flow exceeded 80% of the time. The method has, however, been criticized as being arbitrary and unsupported (Morhardt 1986). The Northern Great Plains Resource Program (1974) presented a similar model by recommending a minimum flow for each month equal to the flow exceeded on 90% of the days for the months in question for the period of record, but excluding from the analysis those months with extreme mean monthly flows (in the highest and lowest 15%). This method has also been criticized for lack of data supporting any of the criteria chosen, which were found to be completely arbitrary (Morhardt 1986). Geer (1980) developed a method to establish minimum winter and summer flows in Utah streams. The minimum allowable winter flow was based on the average of the minimum monthly flow for the months of October to March, whereas the minimum allowable summer flows were taken as the average of the minimum monthly flow from April to September.

B.2.2.4 Discussion

The singular advantage of Tennants method is that the only data it requires is the mean annual flow, which is readily available for most streams in North America. However, from a hydraulic perspective it should be noted that this approach does not account for the magnitude of discharge fluctuations (i.e. the standard deviation associated with the mean annual flow) and it has been reported that the method overestimates minimum flow recommendations for streams with a large seasonal variability (Bietz et al., 1985; Cuplin and Van Haveren, 1979). Although it was intended by its author as a technique for setting operational flows in a stream, the method can be used to justify a wide range of flows, and recommendations based on it are therefore neither specific nor easy to defend (Morhardt, 1986).

In general, the main criticism of discharge methods stems from their inability to account for seasonal or annual variability of stream flows. Those methods that do attempt to consider at least seasonal variability have been criticized for the arbitrary way in which their criteria are determined. Given that discharge methods can only provide guidelines for describing the impact of proposed changes in discharge on fish habitat in a qualitative way, and that they cannot quantify the impact on available habitat area or fish biomass, refinement is likely not worthwhile. However, their use should be limited to feasibility level studies as they provide no site specific evaluation of proposed water management projects nor any predictive capability.

B.2.3 Methods based on Channel Hydraulic Characteristics

B.2.3.1 General

The fundamental concept underlying these methods (which are also known as hydraulic rating methods) is that the minimum discharge required to ensure adequate fish habitat can be related to some representative characteristic of the stream channel that is important to fish habitat or fish survival, such as water surface width, wetted perimeter, flow area, depth or velocity (Bietz et al., 1985). In general, stage and streamflow data measurements and/or cross section surveys are required to develop a rating curve between the discharge and the parameter of interest.

B.2.3.2 Wetted Perimeter Inflection Point Method

In this method, originally developed and tested by Nelson in 1984 for use in Montana streams, it is assumed that the wetted perimeter adequately represents limiting habitat conditions. The method is based on the assumption that the loss of habitat quality is correlated with low discharges which are associated with stages falling below the cover provided by undercut banks and riparian vegetation. The point, or points, at which this habitat loss becomes critical is defined by the relationship between wetted perimeter and discharge.

To illustrate the method, consider the cross section drawn in Figure B.1 (a), and its corresponding wetted perimeter versus discharge curve, shown in Figure B.1 (b). It is observed that the rate of increase of wetted perimeter is high from 0 to P_1, where the chan-

nel width approaches its maximum. Beyond this stage the rate of change of top width with respect to stage, is small. At higher stages, an increase in discharge results in a much smaller increase in wetted perimeter than is observed at lower stages. Nelson (1984) refers to this point on the stage-discharge curve as the inflection point[1]. A minimum recommended discharge for a particular study reach is based on the average wetted perimeters computed from at least 3 to 10 critical cross sections, although more than 20 cross sections have been used in some cases (Bietz et al., 1985). The reach averaged wetted

1. From a mathematical point of view, calling p_1 an inflection point is incorrect, because a point of inflection is defined as a point where the curvature of a curve changes sign, i. e. the point where the rate of change of the first derivative (slope) is zero. In fact, point p_1 represents the point on the wetted perimeter versus discharge curve, where the rate of change of the slopes is a maximum.

perimeter is then plotted against discharge to identify the inflection point(s) (Randolph and White, 1984).

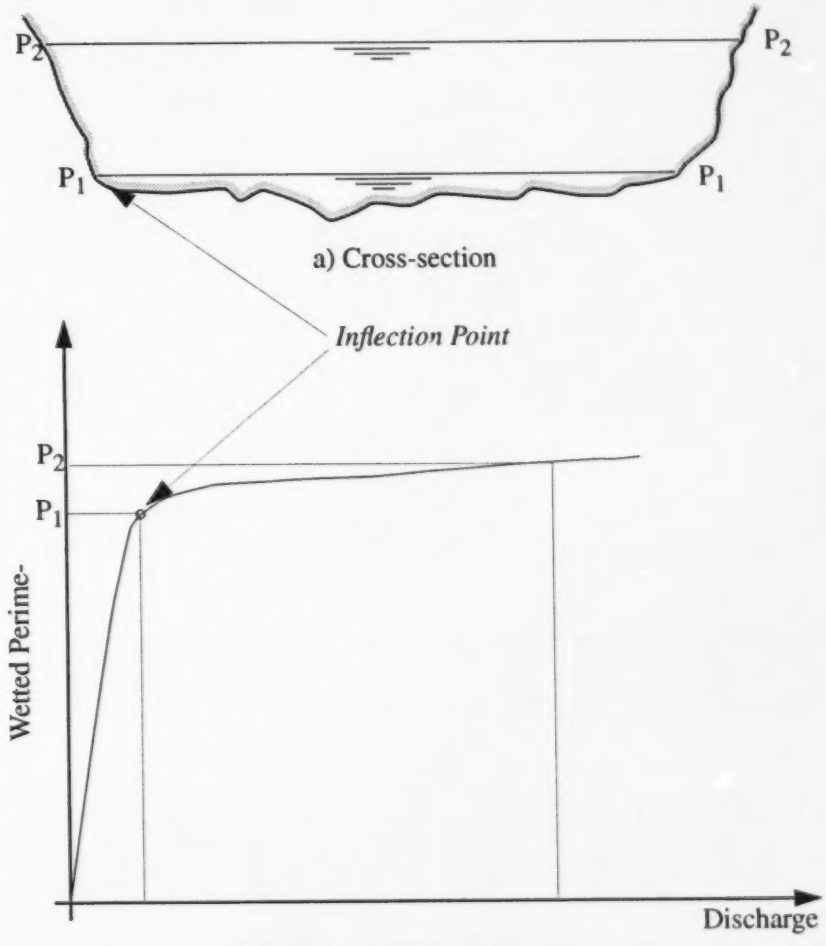

Figure B.2 Wetted Perimeter Inflection Point Method

Implementation of this method first requires development of a rating curve. A survey of the cross section geometry at each of the critical sections is then used to provide the relationship between stage and wetted perimeter. The rating curves are usually developed by assuming uniform flow and estimating water stage for unmeasured flows, although both

Bietz et al. (1985, referencing Leathe and Graham, 1982) and Randolph and White (1984), suggest that inflection points are more easily identified when the rating curve is developed using measured-stage discharge data. Consideration of this recommendation may expose a fundamental weakness of this method in that, typically, the development of the rating curve based on measured stage-discharge data is based on as few as 3 data pairs. Thus, inflection points observed in the resulting wetted perimeter versus discharge curve might be solely attributable to a coarsely discretized rating curve, rather than to the physical attributes of the channel. Although this effect can also occur when developing a theoretical rating curve, it is somewhat less likely, as there is often a tendency to employ a fine discretization in computing the stage discharge relation. In fact, although many authors present the inflection point as a discontinuity in the wetted perimeter versus discharge relationship (Bietz et al., 1985; Randolph and White, 1984; Bovee and Milhous, 1978) its proper recognition as the point where the curvature is a maximum might facilitate a more reliable and consistent means of identification.

It should be noted that averaging the wetted perimeter versus discharge relationship over a reach might, in some cases, prevent physically based inflection points from being identified. Finally, given the weak hydraulic basis of this method, and given the questionable implementation practices currently in use, it is likely that physical identification of a critical stage in the field and a proper hydraulic analysis to determine the associated discharge would be a more accurate approach.

B.2.3.3 Other Methods Based on Channel Characteristics

Swift (1976) chose a parameter which he called toe width which was defined as the horizontal distance from the point where the streambed and one bank join to the ground surface on the other bank. Thus, this method could be correlated to the Wetted Perimeter Inflection Point Method, as the toe width as it is defined, and as it appears from drawings in Swift's report (1976), is close to the width of the water surface for the flow at which the inflection point exists on the wetted perimeter versus discharge curve. Swift (1976) presented empirical relations which yielded preferred discharges for spawning and rearing for trout as a function of the toe width. It has been stated that this method when applied to streams in Washington produced coefficients of determination of 0.9 for spawning and 0.87 for rearing habitat (Morhardt, 1986). It is not clear, how these coefficients were

arrived at. This method provides an interesting alternative to the Wetted Perimeter Inflection Point method, as less effort would be involved in determining the toe width, as it is a single parameter which has to be measured in the field. Further testing of the method would be required for other regions and species.

B.2.3.4 Discussion

These methods represent a slightly more sophisticated IFN tool than the discharge methods, both due to the greater amount of data and analysis required, and due to their consideration of site specific characteristics. Of particular importance, however, is a proper understanding and implementation of the hydraulic theory.

A key limitation of these methods is that the characteristics of the stream are examined only at specific locations. Therefore, it is important to select sections which are critical in terms of providing adequate habitat, that is, where food production tends to occur and where spawning and rearing habitat is located (Bietz et al., 1985). Critical sections have also been defined as those which exhibit sensitivity of width, depth and velocity to changes in streamflow (Bovee and Milhous, 1978; Randolph and White, 1984). Typically, these critical sections are found to be located at riffles (Bietz et al., 1985; Randolph and White, 1984).

Of particular importance in the application of these methods is the appropriate choice and implementation of a hydraulic model for the rating curve. A constraint to this method is introduced through the analysis of critical sections only. As these sections are typically located at riffle sections, the investigator should be aware that local water surface slopes would be expected to be steeper than the reach averaged water surface, or bed slopes. The development of a theoretical rating curve based on a reach average slope (extending over a number of pool-riffle sequences) would most certainly produce erroneous results.

Although implementation of a gradually varied flow analysis in conjunction with these methods may not be common, it could prove to be a significant improvement. A similar quantity of data would be required, although a variety of representative sections would have to be measured rather than just riffle sections. This could have the added advantage of considering habitat characteristics throughout the study reach rather than just

at critical sections. Given that the almost exclusive choice of riffle sections for these methods has been, to a large extent, tied to the ease with which the inflection points may be identified at these, often nearly rectangular, sections (Bietz et al., 1985), the recognition of the inflection point as the point of maximum curvature (though not necessarily a discontinuity) would simplify implementation of this refinement. However, it should be stressed that this refinement is intended to facilitate the development of realistic rating curves at the critical sections, not to extend the evaluation of a recommended minimum acceptable discharge to non-critical sections.

B.3 Multi-variable Methods

B.3.1 General

Multi-variable Methods, as the name suggests, employ several variables which are known to be correlated with fish preferences. Among these methods are empirical methods, which are based on a statistical analysis of stream data to obtain an understanding of factors governing habitat quality. The objective of such methods is usually to develop empirical relations which relate these variables to available usable habitat or fish biomass. The Habitat Quality Index (HQI) method, which is used intensively in the state of Wyoming in the U.S.A., is discussed below as an example of these methods. Another Multi-variable Method is the Instream Flow Incremental Methodology (IFIM), which considers physical habitat characteristics in the development of relationships between streamflow and usable habitat area for different life stages of fish species. This method is widely used in North America. In the U.S.A. it is used in about 35 states and required by law in many of these states (Reiser, 1992). In Canada it has been used for IFN assessments in the provinces of British Columbia, Alberta, Saskatchewan and Manitoba (Fernett, 1992).

B.3.2 Empirical Methods

B.3.2.1 The Habitat Quality Index (HQI) Method

Binns and Eiserman (1979) developed this method to predict the trout standing crop (biomass) in Wyoming streams, based on the assumption that the best habitat for trout is associated with a high standing crop. Data were collected from 44 study sites on Wyo-

ming streams to span a wide array of habitat types. The surveyed streams ranged in elevation from 1,146 to 3,042 m, the average late summer stream width varied from 1.4 to 44 meters (m), the average daily flow was between 0.6 and 14.6 m^3/sec and stream gradients from 0.1 to 10% were observed.

Multiple regression analyses were applied to 22 different attributes representing physical, chemical and biological characteristics of the streams. Thirteen physical attributes (late summer stream flow, annual stream flow variation, maximum summer stream temperature, water velocity, turbidity, cover, stream width, stream depth, stream morphology, eroding banks, substrate, bed material, and silt deposition), five chemical attributes (nitrate nitrogen, total alkalinity, total phosphorous, total dissolved solids, and Hydrogen ion) and four biological attributes (stream bank vegetation, fish food abundance, fish food diversity, and fish food type) were tested.

The determination of some of the attributes required specific defining criteria. Late summer stream flow was rated by comparing average daily flow during August and the first half of September to year-round average daily flow. A proportion of less than 10% was considered inadequate to support trout while greater than 55% was regarded as completely adequate. The water velocity was calculated as the thalweg length of the study reach divided by the time a fluorescent dye took to travel that distance. Cover was identified as anything that allowed trout to avoid the impact of the elements or enemies (Binns and Eiserman, 1979) such as water depth, surface turbulence, loose substrate, large rocks and other submerged obstructions, undercut banks, aquatic and overhanging terrestrial vegetation, dead snags and other debris lodged in the channel (a very broad and subjective definition). The percentage of eroding banks was estimated by dividing the sum of lengths in which bank erosion is observed by the total bank length of the study reach. Substrate condition was judged based on the availability of submerged aquatic vegetation (including algae and moss growing on rocks).

Each attribute was assigned an integer number from 0 (worst) to 4 (best) to rate it's suitability for trout life. From these attributes the ones which showed the highest correlation to trout standing crop were chosen to build two empirical predictive models. The first model (Model I) was developed from data obtained from sites 1 to 20 and verified on sites 21 to 36. This model relates ten habitat attributes to trout standing crop. The development

of the second model (Model II) was based on data from test sites 1 to 36, and was verified for study sites 37 to 44. The models were found to explain up to 96 % of the variation in trout standing crop (Binns and Eiserman, 1979).

The authors claimed that the method has been used to understand potential changes in habitat which occurred due to a water diversion project and to assess habitat improvement potential. It has been claimed that the HQI should prove useful in other areas as it performed satisfactorily in Wyoming (Binns and Eiserman, 1979).

With respect to the hydraulic component of the HQI empirical models, it should be stated that among the four variables: depth, width, discharge and velocity; deterministically speaking, one is redundant. However, as the regression is performed on variables representing the suitability of these hydraulic parameters, rather than the physical variables themselves, this redundancy might not affect the statistical significance of the proposed models.

B.3.2.2 Other Empirical Methods

A number of other empirical methods have been proposed. For example, Layher (1983) presented a series of empirical relations based solely on chemical variables for predicting standing crop of different species of fish in prairie streams in Kansas as well as other relations which included also physical variables such as mean width, percent runs, percent pools and turbidity. Rabern (1984) presented another collection of empirical relations for predicting standing crop of several fish species in Georgia streams. The relations employed hydraulic, chemical and biological variables. White et al. (1976) developed empirical relations for trout in Midwestern U.S. streams. The relations relied on discharge variables such as mean monthly flow, maximum monthly flow, maximum daily flow and peak momentum flow. Although these empirical methods consider hydraulic parameters in their regressions, they do not employ hydraulic models.

B.3.2.3 Discussion

A major limitation facing the empirical methods in general is the large amount of data and analysis required, and their site- and species-specific nature. Binns and Eiserman, 1979, claimed that the HQI method should prove useful in other areas as it performed sat-

isfactorily in Wyoming. However, Bowlby and Roff (1986) tested the two models for trout biomass in Ontario streams and reported a very poor performance with the models accounting for only 6.7 and 9.2% of the variation in trout biomass at Ontario sites. Bowlby and Roff also found that only late-summer stream flow, annual stream flow variation and maximum summer stream temperature were significantly correlated with trout biomass in Ontario, whereas in contrast Binns and Eiserman (1979) found that of the eleven variables in their two models, late summer stream flow and maximum summer stream temperature were the only variables not significantly correlated with trout biomass. Bowlby and Roff concluded that clearly, different factors limit trout biomass in Wyoming than in southern Ontario streams, which would indicate that this empirical model is only regionally valid, at best, and may vary dramatically in form because different aspects of habitat become the critical, limiting elements for particular species in different regions, or even in different streams within a region (Hogan and Church, 1989). Consequently, the HQI method developed by Binns and Eiserman (1979) does not present a generic predictive model for fish habitat evaluation. It is an empirical model for *trout* standing crop prediction in *Wyoming* streams. New models could be developed for other species and/or regions following a similar procedure. Considerable research and testing would be required to identify the attributes correlated to fish biomass and to develop an empirical formula. Furthermore, the model would not be usable for impact prediction, unless tools are available to forecast the physical, chemical and biological impact of any anticipated project or habitat improvement plan.

Binns and Eiserman, 1979, claimed that the method has been used to understand potential changes in habitat which occurred due to a water diversion project and to assess habitat improvement potential. However it is not mentioned how the changes in the variables that would be expected from these projects could be predicted. In order for the method to be useful in such applications, tools would be required to estimate anticipated changes in the attributes involved in the empirical models. Among these tools are hydraulic models as well as models to predict changes in temperature and water quality. Such models have not been addressed by the authors.

B.3.3 Instream Flow Incremental Methodology

B.3.3.1 General

Because of the natural variability in stream characteristics and the unique habitat requirements of different fish species, a deterministic approach to the assessment of proposed water management plans is often desirable, particularly as habitat needs usually vary for different life stages and/or activities of a given fish species. One way to evaluate the suitability of a certain habitat for fish life under different water management plans is the Instream Flow Incremental Methodology (IFIM). The IFIM is essentially a collection of computer models and analytical procedures which combines information about the biology and life habits of the species under study with computer models that can predict the impact of different water management policies on the available habitat. The effect of a disturbance on a system is quantified by incrementally evaluating the impact of the disturbance on the variables describing the system. For example hydraulic models may be used to calculate water depth and flow velocity for a given discharge, sediment transport models can help forecast geomorphological adjustments to proposed channel modifications, and environmental models assist in the predicting of the impacts of proposed water management plans on the water quality or temperature distribution.

Because of the modular approach used, an IFIM system may be continuously updated and improved by modifying, replacing or adding modules. This modular approach facilitates growth and expansion of the IFIM system as improved models for the various physical components are developed. Also new information about the biology and preferences of the evaluation species can be incorporated into the model.

Implementation of the IFIM method has lead to the development of the Physical Habitat Simulation System, or PHABSIM, which was developed by the Instream Flow and Aquatic Systems Group (IFG), U.S. Fish and Wildlife Service in 1981. An updated version of the model was released in 1989. Because of its deterministic and modular approach and its predictive capabilities, the PHABSIM model has gained wide acceptance for use in IFN assessment studies in North America. Therefore, the following discussion concentrates on this model.

B.3.3.2 Method Description

PHABSIM is used to simulate the physical habitat of fish as a function of discharge and to transform this information, through knowledge about fish preferences at various life stages, into a measure of usable habitat (Orth and Maughan, 1982). These relationships are usually represented as continuous functions between the weighted usable area of habitat and discharge, as each species exhibits preferences within a range of habitat conditions that it can tolerate. If these ranges can be defined for each species, the area of the stream providing these conditions can be quantified as a function of discharge and channel structure. This approach assumes that any change in, or impact on, the fish habitat can be adequately described by the four variables: depth, velocity, substrate and cover. It also assumes that the entire stream can be modeled on the basis of one or more representative study reaches and that there is a positive linear relationship between weighted usable area and fish standing crop. In order to find the usability of a stream for fish life, habitat suitability functions have been developed for different types and life stages of species (Bovee, 1986). These functions represent the relationship between habitat suitability and the four variables in mathematical terms. If such functions are not available for the species and/or region under investigation, extensive field measurements, analysis and testing would be required to establish these functions. The reader is referred to Bovee (1986) for more details on this subject.

To facilitate the computer analysis, the stream surface area is divided into a number of quadrilateral cells. These cells are located in such a way to represent an area having fairly uniform habitat characteristics. These physical characteristics are measured and/or computed along verticals at a number of locations across the stream width, the spacing of which determines the cross-stream cell dimension. The longitudinal extent of a cell is equal to one half the distance between adjacent upstream and downstream measurement stations or transects. From these measurements, a representative value for each of the four variables: depth; velocity; substrate; and cover, is obtained for every cell.

Information about cover and substrate are obtained from field observations and bed material samples and, generally, no computer simulation is used to provide estimates for these variables. Hydraulic simulation models are used to forecast changes in depth and

velocity. This hydraulic modeling is done in two steps. First, a stage-discharge relationship is developed. Then, the velocity distribution across the channel is determined.

i)Development of a Rating Curve

In PHABSIM, the stage-discharge relationship can be determined in one of three ways:

1.the use of a stage-discharge regression model (IFG-4);

2.a uniform flow model (MANSQ); or

3.a gradually varied flow model (WSP).

The last two models are used in situations where geometric data is available for the study reach, but actual measurements of corresponding stage discharge data are scarce or altogether unavailable. The use of a stage-discharge regression model requires that sufficient stage-discharge data be available to define the stage-discharge relationship over the range of anticipated discharges. For all three models, it is assumed that no scour or deposition will take place for the type of projects and range of flows considered. Unlike the gradually varied flow model, the uniform flow and stage-discharge regression models simulate each cross-section independently of the other cross-sections in the study reach. Care must be taken to assure that the models used adequately describe the physics of the flow. In particular, water management proposals in which channel modifications or hydraulic structures are involved, would alter the stage-discharge relationship and, therefore, a stage-discharge relationship derived for conditions before the project would be invalid for predictive purposes.

For most natural streams, particularly gravel bed streams exhibiting pool and riffle sequences, the uniform flow approximation is invalid. Flow velocities and water surface slopes are small in pools while depths are large (relatively speaking), whereas flow velocities and water surface slopes are large and depths shallow over the riffles. Clearly, a proper evaluation of the hydraulics warrants a gradually varied flow analysis. The gradually varied flow calculations in PHABSIM are performed through the Water Surface Profile (WSP) program (also referred to as IFG-2) originally developed by the U.S. Bureau of Reclamation in 1968 and later modified for use in PHABSIM (Milhous et al., 1989). It is

based on the standard step method and also includes options which provide for step changes in discharge between cross sections and a variety of methods for averaging friction slopes between cross sections.

An alternative to the WSP program is the Water Surface Profile Calculation program, HEC-2, developed at the Hydraulic Engineering Center of the U.S. Army Corps of Engineers. Although it is not an integral part of PHABSIM, HEC-2 does have a number of attractive advantages. First, its wide acceptance across North America makes it a familiar tool for the analysis and one for which data sets may already be available. In addition, along with the standard step gradually varied flow analysis, HEC-2 incorporates numerous options which may facilitate the analysis of reaches containing bridges (and piers), culverts, and other hydraulic structures. In addition the effects of flood plain flow and ice covers may also be evaluated. It is important to realize, however, that these complex flow problems are handled in an empirical way and therefore the accuracy of the results will depend heavily on the expertise of the user.

Both WSP and HEC-2 offer an option to calculate the variation in channel roughness in the study reach using a set of calibration measurements (discharge and water surface elevation measurements). Some authors have recommended against the use of this option because the calibration process is difficult to perform, has limited accuracy and because the final results in PHABSIM are sensitive to velocities (Milhous et. al. 1989; Bovee and Milhous 1978). However, many engineers have overcome the difficulties associated with calibration by avoiding these optional routines and calibrating their model manually. This merely involves estimating reasonable values of the loss parameter (Manning's n) for the initial run and then adjusting these in subsequent runs of the model until the measured water surface profile is reproduced. A systematic and theoretically sound approach simplifies the calibration process significantly. For example, large variations in n between adjacent cross sections are physically unrealistic. It should be considered as a reach characteristic and should only be changed on a reach by reach basis where physical evidence suggests that such a change is warranted. In fact, this is the source of much of the frustration associated with the use of the calibration routines within the programs, as these computer routines have no ability to introduce judgment and qualitative assessment into the process. Another factor to keep in mind during the calibration process is the spatial direction of the calculations. If the flow is subcritical for example (calculations step in the

upstream direction), then changes to n values at downstream sections will be reflected in the computed water surface levels at upstream sections. Consequently, calibration adjustments should start at the downstream end for subcritical flow calculations. Again, this is an approach not necessarily implemented in the automated calibration routines. Finally, it is important for the modeler to appreciate that dramatic changes in n between sections or reaches and/or unrealistic values of n required to achieve calibration may be indicative of a flow regime change (subcritical to/from supercritical) which requires special modeling techniques.

ii)Determination of the Velocity Distribution Across the Channel

Once a stage discharge relationship has been obtained, the program IFG-4 is used to find the velocity distribution across each transect (cross section). These velocity values, essential to the habitat simulation phase, are quantified by establishing a velocity versus discharge relation for each vertical within each cross section. As with the development of a rating curve, the method used to obtain the velocity-discharge relationship depends on the type and amount of data available.

One approach for establishing a velocity versus discharge relationship for each vertical within each transect, is to perform a linear regression between the logarithms of the discharge and velocity. This approach assumes that the velocity at each vertical exhibits a log-log linear relation with discharge and that no change in channel morphology, vegetation or flow regime occurs. A minimum of three velocity-discharge measurements taken at all verticals at all transects are required and these data must be taken at exactly the same verticals each time.

An alternative to this data intensive approach was introduced in version II of IFG-4 (Milhous et al., 1989) which facilitates the evaluation of the velocity versus discharge relation for each vertical within each transect using only one set of velocity versus discharge data. First, this calibration set of velocity measurements across the channel is used to determine the distribution of roughness across the channel, based on the Manning's equation, as follows:

$$n_i = \frac{H_i^{2/3} S_f^{1/2}}{v_i} \qquad [B.1]$$

where n_i is Manning's n value for the cell i, v_i is the depth averaged velocity measured for the vertical, H_i is the corresponding water depth at the same vertical and S_f is the slope of the energy grade line, which is assumed to remain constant across the channel width at each transect. The magnitude of S_f may be input by the user or the program will assign a default value of 0.0025.

Once the flow distribution has been calibrated using equation [B.1] at all verticals across a transect, cell velocities may be computed for other discharges by weighting the cell velocity based on conveyance using the formula:

$$v_i = \left(\frac{r_i^{2/3} S_f^{1/2}}{n_i} \right) \{ \frac{Q}{Q_t} \} \qquad [B.2]$$

where r_i is the hydraulic radius, Q is the total discharge through the cross section for which the subsection velocities are required and Q_t is the total discharge based on a summation of subsection conveyances, that is:

$$Q_t = \sum_{i=1}^{n} \{ \frac{a_i r_i^{2/3} S_f^{1/2}}{n_i} \} \qquad [B.3]$$

in which a_i is the subsection area perpendicular to the flow.

iii)Determination of the Velocity Distribution Through the Depth

An option has been included in PHABSIM in the habitat simulation program HABTAT, to account for the variation of velocity in the vertical direction. However, it should be noted that the accuracy of these calculations are, at best, only as good as the initial calculations of the depth averaged column velocity performed in IFG-4. The user can specify a certain vertical distance which is excluded from the top and the bottom of the cell (a default value of 30 mm is set by the program). Then it is assumed that the fish is free to move vertically in the remaining portion to select an optimum velocity for its activity. The variation of the velocity in the vertical direction can be calculated either by using a power relation or the log-law for rough bed (Milhous et. al. 1989).

B.3.3.3 Discussion

First, a brief discussion of the terminology used in hydraulic modeling in PHABSIM, specifically the use of the name "one-dimensional" model. Generally, a one-dimensional approach looks at the stream as a number of cross-sections. Each cross-section is described by cross-section average variables. Thus, for each cross section there exists one representative stage and one representative cross-section average velocity. Hydraulic principles are applied to relate these cross-sections to each other and solve for the cross-section average variables. Among the assumptions underlying the one-dimensional model are (Abbott, 1979) that the flow varies only in the longitudinal direction, or at the least that variations in the plane normal to the flow can be considered negligible and that the velocity distribution is uniform across the channel. Examples for the one-dimensional approach are the stage determination in PHABSIM using WSP or HEC-2.

However, if we look at the velocity determination in PHABSIM, we find that the cross-section is devided into cells and verticals, and velocity at each vertical is determined from measured velocity values at different discharges at that vertical. The vertical is not tied in any way to other verticals around it through hydrodynamic principles. Therefore, this approach of velocity determination should be more correctly termed a zero-dimensional approach, which relies solely on interpolation from measured values and not on physical principles.

Now, looking at the velocity determintation using only one set of velocity measurements together with "Manning's equation", since the subsection roughnesses are calibrated based on uniform flow in [B.1] and the computed velocities in [B.2] are based on the gradually varied flow solution, the factor Q/Q_t is required to adjust the velocities. In this context then, n_i does not really represent a roughness so much as a weighting factor. This also illustrates why the magnitude of the slope, if assumed constant across the channel, is not a factor in the analysis and is likely included only to assign a realistic scale to the values computed for n_i. It should be mentioned here, that the use of IFG-4 with only one velocity set is strongly discouraged in PHABSIM's User's Manual (Milhous et al., 1989). Hence, it is important to make a distinction between the approaches used for determination of stage and the determination of velocities in PHABSIM.

Regarding the techniques applied for the evaluation of the stage at different cross sections, specifically the use of HEC-2 or WSP, are based on sound and widely accepted hydraulic principles of one-dimensional open channel flow, and, if properly applied under consideration of the basic underlying assumptions, can provide reliable estimates for the stage at each cross-section for unmeasered flows.

Now, if we look at practical river situations, we find several difficulties in conforming to the requirement of three velocity sets. For example, considering the cross-section in Figure B.1 of a natural channel where velocity measurements are taken for three well-spaced discharges as required by the zero-dimensional model, the three horizontal lines a-a', b-b' and c-c' represent the water surface at low, medium and high flow, respectively.

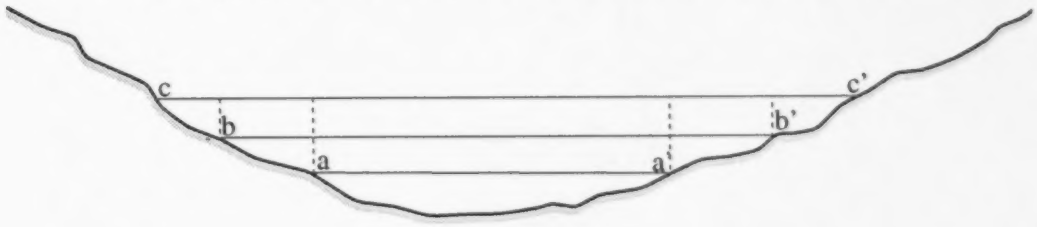

Figure B.2 Cross section in a Natural Stream

It can be seen that verticals in the region a-a' will have three velocity measurements. However, verticals in the regions b-a and a'-b' will have two, and verticals in c-b and b'-c' only one velocity measurement. Further, for simulating higher unmeasured flows, the water surface will become even wider, exposing new regions with no velocity measurements. However, from a biological point of view, these regions near the banks (or near islands) might be quite interesting, but would not be properly simulated when using the standard IFG-4 approach. Also, considering the situation of non-wadable rivers, for the standard IFG-4 approach to work properly, velocity measurements for different discharges have to be taken at exactly the same verticals. This might be quite difficult to achieve in the case of large rivers. Also, in some studies the IFG-4 model has been used to analyze river enhancement designs. Although this might have been the only tool available, it is obvious that once any structure is placed in the river the flow regime, energy grade line... etc. (not to mention channel morphology) may be changed drastically, and thus velocity

measurements taken before the modifications would be irrelevant. Further, in natural streams flow phenomena such as eddies and recirculation are encountered, which cannot be resolved using a zero- or one-dimensional approach, which assumes a priori a flow direction perpendicular to the cross section. In the one-dimensional approach the stream is assumed to be straight, and thus the effect of meanders on the redistribution of longitudinal velocity are neglected. Therefore, the argument is that even if all the funds, manpower and time required to use the standard IFG-4 model are available, there are many situations where it is practically very difficult or impossible to apply. Further, Milhous et al., 1989, page II.127 stated that the weighted usable area predicted by the habitat simulation programs is much more sensitive to errors in velocities than to errors in depth values. This suggests that a more rigorous approach should be adopted for the determination of velocities.

B.3.4 Other Multi-variable Methods

A number of other conceptual multi-variable models have been developed. Swank and Philips (1976) based their recommendations of IFN on the channel usable width, defined as the channel width having depth and velocity within prescribed limits which depend on the fish activity under consideration. Waters (1976) presented a method which calculated relative habitat units (RHU) based on the four variables velocity, depth, substrate and cover. This method is the precursor of the PHABSIM model. None of these models have gained widespread use.

B.4 Discussion of IFN Methods

The hydraulic models employed in the widely used IFN studies fall into the restrictive category of approximations within one-dimensional, steady, rigid boundary models known as uniform flow and gradually varied flow. Given the simplistic approach of some of the IFN tools, such as the single variable methods, the elementary nature of the hydraulic solution is likely no more limiting than their biological simplicity. From a hydraulic viewpoint, these models are adequate for preliminary level studies, although proper application of the hydraulic theory cannot be stressed enough.

With respect to the multi-variable methods, empirical models involve only limited application of hydraulic theory in terms of the collection and statistical analysis of hydraulic data. Given their site and species specific success and data intensive approach, hydraulic modeling criteria are likely of secondary importance in evaluating the applicability of such models to IFN studies.

Clearly, for planning and design level studies, the IFIM approach and in particular the PHABSIM model is the most promising. However, there is a lack of sophistication in the hydraulic models. For example, even though the determination of the velocity distribution in the stream is a key factor in assessing habitat quality, the hydraulic models currently in use are woefully inadequate. In particular, projects which propose modification to the channel or instream structure require more sophisticated modeling techniques.

Fortunately, the modular and deterministic approach used in the PHABSIM model easily facilitates the use of more sophisticated hydraulic models, the selection of which depends on the needs and characteristics of the given problem. It is important to note that many of these models do not require prohibitive amounts of data (which is the reason for using hydraulic models in the first place) and may even, in some cases, require less data than the one-dimensional models currently used.

It should be mentioned here, that other authors have realized the limitations in the present IFN assessment methods and have moved to using more sophisticated hydraulic modeling techniques. Leclerc et. al., 1994, used a two-dimensional finite element model based on the mixed interpolation technique to model spawning habitat in a reach of the Ashuapmushuan River, Quebec. However, it is observed that the general understanding and acceptance of such techniques from most IFN workers is still unsatisfactory. Further, as shown in Chapter 1, there is room for improvement on the available two-dimensional hydraulic models. Therefore, this thesis has two major objectives. First, to increase the acceptance of advanced hydraulic models and help bridge the gap between hydraulics and biology, and second, to present numerical modeling techniques for overcoming the difficulties underlying the solution of the two-dimensional shallow water flow equations.

Appendix C

Evaluation of the Square Root of the Convection Matrix

The matrices $\mathbf{W_x}$ and $\mathbf{W_y}$ are given by equations [2.40] and [2.41]. The square root of the matrices is calculated numerically using the Cayley-Hamilton theorem (Hoger and Carlson, 1984) as follows:

$$s_1 = \sqrt{U^2 + V^2 + c^2} \qquad [\text{C.1}]$$

$$s_2 = (\sqrt{3c^2 + 2U^2 + 2V^2 + c\sqrt{c^2 + 16U^2 + 16V^2}}) / (\sqrt{2}) \qquad [\text{C.2}]$$

$$s_3 = (\sqrt{3c^2 + 2U^2 + 2V^2 - c\sqrt{c^2 + 16U^2 + 16V^2}}) / (\sqrt{2}) \qquad [\text{C.3}]$$

$$i_1 = s_1 + s_s + s_3 \qquad [\text{C.4}]$$

$$i_2 = s_1 s_2 + s_2 s_3 + s_3 s_1 \qquad [\text{C.5}]$$

$$i_3 = s_1 s_2 s_3 \qquad [\text{C.6}]$$

$$j_1 = s_1^2 + s_2^2 + s_3^2 \qquad [\text{C.7}]$$

$$j_2 = s_1^2 s_2^2 + s_2^2 s_3^3 + s_3^2 s_1^2 \qquad [\text{C.8}]$$

$$j_3 = i_3^2 \qquad [C.9]$$

$$\text{div} = j_3 (i_3 + i_1 j_1) + i_1^2 (i_1 j_3 + i_3 j_2) \qquad [C.10]$$

finally,

$$(\mathbf{A}_x^2 + \mathbf{A}_y^2)^{-1/2} = (i_1 (i_1 i_2 - i_3)\mathbf{A}^2 - (i_1 i_2 - i_3)(i_3 + i_1 j_1)\mathbf{A}^2 + (i_2 i_3 (i_3 + i_1 j_1) + i_1^2 (i_2 j_2 + j_3))\mathbf{I}) / \text{div} \qquad [C.11]$$

where **I** is the identity matrix.